

DRUG RESISTANCE IN BRAF-DRIVEN TUMOURS: THE SEARCH FOR  
CANDIDATE MEDIATORS AND BIOMARKERS

by

Nourah Mohammad Obaid

Submitted in partial fulfilment of the requirements  
for the degree of Master of Science

at

Dalhousie University  
Halifax, Nova Scotia  
March 2017

© Copyright by Nourah Mohammad Obaid, 2017

رَبِّ أَوْزِعْنِي أَنْ أَشْكُرَ نِعْمَتَكَ الَّتِي أَنْعَمْتَ عَلَيَّ وَعَلَىٰ وَالِدَيَّ  
وَأَنْ أَعْمَلَ صَالِحًا تَرْضَاهُ وَأَصْلِحْ لِي فِي ذُرِّيَّتِي ۖ إِنِّي تُبْتُ إِلَيْكَ وَإِنِّي مِنَ الْمُسْلِمِينَ

[الأحقاف:15]



"O my Sustainer! Inspire me so that I may forever be grateful for those blessings of Thine with which Thou hast graced me and my parents, and that I may do what is right <sup>1</sup> that will meet with Thy goodly acceptance; and grant me righteousness in my offspring [as well]. Verily, unto Thee have I turned in repentance: for, verily, I am of those who have surrendered themselves unto Thee!"

(*Qur'an*, *Al-Ahqaf* 46.15), *Asad Translation* <sup>1</sup>

# TABLE OF CONTENTS

LIST OF TABLES .....	vi
LIST OF FIGURES .....	vii
ABSTRACT .....	x
LIST OF ABBREVIATIONS USED .....	xi
ACKNOWLEDGEMENTS .....	xvi
CHAPTER 1 INTRODUCTION .....	1
1.1 CANCER .....	1
1.1.1 Biomarkers in Cancer .....	3
1.2 BRAFV600E POSITIVE TUMOUR/ AS BIOMARKER.....	3
1.2.1 BRAF gene and the BRAFV600E mutation.....	3
1.2.2 BRAF gene and MAPK pathway .....	7
1.2.3 The role of BRAF in the MAPK/ERK kinase pathway.....	9
1.2.4 Feedback regulation of the MAPK pathway .....	10
1.2.5 Current approaches for detecting BRAFV600E mutations .....	13
1.3 CONFERRED RESISTANCE MECHANISMS IN BRAFV600E TUMOURS .....	14
1.3.1 Resistance through MAPK pathway reactivation.....	15
1.3.2 Resistance involving insensitivity to MAPK regulators.....	17
1.3.3 Other mechanisms of resistance .....	18
1.4 CHALLENGES ENCOUNTERED BY COLORECTAL CANCER (CRC) PATIENTS WITH BRAFV600E MUTATION .....	20
1.4.1 Evidence of specific resistance mechanisms in BRAFV600E mutated CRC 20	
1.5 EMERGING INSIGHTS INTO THE ROLE OF REACTIVE OXYGEN SPECIES (ROS) IN BRAF MUTATED TUMOURS .....	23
1.6 HYPOTHESIS AND OBJECTIVES.....	27
CHAPTER 2 MATERIALS AND METHODS.....	31
2.1 CLINICAL SPECIMENS AND CELL CULTURES .....	31
2.1.1 Clinical specimens (Project 1).....	31
2.1.2 Cell cultures (Project 2).....	38

2.2	RNA EXTRACTION.....	41
2.2.1	FFPE samples .....	41
2.2.2	Cell Lines.....	43
2.3	REAGENTS.....	44
2.3.1	Kinase inhibitors.....	44
2.3.2	ROS scavenging agents .....	44
2.4	RNA QUALITY AND QUANTITY ANALYSIS .....	45
2.5	DNASE I DIGEST TREATMENT.....	45
2.6	REVERSE TRANSCRIPTION (CDNA SYNTHESIS) .....	46
2.7	PLASMID PREPARATION, PURIFICATION AND QUALITY ANALYSIS .....	46
2.8	PRIMERS DESIGN.....	50
2.9	QUANTITATIVE REVERSE TRANSCRIPTASE POLYMERASE CHAIN REACTION (RT- qPCR) .....	53
2.9.1	TaqMan based RT-qPCR Assay .....	54
2.9.2	SYBR Green based RT-qPCR Assay .....	55
2.9.3	Quantitative Digital Droplet PCR.....	57
2.10	CELL VIABILITY ASSAY .....	61
2.11	AMPLEX RED ASSAY .....	61
2.12	STATISTICAL ANALYSIS.....	66
CHAPTER 3 RESULTS .....		67
3.1	PROJECT 1: UTILIZATION OF RT-QPCR AND ddPCR IN THE DETECTION OF BRAF IN PATIENT’S TUMOUR SAMPLES.....	67
3.1.1	Assessment of a TaqMan-based RT-qPCR method and ddPCR method in detecting BRAF expression in FFPE tumour samples.....	67
3.2	PROJECT 2: UTILIZATION OF CELL CULTURE BASED MODEL TO INVESTIGATE THE UNDERLYING MECHANISMS AND POTENTIAL TARGETS TO OVERCOME RESISTANCE.....	75
CHAPTER 4 DISCUSSION .....		100
4.1	PROJECT 1 .....	100
4.2	PROJECT 2 .....	107
4.3	LIMITATIONS AND STRENGTHS.....	111
4.4	CONCLUSION.....	112

REFERENCES ..... 114

APPENDIX A : SUPPLEMENTAY MATERIALS ..... 149

## LIST OF TABLES

Table 1 List of genes products turned on by MAPK pathway signaling. ....	12
Table 2 Melanoma FFPE samples. ....	32
Table 3 Papillary thyroid cancer FFPE samples. ....	33
Table 4 Colorectal cancer FFPE samples. ....	34
Table 5 Assessment of V600E BRAF mutant expression in melanoma samples by IHC with monoclonal antibody mutation specific (VE1). IHC staining was assessed by Dr. Huang. ....	35
Table 6 Assessment of V600E BRAF mutant expression in PTC samples by IHC with monoclonal antibody mutation specific (VE1). IHC staining was assessed by Dr. Huang. ....	36
Table 7 Assessment of V600E BRAF mutant expression in CRC samples by IHC with monoclonal antibody mutation specific (VE1). IHC staining was assessed by Dr. Huang. ....	37
Table 8 Cell lines characteristic and mutational changes. ....	39
Table 9 List of Primers Used Throughout the Project. ....	48

## LIST OF FIGURES

Figure 1 The abundance of BRAF RNA expression in various tissues.....	5
Figure 2 RAS/RAF/MEK aberrant signaling and mechanisms of resistance to inhibition in melanoma.....	8
Figure 3 RAS-RAF-MEK-ERK Signalling Pathway and its most important regulatory component.....	11
Figure 4 Processes followed when choosing cell lines.....	40
Figure 5 RNA extraction of FFPE tissue specimens from each patient.....	42
Figure 6 10 fold serial dilution of plasmid with known concentration for GUSB as a reference gene, wild-type BRAF, and V600E BRAF.....	51
Figure 7 Representation of standard serial dilution of plasmid with known concentration after expanding the dilution range.....	52
Figure 8 Steps followed in the development and assessment of a TaqMan-based RT-qPCR assay.....	56
Figure 9 A graphical representation of the fluorescence amplitudes of droplets detected.....	58
Figure 10 QuantaSoft software (BioRad) data output.....	59
Figure 11 A graphical representation of the intermediate droplets “rain”.....	62
Figure 12 Alamar Blue assay principle.....	63
Figure 13 Representative Standard curve of peroxide.....	65

Figure 14 Gene expression (ag/μl) from FFPE melanoma patients' samples as determined from known standard serial dilution curve. ....	69
Figure 15 Gene expression (ag/μl) from FFPE PTC patients' samples as determined from known standard serial dilution curve. ....	70
Figure 16 Gene expression (ag/μl) from FFPE colorectal cancer patients' samples as determined from known standard serial dilution curve. ....	71
Figure 17 Correlation between V600E BRAF mutant protein expression from IHC score and V600E BRAF mutant mRNA expression from QRT-PCR.....	72
Figure 18 Comparison between quantitative reverse transcriptase PCR (RT-qPCR) and digital droplet PCR (ddPCR) in detecting BRAF expression from FFPE samples. ....	74
Figure 19 Cell Lines gene expression as obtained from available online expression profiling study.....	77
Figure 20 Cytotoxicity effect of BRAF inhibitor (dabrafenib) on A375 melanoma cells.	79
Figure 21 Cytotoxicity effect of BRAF inhibitor (dabrafenib) on RKO colon carcinoma. ....	80
Figure 22 Comparison of cytotoxicity effect of BRAF inhibitor (dabrafenib) on naïve and resistance A375 melanoma cells. ....	82
Figure 23 Comparison of cytotoxicity effect of BRAF inhibitor (dabrafenib) on naïve and resistance RKO colon carcinoma. ....	83
Figure 24 Effect of dabrafenib treatment on gene expression. ....	84
Figure 25 Effect of dabrafenib treatment on gene expression. ....	85



Figure 26 Cytotoxicity effect of MEK inhibitor (trametinib) on naïve A375 melanoma and RKO. ....	86
Figure 27 Enhanced dabrafenib (BRAF inhibitor) potency after combination with trametinib (MEK inhibitor).....	88
Figure 28 Enhanced dabrafenib (BRAF inhibitor) potency after combination with trametinib (MEK inhibitor).....	89
Figure 29 Concentration-dependent effect of trolox on scavenging ROS in A375 naïve and resistance cells.....	91
Figure 30 Concentration-dependent effect of trolox on scavenging ROS in RKO naïve and resistance cells.....	92
Figure 31 Evaluation of Reactive Oxygen Species (ROS) productions in A375 melanoma cells. ....	93
Figure 32 Evaluation of Reactive Oxygen Species (ROS) productions in RKO colon carcinoma cells.....	94
Figure 33 Representative curves comparing the cytotoxicity effect of BRAF inhibitor (dabrafenib) alone and in combination with trolox.....	96
Figure 34 Representative curves comparing the cytotoxicity effect of BRAF inhibitor (dabrafenib) alone and in combination with trolox.....	97
Figure 35 EC50-half-maximal response comparison in naïve and resistance A375 melanoma cells.....	98
Figure 36 Linear regression curve comparisons in naïve and resistance RKO colon carcinoma cells.....	99

## **ABSTRACT**

Activating V600E mutation of the *BRAF* gene has been identified as being a biomarker for poor prognosis and overall survival. Targeted therapy for this mutation is available, nonetheless, melanoma and colon carcinoma with the BRAFV600E mutation display differences in their response and resistance to therapeutic agents. This work aims to contribute to our understanding the underlying causative mechanisms involved in the resistance to therapy.

Herein, the focus of our attention was on the identification of functional differences that might point towards the mechanisms leading to the development of resistance to treatment and to explore the feasibility of using RNA based methodologies to detect the transcript from FFPE tumour specimens. The findings obtained in this study point toward the potential of digital droplet PCR as an assessment tool and shed the light on the role that ROS might play in the development of resistance to BRAF targeted therapy.

## **LIST OF ABBREVIATIONS USED**

aa	Amino Acid
AB	Alamar Blue
ag	Attogram
AmR	Amplex Red
ATCC	American Type Culture Collection
Bad	Bcl-2 Associated Agonist of Cell Death
BIM	Bcl-2 like proteins
bp	Base Pairs
BRAF	V-Raf Murine Sarcoma Viral Oncogene Homolog B1
c-Fos	Fos proto-oncogene
c-Jun	Jun proto-oncogene
c-Myc	v-myc avian myelocytomatosis viral oncogene homolog
CAT	Catalases
CCND1	Cyclin D1
cDNA	Complementary DNA
Cq	Quantification Cycle
CRC	Colorectal Cancer
ddPCR	Droplet Digital PCR
DMEM	Dulbecco's Modified Eagle Medium
DMSO	Dimethyl Sulfoxide
DNA	Deoxyribonucleic Acid
dNTP	Deoxyribonucleotide Triphosphates

DPI	Diphenyleneiodonium
DUSP4	Dual Specificity Phosphatase 4
DUSP6	Dual Specificity Phosphatase 6
EC50	Half-Maximal Response
EDTA	Ethylenediaminetetraacetic Acid
ELK	ETS domain-containing protein Elk-1
EMEM	Eagle's Minimal Essential Medium
FBS	Fetal Bovine Serum
FFPE	Formalin Fixed Paraffin Embedded
fg	Femtogram
G	Glutathione Peroxidases
Gab2	GRB2 Associated Binding Protein
GAP	GTPase Activation Protein
GEO	Gene Expression Omnibus
GUSB	Beta-Glucuronidase
h	Hour
H <sub>2</sub> O <sub>2</sub>	Hydrogen Peroxide
HGNC	The Human Gene Nomenclature Committee Site
IDT	Integrated DNA Technologies
IHC	Immunohistochemistry
IRS1	Insulin Receptor Substrate 1
kDa	Kilodalton
l	Liter

LB	Lysogeny Broth
log	Logarithm
M	Molar
M	Mean
M-MLV RT	Moloney Murine Leukemia Virus Reverse Transcriptase
mAb	Monoclonal Antibody
Mg <sup>++</sup>	Magnesium
MgCl <sub>2</sub>	Magnesium Chloride
MgSO <sub>4</sub>	Magnesium Sulphate
min	Minute
MITF	Microphthalmia-Associated Transcription Factor
MKP-3	Map Kinase Phosphatase-3 Short Name For Mitogen-Activated Protein Kinase Phosphatase
ml	Milliliter
mRNA	Messenger RNA
Mut	Mutant
NaCl	Sodium Chloride
NCBI	National Center for Biotechnology Information
ng	Nano gram
nl	Nano Liter
NOX1	NADPH Oxidase 1
NOX4	NADPH Oxidase 4
Nrf2	Nuclear Factor-Erythroid 2-Related Factor 2

OIC	Oncogene-Induced Senescence
P	Penicillin
PBS	Phosphate-Buffered Saline
PCR	Polymerase Chain Reaction
	Peroxisome Proliferator-Activated Receptor Gamma Coactivator
PPARGC1 $\alpha$	1-A
PTC	Papillary Thyroid Cancer
RB	retinoblastoma
REB	Research Ethics Board
RefSeq	Reference Sequences
RNA	Ribonucleic Acid
ROS	Reactive Oxygen Species
rpm	Revolutions Per Minute
RPMI	Roswell Park Memorial Institute 1640 Medium
RQI	RNA Quality
RT	Room Temperature
RT-qPCR	Reverse Transcription– Quantitative Polymerase Chain Reaction
S	Streptomycin
SD	Standard
sec	Second
SODs	Superoxide Dismutases
SOS	Ras/Rac Guanine Nucleotide Exchange Factor
SPRY	Sprouty

VE1	Anti-BRAF V600E (Cytoplasmic Stain of Tumour Cell)
Vif	Virion infectivity factor
WT	Wild Type
$\beta$ -ME	B-Mercaptoethanol
$\Delta$ Ct	Delta Ct (Cycle threshold)
$\Delta\Delta$ CT	Delta Delta Ct
$\mu$	Micro

## **ACKNOWLEDGEMENTS**

“No one who achieves success does so without acknowledging the help of others. The wise and confident acknowledge this help with gratitude.” Alfred North Whitehead

First and foremost I would like to show my gratitude toward the almighty God whom without his blessing and guidance I would not be the person that I am. Thank you Allah for giving me all the skills required to survive in this life. Thank you for giving me the gift of family, health, marriage, parenthood, learning, peace, contentment, believing, and simply knowing you. You have proved to me that even the unpleasant, devastated destinies in my life have reasons, and I without a doubt know those predeterminations are always followed with best and better options.

Great thanks goes to my wonderful parents Mohammad and Fawzya; Papa, and Mama, and to my younger siblings (Habosh, Saronah, Btool, Gogo, Raghodah, and Fasoly). Thank you so much for the love, support and just being so patient with my craziness. You have been always looking up to me and I do not know if I did justice. My lovely hubby, Ahmad I cannot describe how important your presence in my life. You are my every thing, my smile, happiness, sadness, best mate and such a precious present from Allah. I would like to apologize for you and to our lovely girl Sarah for taking so much time away from both of you. May Allah grant our family and us a place in Jannah with our baby boy Abody.



This is a wonderful chance to thank my Canadian family who host us for the first couple months “Mom” Connie and Doug. I would like to thank Joan O’Keefe, Annette Scott for being there with us supporting us with the birth of Abody and Sarah, and for helping us grieving the loss of our baby boy. Thank you guys for your continued care and love. Special thanks to Emma Al-ammasi and her family for taking such good care of Sarah. I am also grateful to my ESL teachers (Krista Gault, David Packer, Andrew Dueck, Cory Walling, Mike Murray, Meredith Stewart) my friends (Maram Hulbah, Dhuha Qorban, and Saki Sultana), Eileen Kaiser, and to Dr. Wenda Greer.

I would like to acknowledge the financial support of the Ministry of Higher Education of Saudi Arabia, and at some stage the Department of Pathology, Dalhousie University; and the assistance of my colleagues at the Bedard Lab, particularly, Mat Nightingale for his technical help in extracting RNA from cell lines; Dr. Linda Chen for her endless help, supervision, and assistance with the tissue culture; Michael Mackley for allowing me to contribute in his project and for developing the assay I am assessing in my study. I also appreciate the effort from Dr. Marshall lab members Drs. Sarah Roberts, Ian Haidl, Liliana Portales Cervantes, and Nong Xu regarding digital droplet PCR, specially, Dr. Sarah Roberts for her kind assistance in explaining how to perform experiments and interpret results. I would like to extend my thanks to Dr. Ryan Pelis for offering us a space in his lab while our lab was undergoing retrofit work; Dr. Paola Marcato for offering a space to keep our cells while we had technical issues with our incubators; Dr. Graham Dellaire for lending us Alamar Blue reagent; Dr. Weei-Yuarn Huang for providing FFPE tumour specimens; my academic advisors at the Saudi Arabian Cultural Bureau in Canada for providing me with all the support needed to successfully complete

my degree particularly Drs. Yousef Abu-Nada and Mohamad Najem Najem; Ziaullah Khan for helping me to find the rough translation for my dedication; and finally Dr. Godfrey Heathcote professor and head of the Department of Pathology. Fruitful discussions of research and experiments with Dr. Karen Bedard are gratefully acknowledged.

I am sincerely and heartily thankful to my supervisors Dr. Karen Bedard and Dr. Weei-Yuarn Huang, to my committee members Dr. Paola Marcato, and Dr. Bruce Colwell, and to the external examiner Dr. Christopher Sinal.

## **CHAPTER 1      INTRODUCTION**

### **1.1 CANCER**

It is not surprising for people to hear that their beloved ones or a close friend have been impacted by cancer. In Canada alone it is estimated that between 2028 and 2032 there will be a 79 % increase in new cancer cases compared to the years 2003 to 2007 <sup>2</sup>. Of those who develop cancer in 2015, 40% will die from this tragic disease. The Canadian Cancer Society statistic from 2015 estimated that two in five Canadians will develop cancer over their life time <sup>3</sup>. It is a rising health issue, with an increasing mortality rate year after year, compelling more scientists and other stakeholders to understand and investigate this disease. The acceleration rate in research is giving rise to a more comprehensive and advanced knowledge of the cellular components and signalling pathways related to cancer. This eventually leads to improvements in diagnosing and managing cancer patients, in predicting outcomes, and in developing new therapeutic treatments.

Two important cellular programs, cell cycle and apoptosis, contribute to regulating cell growth and cell death. Both of these are tightly controlled by numerous gene products. In the case of cancer, two significant categories of genes play an essential role in suppressing cancer cell death or in promoting cancer cell growth, known as tumour suppressor genes or oncogenes, respectively <sup>4</sup>. Tumour suppressors are genes that play an important role in repairing damaged DNA, limiting cell growth, and promoting cell death;

they are also referred to as anti-oncogenes due to their unique ability to stop tumour growth <sup>5</sup>. Thus, conditions that lead to the loss of expression or the loss of function of those gene products can lead to cancer. Oncogenes refers to those genes that when over expressed or activated have the potential to trigger cancer <sup>6</sup>. Normally, the expression and activity of tumour suppressors and oncogenes are strictly regulated to control cell growth. However, mutations in the DNA, either inherited or acquired over one's lifetime, can alter the expression or the function of tumour suppressors or oncogenes, and this can lead to the development of cancer. Endogenous or environmental DNA damage factors including UV radiation, alkylating agent, and replication errors <sup>7</sup> can induce mutations to DNA. Such alterations in DNA occur routinely, and are usually repaired by DNA repair mechanisms, or in cases where the DNA cannot be repaired, cell division is arrested, and cells undergo apoptosis. In some cases however, these aberrant changes lead to loss of function of tumour suppressor genes and/or gain of function of proto-oncogenes; this may initiate tumorigenesis.

Many of the key concepts underlying our understanding of cancer were brought into focus by the remarkable review article that published in January 2000 by Hanahan and Weinberg in the journal *Cell* <sup>8</sup>. The authors outlined six underlying properties shared by cancer cells to breach the normal anticancer defense machinery that are hardwired in normal cells. These six distinct hallmarks detailed the key changes that can allow a cell to progress towards cancer. These properties are “self-sufficiency in growth signals”, “insensitivity to anti-growth signals”, “evading apoptosis”, “infinite replicative immortality”, “sustained angiogenesis”, and “tissue invasion and metastasis”. In March

2011<sup>9</sup>, the authors revised their list of cancer hallmarks to incorporate four new principles: “genome instability and mutation”, “tumour-promoting inflammation”, “reprogramming energy metabolism”, and “evading immune destruction”. These ten distinctive features enlighten scientists to describe “cancers” as a group of diseases that characterized by continuous cell growth and division with a failure in regulatory control.

### 1.1.1 Biomarkers in Cancer

Although there are features common among all cancers, at the molecular level, cancers are in fact remarkably diverse. In the era of precision medicine, the need for developing and finding specific biological markers becomes an emerging field in cancer treatment<sup>10,11</sup>. Biomarkers may be classified into three categories based on the purpose for which they will be used: diagnostic markers, prognostic markers, and predictive/therapeutic markers<sup>10,12</sup>. Occasionally, the significance of some of these biomarkers as both diagnostic and therapeutic markers makes them quite powerful for patient care. In this case, they are called “dual-duty biomarkers”<sup>13</sup>.

## 1.2 BRAFV600E POSITIVE TUMOUR/ AS BIOMARKER

### 1.2.1 BRAF gene and the BRAFV600E mutation

Retroviral oncogenes RAF discovery in 1983 led to the finding of the proto-oncogene of RAF family<sup>14</sup>. Five years later, in 1988 to be precise, Ikawa *et al.* discovered the *BRAF* gene<sup>15</sup>. *BRAF* short for (short for v-raf murine sarcoma viral oncogene homolog B) is a protein-coding gene, encoded on chromosome 7q34<sup>16</sup>. The

*BRAF* gene consists of 18 exons encoding a transcript 2949 base pairs (bp) in length. In mice, *BRAF* undergoes alternative splicing that results in the production of various *BRAF* products that differ in their biological functions and range from 2046 to 2727 bp<sup>17,18</sup>. In human however, the normal *BRAF* gene encodes a single transcript leading to a 766 amino acid (aa) (UniProtKB ID P15056). Even though BRAF expression was described by Storm *et al.* in 1990 as displaying a “restricted pattern”<sup>19</sup>, with the highest expression of BRAF is found in the neural tissue<sup>20</sup>, a later study showed that, BRAF is actually expressed in vast majority of tissues to varying degrees<sup>17,21</sup> (see Figure 1). It expressed in gonads (mainly in testes), kidney, thymus, liver, spleen and heart. Compared to normal skin and colon, thyroid gland displayed a higher BRAF mRNA expression with 18.7 TPM (transcripts per million) followed by skin and colon, as reported in the Human Protein Atlas<sup>22</sup>.

In 2002, BRAF mutations were first identified in human cancer<sup>23</sup>. Since then, it has been found that eight percent of all cancers have mutations in the *BRAF* gene<sup>23</sup>. Mutations of *BRAF* is present in a widespread range of malignant tumour including ~50% of melanoma<sup>24</sup>, ~40% papillary thyroid cancer (PTC)<sup>25,26</sup>, ~30% of serious ovarian cancer<sup>27</sup>, ~10% colorectal cancer (CRC)<sup>25</sup> and lung cancer<sup>23,28,29</sup>. Additionally, it is also found to be mutated in a pre-malignant colon polyps<sup>30</sup>, likewise in benign skin lesions<sup>31,32</sup>.

There are more than fifty distinctive mutations that have been detected in the *BRAF* gene<sup>23</sup>. Three single nucleotide point mutations were identified and among these

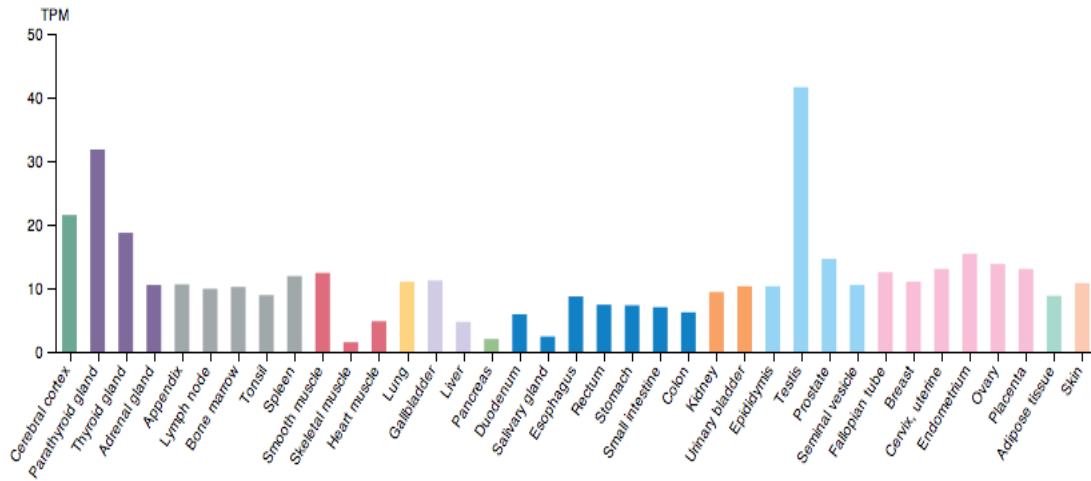


**Figure 1 The abundance of BRAF RNA expression in various tissues.**

An estimation of the BRAF RNA expression in different tissue types (x-axis) obtained by RNA-seq analysis of 115 cell line samples and 172 tissue samples on Illumina HiSeq2000 and 2500 machines (Illumina, San Diego, CA, USA) using the standard Illumina RNA-seq protocol with a read length of 2x100 bases. The abundance of BRAF transcript was reported as number of transcripts per million (TPM) (y-axis). Individual bar represents the highest expression score found in a particular group of tissues. [Credit: image from Human Protein Atlas available from [www.proteinatlas.org](http://www.proteinatlas.org); BRAF RNA expression overview/HPA dataset].

(<http://www.proteinatlas.org/ENSG00000157764-BRAF/tissue>)

substitutions, greater than 90% occur at codon 600 in exon 15, the most common single – base changes account for a thymine (T) to adenine (A) replacement at position 1799 of the mRNA (NM\_004333.4; c.1799T>A). This missense mutation results in the substitution of the amino acid valine (V) to glutamic acid (E). This mutation is well-known as BRAFV600E (p.Val600Glu)<sup>23</sup>.

Biochemically, even though amino acids have slightly similar structure, each one of them has its unique side chain that would determine its properties in the protein final product. In the case of BRAFV600E substitution, a slightly small-sized hydrophobic valine has been replaced by a negatively charged glutamic acid which interrupts the hydrophobic interaction of the valine<sup>23,26,33,34</sup>. The negatively charged side chain of the glutamic acid mimics the effect of phosphorylation, and the BRAF protein becomes active in the absence of upstream signalling pathways.

In an *in-vivo* study done by Hoeflich *et al.* in 2006 illustrated that, suppression of mutant BRAFV600E in melanoma xenograft model slowed tumour growth<sup>35</sup>. This suggests the significance roles that gain-of-function BRAF plays in maintaining tumour proliferation. However the presence of mutant BRAF V600E is itself not always enough for cancer progression<sup>36</sup>. The formation of nevi lesions, benign skin lesions, in transgenic zebrafish expressing BRAFV600E indicate that mutant BRAF has a critical role in initiating the tumour but that a combination of other factors is required for tumour progression<sup>37,38</sup>.



### 1.2.2 BRAF gene and MAPK pathway

Errant signalling of MAPK has been linked to a number of tumour types<sup>39</sup> and it can lead to uncontrolled cell proliferation, resistance to apoptosis; the programmed cell death, and resistance to therapies<sup>40,41</sup>. Malignant cells are independent from external growth signals and do not respond to any normal stimuli. This self-sufficient feature is one of the Hallmarks of cancer and it allows them to continue dividing without stopping. Gain-of-function mutation in the *BRAF* gene can cause a conformational change in the activation segment locking the BRAF protein in the “on” state. This will continuously transmit signals resulting in uncontrolled proliferation and tumour development. This pathway is described in Figure 2.

*BRAF* is part of the well-established mammalian signalling pathway known as the Mitogen-activated protein kinase (MAPK), originally called Extracellular signal-regulated kinase pathway (ERK). The discovery of the transforming activities of the retroviral oncogene form of *RAS* (originally named from rat sarcoma) and *RAF* (originally named from rapidly accelerated fibrosarcoma) led to a major breakthrough of what we know today about *RAS* and *RAF* oncogene<sup>42</sup>. Prior to the discovery of BRAF mutations, this pathway was already known to be important in cancer progression, as mutations in *RAS* gene were known to be important drivers of cancer.

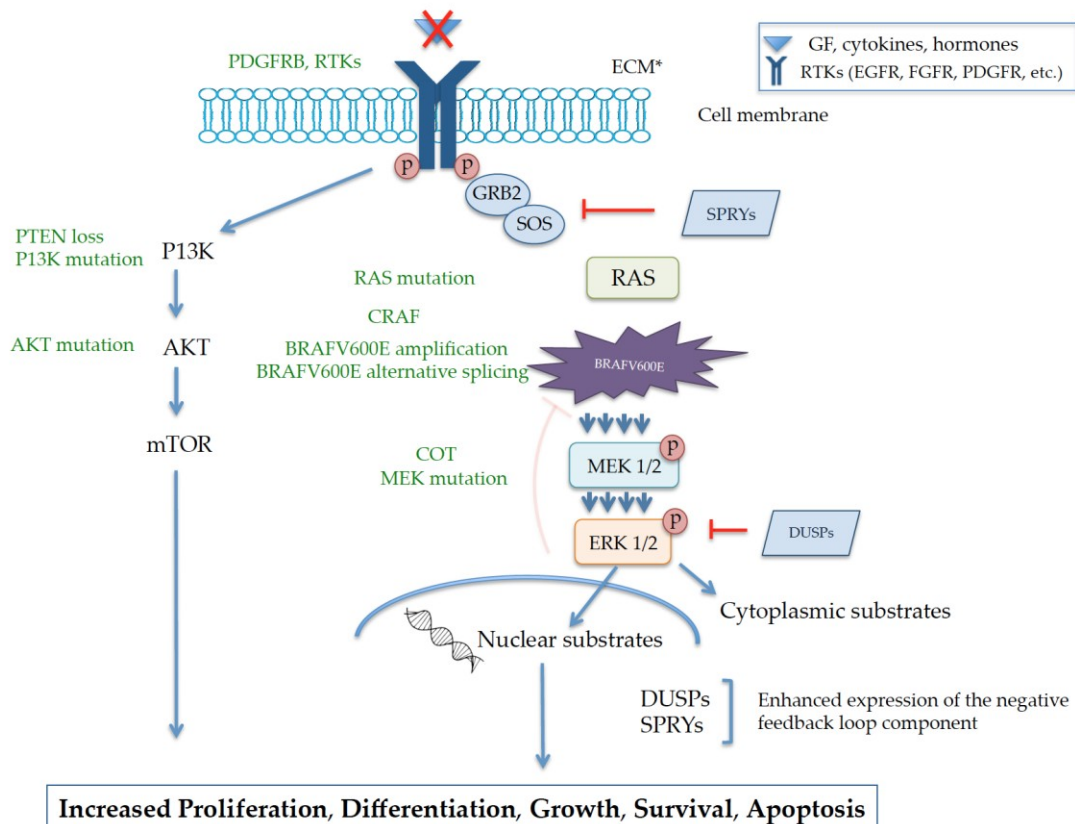


**Figure 2 RAS/RAF/MEK aberrant signaling and mechanisms of resistance to inhibition in melanoma.**

Oncogenic BRAFV600E cells become independent from external growth factors (GF) (triangle symbol marked with an X) and other stimuli leading to constitutive activation of the MAPK pathway. Increased MAPK signalling (four arrows) eventually leads to enhanced gene expression including MAP kinase phosphatases (DUSPs) and sprouty proteins (SPRYs). Despite elevation of those important inhibitory regulators (T lines) of the MAPK pathway, tumour cells adapt and rely on neighbour pathways, such as the PI3K pathway, to grow and survive, Furthermore, negative inhibitory mechanisms of the MAPK pathway, including inactivation of BRAF via ERK1/2, are now lessened (faded T) due to conformational changes in the BRAF. Conferred mechanisms of resistance to BRAF inhibitors including up-regulation of PDGFRB, RAS mutations, elevation of CRAF, BRAFV600E amplification, alternative splicing of BRAFV600E, elevation of COT (MAP3K8), MEK mutation, PTEN loss, PI3K and AKT mutations were highlighted in green. Note: this figure has also been used in publication <sup>43</sup>.

### 1.2.3 The role of BRAF in the MAPK/ERK kinase pathway

*BRAF* is part of the RAS-RAF-MEK-ERK pathway. It is present in all eukaryote cells, and controls and regulates essential cellular mechanisms including cell proliferation, differentiation, survival and apoptosis<sup>44,45</sup>. *BRAF* is one of the three isoforms of RAF family of serine/ threonine protein kinase: BRAF, CRAF, and ARAF. Among the RAF members, BRAF has the highest basal kinase activity and it easily activated by RAS<sup>21,46</sup>. Unlike CRAF; a member of the RAF kinases family, BRAF has a higher MEK kinase activity due to its high affinity for MEK<sup>47</sup>, resulting in more efficient phosphorylation of MEK. Thus, BRAF plays a key regulatory role in the MAPK /ERK pathway<sup>48,49</sup>.

In normal cells (with a wild type BRAF), this pathway is activated by extracellular signals such as, cytokines, hormones and, growth factor binding<sup>50,51</sup> to their receptor on the cells' surface RTK. Once a ligand is attached to the cell surface membrane it will activate and phosphorylate the tyrosine residues, which in turn start a cascade activity events inside the cell, where signals is passed from one protein to another. These signals are initiated by the activation of the small GTPase protein RAS<sup>52</sup>. The RAS-GTPase complex binds to the RAS binding domain (RBD) and to the cysteine-rich domain (CRD)<sup>34</sup> of the BRAF protein resulting in its recruitment to the cell membrane, which start a signal transduction in the plasma, starting with BRAF activation followed by activation of its downstream substrate MEK 1/2 and ERK 1/2. Ultimately, the signals end up in the cell's nucleus where DNA is found, which turn on transcription, which eventually result

in gene expression of genes that allow cell to grow and survive (Figure 3). Some examples of gene products turned on by BRAF signalling pathway are listed in Table 1.

Active RAS-GTPase complex then becomes inactive shortly after its activation to avoid undesirable effects via binding to GTPase activation protein (GAP). Thus, BRAF can no longer be recruited and the MAPK pathway is turned off. Additional negative regulatory mechanisms that inhibit the MAPK pathway involve the negative feedback loop incorporating a number of mechanisms including two sets of proteins: the dual-specificity phosphatase (DUSP) enzymes family and the sprouty protein (SPRY), and other regulatory protein family.

#### 1.2.4 Feedback regulation of the MAPK pathway

Homeostatic balance is essential for almost every physiological process in the human body<sup>43</sup>. In non-transformed cells the MAPK pathway is balanced by inhibitory regulators, which provide a negative feedback signal. The MAPK pathway is in part regulated through a classical negative feedback loop, which is controlled by ERK activation of DUSPs<sup>53</sup>, and other molecules such as SPRYs<sup>54</sup>, KSR1<sup>55,56</sup>, and RKIP<sup>57,58</sup>. DUSPs can inhibit ERK directly while SPRYs proteins inhibit MAPK pathway at an upstream level indirectly through inhibiting RAS activation. ERK itself can also directly inactivate the MAPK pathway at several levels by directly inhibiting RTKs, RAS activation, and RAF dimerization. One of these inhibitory mechanisms is through regulation BRAF itself. Activated ERK can phosphorylate BRAF in two sites: Ser750, and Thr753, resulting in its inhibition<sup>59</sup> (Figure 3).

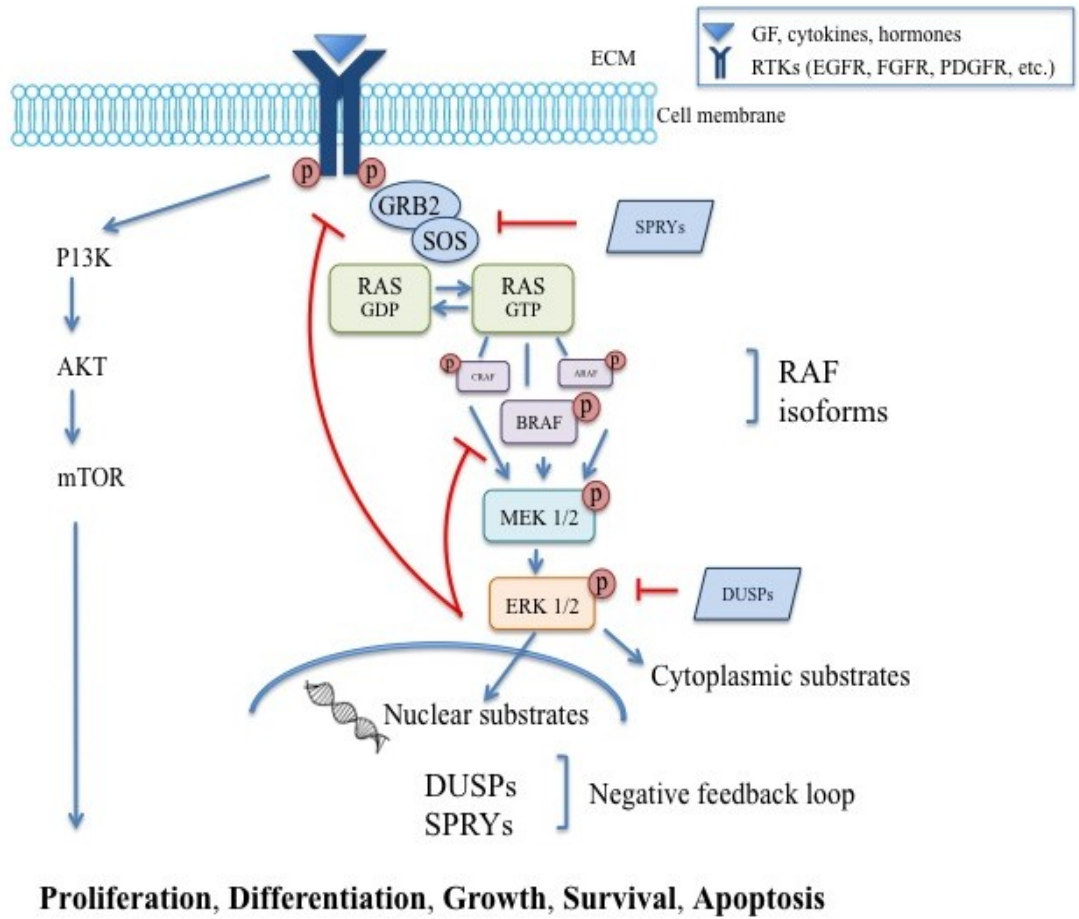


**Figure 3 RAS-RAF-MEK-ERK Signalling Pathway and its most important regulatory component.**

Under normal physiological conditions the ligand binding to RTKs will recruit a cascade of activation, starting with the activation of the small GTPase protein RAS, which in turn binds to and activates BRAF, followed by activation of its downstream MEK1/2 and ERK1/2. In order to prevent undesirable excessive growth signaling, this pathway becomes inactive as ERK will negatively regulate the pathway through direct actions or indirectly through upregulation of negative feedback regulators DUSP and SPRY.

**Table 1 List of genes products turned on by MAPK pathway signaling.**

<b>Category</b>	<b>Protein</b>	<b>Effect of ERK phosphorylation on its functions</b>	<b>Ref.</b>
Kinases and phosphatases	MEK1/2	Either enhances its activity or reduces it depending on the phosphorylation site	60
	CRAF	Inhibits its activity	61,62
	BRAF	Inhibits its activity	63
	RSK	Activation and further signal transduction	64
	S6K	Activation	65,66
	DUSPs	Negative feedback loop- indirectly via dephosphorylating ERK1/2	67-69
	SPRYs	Negative feedback loop- directly inactivating upstream	70,71
Signalling proteins	EGFR	Downregulation of MAPK pathway	72
	Gab2	Reduces its activation	73
	SOS	Negative feedback mechanism via preventing its association with Gab2	74
	IRS1	Impaired its downstream signalling	75
	TSC2	Weakens its ability to pair with TSC1 therefore impairs its ability to inhibit mTOR signalling	76
Cytoskeletal proteins	Crystalline $\alpha$	Anti-apoptotic protection	55,77
Transcription Factors	ELK	Transcription of c-Fos	77,78
	c-Fos	Acts as a sensor for ERKs' signal duration	79
	c-Jun	Transcription of c-Jun	80
	p53	Tumour suppressor protein, play a role in cell cycle	81,82
	c-Myc	Transcription	72
Apoptotic proteins	BIM	Inhibit its pro-apoptotic function	83
	Caspase9	Reduce its pro-apoptotic function	84
	Bad	Inhibit its pro-apoptotic function	85
Other proteins	RB	Cell cycle progression	86
	Vif	Activates HIV-1 replication	87

Note: this table has also been used in publication <sup>43</sup>.

In BRAFV600E mutations, the negative feedback mechanisms can be impaired (Figure 2 on page 8). The mutation itself can also impair the feedback inhibition. For example, negative feedback inhibition through SPRYs proteins is impaired because the SPRY proteins are unable to bind to BRAF due to disruption by mutation<sup>88</sup>. Constitutive activation of mutant BRAF results in hyperactive ERK that in turn can increase the expression of DUSPs and SPRYs proteins<sup>89</sup>. However, this surge in expression of inhibitory regulators no longer acts as efficiently as in healthy cells.

### 1.2.5 Current approaches for detecting BRAFV600E mutations

Until 2011, the presence of BRAF mutations was detected by analysis of tumour DNA for BRAF mutations. Techniques such as direct Sanger sequencing, SNaPshot assay, pyrosequencing, or locked nucleic acid-PCR sequencing have been employed<sup>90-92</sup>. More recently, Capper *et al.* developed a monoclonal mouse antibody specific for recognizing the mutant BRAFV600E protein. This antibody is specific for the BRAFV600E mutation, and does not detect the WT BRAF protein, and can be used in formalin-fixed and paraffin-embedded tissue (FFPE)<sup>93</sup>. This BRAFV600E (VE1) antibody was initially used as an *in-vitro* diagnostic antibody for both immunohistochemistry (IHC) and western blotting. There are numerous advantages for utilizing IHC in diagnosis, such as low-cost, routine methodology, the ability to distinguish the spatial distribution and intensity of the mutation, and the capacity to assess the mutation status in small-sized that favour this technique as a clinical tool. Although, this technique is widely used in clinical practice, in recent study<sup>94</sup> done by Adackapara *et al.* showed that, visualizing mutant BRAFV600E using this staining technique is not

sufficiently sensitive across tumour types. Another drawback for the technique is that there is no recommended scoring system for the interpretation of the immunohistochemical analysis and it is mainly subjected to the pathologist when judging and evaluating the status of the mutant protein<sup>95</sup>. Further, the presence and level of expression of the BRAFV600E mutation does not in and of itself predict how well a tumour will respond to therapy, so additional markers may need to be added for predictive and prognostic value. IHC based methods may not be most ideal for testing multiple targets. So, while the development of this mutant-specific antibody (VE1) improved the detection method for BRAFV600E mutation, there is a need for developing a more sensitive, quantitative, and multiple-target compatible tool. One possible solution to this problem is to use mRNA as a target when evaluating tumour samples as it might help us understanding the correlation between BRAF as well as other gene expression and why there is a variation in patients' response to treatment and what the unique difference between each tumour type amongst tumour type regarding drug response.

### 1.3 CONFERRED RESISTANCE MECHANISMS IN BRAFV600E TUMOURS

The development of drugs to target the hyperactivation of the BRAF-MAPK-ERK signaling pathway has led to substantial advances in patients' overall survival and progression-free survival for melanoma, and the further addition of MEK inhibitors given in combination has improved response rates and survival compared to monotherapy<sup>96</sup>. Unfortunately, the story of BRAF inhibitors is not entirely one of success. While most melanoma cancers initially respond well to therapy, most patients will relapse with tumours that are now resistant<sup>97,98</sup>. For tumours other than melanoma, the combined



targeted therapy is not always effective. For example, while some success with combination BRAF-MEK1/2 inhibition was observed in colorectal cancer<sup>99</sup>, the efficacy of this combination strategy is still far less than is observed for BRAF mutant melanoma. In addition, there are some circumstances where therapy can actually result in increased tumour growth. This is a result of the inhibitors' ability to induce a paradoxical activation of downstream signaling in WT BRAF cells and in cell harbouring RAS mutations<sup>100-103</sup>. Here the main mechanisms for the resistance to therapy will be discussed.

### 1.3.1 Resistance through MAPK pathway reactivation

In the case of BRAFV600E, the reactivation of the MAPK signaling pathway accounts for the majority of acquired resistance mechanisms<sup>43,104</sup>. In a study of 100 primary and 134 follow-up samples from melanoma patients (where 87% were BRAFV600E positive), resistance mechanisms in the recurrent section could be identified in approximately 58% of the cases. These largely represented *BRAF* splice variants (29%) or BRAF gene amplification (8%)<sup>105,106</sup>, however, secondary mutations in other genes in the RAS-RAF-MEK-ERK pathway, such as NRAS<sup>107</sup>, and MEK<sup>108,109</sup> can lead to resistance to therapy. These mechanisms involve BRAF-independent activation of the MAPK pathway.

Secondary mutations within the *BRAF* gene have only rarely been linked to the resistance to BRAF inhibitors<sup>110-112</sup>. One exception to this is the identification of an alternative splice form of the BRAFV600E which lacks the dimerization domain has been observed as a mechanism of resistance<sup>113</sup>. Resistance to BRAF inhibitors can be a result

of BRAFV600E amplification <sup>110</sup>. Whole-exome sequencing of 20 melanoma patients before and after treatment with BRAF inhibitors identified four patients with disease progression had BRAFV600E copy-number gain relative to baseline tumours from the same patient. Quantitative PCR confirmed an increase in *BRAFV600E* expression in these patients, and a cell culture model was used to demonstrate that the copy-number gain of BRAFV600E did indeed induce resistance to BRAF inhibitors while sensitivity was restored by its knockdown <sup>110</sup>.

Acquired mutations in NRAS have been associated with acquired resistance to BRAF inhibitors. Comparing melanoma tumours collected before BRAF inhibitor therapy, to resistant tumours in the same patient after therapy identified acquired NRAS mutations in many of these tumours, including in tumours that continue to harbor the BRAF mutations <sup>114</sup>. The KRAS mutation G12D has been identified in many tumour types, including colorectal cancers. The acquisition of this activating mutation following BRAF inhibitor exposure has been linked to the development of resistance in BRAFV600E mutant parathyroid cancer cell line <sup>115</sup>. Similarly resistance in a colorectal cell line has been linked to the appearance KRAS G12D and G13D mutations <sup>116</sup>, suggesting activating mutations in this RAS pathway may contribute to intrinsic and acquired resistance. Post treatment acquisition of MEK1 and MEK2 mutations have also been associated with acquired resistance <sup>105,116</sup>.

Besides secondary mutations to elements of the MAPK pathway, changes in gene expression level for elements of the MAPK pathway have been linked to resistance. By screening the effect of overexpressing 597 kinases, MAP3K8 (COT) kinase and C-RAF

emerged as among the genes that could confer resistance to BRAF inhibitor therapy. BRAFV600E positive cancer cell lines that express higher levels of MAP3K8 tended to be less sensitive to BRAF inhibitor drugs, MAP3K8 expression increased in the tumours of patients treated with BRAF inhibitors, and was even further elevated in drug resistance relapse tumour samples<sup>117</sup>. Similarly, Montagut *et al.* found that elevated CRAF expression was observed in cells resistant to the RAF inhibitor AZ628 compared their sensitive parental cell, and that elevated CRAF can activate the MAPK pathway independent of BRAF activity<sup>118</sup>.

Both MAP3K8 and CRAF elevations can confer resistance either as primary or acquired resistance mechanisms. One approach that has been employed in an attempt to overcome resistance resulting from elevated expression was the use of agents that bind to and inhibit heat shock protein 90 (HSP90)<sup>118</sup>. HSP90 is required for the conformational stability of mutant BRAFV600E and RAF related family members<sup>119-121</sup>, making blockade of HSP90 a potential strategy for overcoming resistance<sup>122,123</sup>. HSP90 inhibitor therapy has been included in some cancer treatment combinations<sup>124</sup>, and has been tried in clinical phase II trials for the treatment melanoma, however, the studies either showed little effect<sup>125</sup> or were inconclusive<sup>126</sup>. Further research into this approach is required.

### 1.3.2 Resistance involving insensitivity to MAPK regulators

Negative feedback regulators of the MAPK pathway including DUSPs and SPRYs have been linked to the development of acquired resistance to BRAF inhibitors<sup>43</sup>. Ordinarily, a balance emerges between the activation of the RAS-RAF-MEK-ERK

pathway, and negative feedback imposed by ERK-induced expression of DUSPs and SPRYs. Activated phosphor-ERK directly inhibits the upstream pathway, dampening the signal, and elevation in DUSPs leads to dephosphorylation of ERK, further dampening the signal cascade. Pratilas and colleagues revealed that despite elevated feedback inhibition signals, BRAFV600E is insensitive to negative feedback regulation by DUSPs<sup>89,127</sup>. The cell falls into a new, distorted balance with elevated ERK and elevated DUSP, but the negative feedback components are overwhelmed by persistent signaling. Similarly, SPRY2 and SPRY4 can provide negative feedback to wildtype BRAF, but are unable to inhibit the BRAFV600E mutation<sup>88</sup>. It has been proposed that resistance to treatment may be related to further disruption in the balance between the negative feedback mechanisms and the activation<sup>128</sup>.

### 1.3.3 Other mechanisms of resistance

The cross-talk that exists between signaling pathways activated by receptor tyrosin kinases (RTK)s, such the RAS-RAF-MEK-ERK and the PI3K-PTEN-AKT pathway, was first identified in 1994 by Chung and colleagues<sup>43,129</sup>. Overexpression of RTKs could be expected to elevate the signaling in both of these arms. Elevations in EGFR<sup>130</sup>, PDGFR<sup>107,131</sup> and IGF1-R<sup>132</sup> have been observed in resistance. Release of hepatocyte growth factor (HGF) from the surrounding stromal cells to activate MET, the HGF RTK on the tumour cell has also been described as a resistance mechanism<sup>133,134</sup>.

The integration between these two signaling pathways and the fact that both are sharing the same upstream RTKs raise the possibility of involvement of activated PI3K

pathway in resistant tumour cells. Shi *et al.*<sup>135</sup> have identified BRAF inhibitor resistant melanomas with gain-of-function mutations in AKT. This AKT-mediated resistance mechanism results in P13K up-regulation. Their data suggested that, in spite of MAPK pathway inhibition through BRAF inhibitors, the BRAF mutated cells evade treatment by adapting to the use of PI3K signaling to survive. In addition to *AKT* mutations, *PTEN* mutations are found in 15.2% in metastatic melanoma leading to a similar resistance mechanism<sup>136</sup>. *PTEN* loss of function promotes AKT activation, which in turn can lead to dysregulation of the pro-apoptotic Bcl-2 like proteins. The resulting impairment of the apoptotic pathway was associated with resistance to BRAF inhibitors, vemurafenib and dabrafenib<sup>137-139</sup>. Figure 2 on page 8 illustrates how aberrant signaling resulting from the V600E mutation in *BRAF* gene led to uncontrolled growth and summarizes hypothesized mechanisms of resistance.

More recently, other mechanisms have been proposed. Treatment with inhibitors that inhibit MEK and ERK phosphorylation prevent the phosphorylation and stabilization of the transcriptional regulator MYC, leading to rapid degradation<sup>140</sup>. MYC promotes modifications to histones that influence transcription, and the loss of MYC following MEK inhibition has been found to cause epigenetic modifications to gene expression through histones and altered binding of regulatory molecules to enhancer regions<sup>141</sup>. While this was not specifically tested in the context of BRAFV600E resistance, this mechanism warrants consideration.

Another emerging mechanism of resistance to BRAF inhibition is through altered expression of microRNAs<sup>43</sup>. MicroRNAs are small non-protein coding RNAs that bind

to the transcripts of other genes and promote their degradation. Recently, the loss of microRNA miR-579-3P has been identified as a potential mechanism of both primary and acquired resistance to BRAF and MEK inhibitor drugs<sup>142</sup>. The mechanism by which loss of miR-579-3p leads to resistance is not fully understood, but Fattore *et al.* observed that this loss results in increases for both BRAF and the MDM2 pathway. MDM2 is an important negative regulator of the tumour suppressor p53, so elevation in MDM2 would reduce this protective tumour suppression pathway.

## 1.4 CHALLENGES ENCOUNTERED BY COLORECTAL CANCER (CRC)

### PATIENTS WITH BRAFV600E MUTATION

The impact of the BRAFV600E mutation in colorectal cancer (CRC) differs from that in melanoma<sup>43</sup>. The BRAFV600E mutation is found in 10% of colorectal cancer (CRC) cases<sup>25,43</sup>. Those patients progress rapidly and tend to not respond well to therapy. This subgroup of patients is distinct from other forms of CRC, and has its own molecular and genetic profile. However, the response rate to Vemurafenib was only 5% in CRCs exhibiting BRAFV600E mutation compared to 60 to 80% of melanoma patients harbouring the same mutation<sup>110,136,143</sup>.

#### 1.4.1 Evidence of specific resistance mechanisms in BRAFV600E mutated CRC

The small subset of BRAFV600E mutant CRC display different tumour biology and different clinical behaviours compared to *RAS* mutant CRC<sup>144</sup>. In a study by Kopetz *et al.*

<sup>145</sup>, BRAF mutated CRC patients had limited benefit from any of the “available standard-of-care therapies”. These findings have raised the attention of many groups to understand why BRAF inhibitor treatment showed little or no response <sup>143,146,147</sup>. In 2012, two independent groups recognized the involvement of EGFR in CRC resistance to BRAF inhibitors. Prahallad *et al.* proposed that inhibition of mutant BRAF led to a powerful feedback activation of EGFR triggering a secondary reactivation of the MAPK pathway <sup>148</sup>. This feedback activation of EGFR increased the activation not only MAPK pathway but also the parallel pathway PI3K generating growth renewal. The group studied the involvement of cell division cycle 25C (CDC25C), which is a downstream substrate of ERK that when activated it can bind to and deactivate EGFR <sup>149</sup>. Treatment with BRAF inhibitors resulted in decreased activation of MEK1/2 and ERK1/2, consequently a failure of ERK to phosphorylate CDC25C. This failure to activate the negative feedback signal of CDC25C leads to a prolonged EGFR activation and greater activation of the P13K pathway <sup>148</sup>. Corcoran *et al.* proposed a slightly different mechanism for the prolonged EGFR activation <sup>110</sup>. This group postulated that negative feedback regulators such as SPRY proteins participated in EGFR reactivation. SPRY proteins comprise a key regulatory function for the MAPK pathway and transcribe in an ERK-dependent manner <sup>150</sup>. SPRYs negatively regulate upstream MAPK at the RTKs and RAS level. BRAF targeted therapy led to decrease level of SPRYs enabling EGFR to rebound and reactivate MAPK pathway <sup>110</sup>. Both groups showed that the efficacy of BRAF inhibitor is improved greatly *in-vitro* when combined with an EGFR inhibitor and that this combined treatment leads to tumour regression *in-vivo*. They further examined EGFR levels in clinical biopsies from patients with the BRAFV600E mutation and compared across CRC,

melanoma and PTC. The majority of BRAF mutated CRC showed high level of active EGFR compared to other tumour types <sup>110,148</sup>. Moreover, single agent treatment with either inhibitor (BRAF or EGFR) produced little to poor response indicating a combination strategy might be more appropriate for patients with BRAF mutated CRC.

Several studies that have been exploring new therapeutic approaches aimed to target resistance-conferring mutations are providing promising treatment options for patients harbouring the BRAFV600E mutation. For example, Mao *et al.* showed that BRAF inhibitor combined with PI3K inhibitors hindered the growth of BRAF mutated CRC cell lines <sup>151</sup>. In addition, epigenetic factors may be playing a role in drug resistance in colorectal cancer. Hypermethylation of CpG islands is observed in colorectal tumours with the BRAFV600E mutation, and results in gene silencing of multiple target genes. Mao *et al.* found that the efficacy of BRAF inhibitor improves after treatment with demethylating agents <sup>151</sup>.

Triple targeted inhibitor combinations are also being examined, combining BRAF and EGFR inhibitors with additional targets, including P13K and MEK1/2 inhibitors <sup>145,152,153</sup>. A more robust response rate was observed compared to monotherapy or BRAF-MEK combination therapy <sup>143,154</sup>. These advances illustrate the importance of understanding the underlying mechanisms of resistance in specific tumour types. New potential therapies may emerge for BRAFV600E positive CRC tumours that failed to respond to therapies designed for melanoma tumours.



## 1.5 EMERGING INSIGHTS INTO THE ROLE OF REACTIVE OXYGEN SPECIES (ROS) IN BRAF MUTATED TUMOURS

The production of ROS has a broad range of effects on cellular function. On the one side, ROS generated by this system can act as cellular signaling molecules, interacting specifically and reversibly with low pKa cysteine residues on many proteins to regulate a wide range of cells signaling processes<sup>155-157</sup>. On the other side, irreversible or non-specific reactions with cellular molecules such as proteins, lipids and DNA can generate oxidative lesions causing genomic instability and oxidative stress and eventually progress into numerous chronic diseases such as inflammation, hypertension and tumorigenesis<sup>158-161</sup>. Increased ROS production can alter cellular signalling pathways, which can either promote cell growth, or can lead to toxicity<sup>162,163</sup>.

One of the sources of increased ROS in cancer cells is the mitochondrial electron transfer chain. Cancer cells are unlike healthy cells in terms of their energy demand. Due to their rapid growth and division, cancer cells require more nutrients to sustain rapid proliferation. The shift in metabolism in transformed cells was first identified in early 1920 by the German physiologist Otto Warburg and since then it also known as “the Warburg effect”<sup>164</sup>. Altered metabolism such as excessive uptake of nutrients including glucose and glutamine and the dependency on glycolysis to metabolize them in an insufficient approach to produce energy<sup>165-170</sup>. The new demands disturb the normal balance of ROS production released as a byproduct of the mitochondria electron transfer chain and breakdown of those ROS products by cellular antioxidant systems such as

glutathione peroxidases (GPx), catalases (CAT), and superoxide dismutase (SODs)<sup>76,171</sup> (for review<sup>172,173</sup>).

Another important source is superoxide generated by the membrane-bound enzyme complex referred to as the NOX family of NADPH oxidases (nicotinamide adenine dinucleotide phosphate-oxidase) which function as ROS-generating NADPH oxidases (see<sup>174,175</sup> for review). This family consists of seven members: NOX1-5, and DUOX1, 2; and they generate ROS by transferring electron to an oxygen molecule. It has been observed that tumour cells generate high level of ROS<sup>176</sup> and cells expressing oncogene in particular have elevated level of ROS as detected in RAS transformed cells<sup>177,178</sup>. Such changes in redox balance have been evident in melanoma, as they tend to be sensitive to redox status, and manipulating this greatly affects their transformation and progression<sup>179-181</sup>.

Given the wide range involvement of ROS in the cell, homeostatic balance is essential in maintaining a healthy level of ROS<sup>182,183</sup>. In order to limit ROS accumulation, cells are compromised with multiple systems including scavenging enzyme and or internal and external antioxidant agents that aid in detoxifying and scavenging ROS molecules. Enzymatic scavenging of ROS involve SODs, CAT and GPx<sup>184</sup>. A series of enzymatic reactions are involved in detoxifying the superoxide anion molecule, which is most often the form of ROS initially generated, and converting it into hydrogen peroxide (H<sub>2</sub>O<sub>2</sub>), which in turn is decomposed into water and oxygen molecule<sup>185,186</sup>. Compared to other ROS molecules, H<sub>2</sub>O<sub>2</sub> has a long lifetime and able to cross cell

membranes with potential oxidative damage to other sites that are far from its original formation site <sup>187</sup>.

In tumour cells the V600E mutation in *BRAF* can initiate hyper-proliferative cells while in cancer-prone cells it can suppress cell proliferation as seen in nevi; a benign skin lesion of melanocytes <sup>188-190</sup>. This effect is known as oncogene-induced senescence (OIC) <sup>191,192</sup>. There are many mechanisms proposed to explain OIC including activation of the DNA damage response, ROS, activation of the negative feedback loop, and stress signalling leading to aberrant oncogene signaling reviewed by Cichowski *et al.* in <sup>193</sup>. One of these proposed mechanisms for the induction of senescence in BRAF V600E melanocytes is an imbalance between ROS generation and ROS detoxification that favours oxidative stress.

In addition, ROS can promote cancer in many ways: ROS can act as cellular signalling molecules to promote cell proliferation, can act as an DNA damage inducing agents that introduce cancer promoting mutations, can signal pro-angiogenesis pathways that promote tumour vascularization, and can also promote cellular invasion <sup>194</sup>. ROS and NOX-derived ROS have been linked in the progression of many cancers including melanomas <sup>195-198</sup> and colorectal cancer <sup>196,199-201</sup>. In addition to tumour progression, Morrison *et al.* <sup>202</sup> have revealed recently ROS involvement in metastasis. In their study, Morrison and colleagues studied the effect of oxidative stress on metastasis by generating NSG mice models that transplanted with stage III melanomas that have different metastasis efficiencies and obtained from different patients. Secondary tumour showed elevated level of the enzymatic activity of the folate metabolism pathway compared to

original site<sup>202</sup>. Likewise, reversible increase in the generation of NADPH enzyme was observed suggesting metabolic adaptation that aids metastasis cells to elude toxic level of ROS.

In recent years, the identification of altered metabolism as a trait of cancer has attracted much attention from research team to target metabolic pathways and or NOX enzymes as an additional approach when treating cancer<sup>203-205</sup>. Much research on the biological and biochemical aspects that differentiate cancer cells relative to normal cells have been done. For instance, the usage of glycolytic inhibitors<sup>206</sup>, ketogenic diet<sup>207</sup>, ROS and ROS-generating NOX inhibitors<sup>208-211</sup> have been widely investigated.

BRAFV600E tumours found to have an elevated level of mitochondrial biogenesis proteins. Mitochondrial biogenesis markers such as microphthalmia-associated transcription factor (MITF), peroxisome proliferator-activated receptor gamma coactivator 1- $\alpha$  (PPARGC1 $\alpha$ ), Transcription Factor A, Mitochondrial (TFAM) and TNF Receptor Associated Protein 1 (TRAP1) were elevated, especially in BRAF-inhibitor resistant tumours in cell lines and in clinical biopsies from patients with progressive tumours<sup>212,213</sup>. Surprisingly, BRAF-mutant tumour cell lines with lower mitochondrial biogenesis marker expression were more resistant to MAPK inhibitors, however, patients with lower level of mitochondrial biogenesis markers showed a better overall survival rate<sup>213</sup>. Herlyn *et al.* investigated whether inducing mitochondrial biogenesis could attenuate drug resistance and improve the efficacy of combination BRAF-MEK1/2 inhibitor treatment. Gamitrinib, a mitochondrial-targeted small- molecule HSP90 inhibitor induced mitochondrial biogenesis genes, and when used in combination with

BRAF inhibitor and MEK inhibitor, diminished the number of viable cells including those with acquired resistance<sup>213</sup>. Thus targeting impaired mitochondrial metabolism in BRAFV600E melanomas seems to enhance a combination approach and most importantly to bypass resistance to therapy. These findings call attention toward potential anti-cancer therapy encompassing ROS, NADPH, and metabolism related pathways.

## 1.6 HYPOTHESIS AND OBJECTIVES

The widespread of activating BRAFV600E mutation in different type of cancer, including melanoma<sup>214</sup> “the most lethal type of skin cancer”, give an additional credit to this mutation as a diagnostic and prognostic biomarker in human cancer<sup>46,214-216</sup>. Patients with activating BRAFV600E display poor prognosis comparing to those with a wild type WTBRF, in particular, in melanoma, colorectal cancer, and thyroid cancer<sup>217-221</sup>. Previous studies (in melanoma) have shown that the expression of either BRAFV600E or WTBRF strongly influence patients’ clinical parameters, as demonstrated in Di Nicolantonio *et al.* (2008)<sup>222</sup>. BRAF expression not only predicts the correlation to the clinical outcomes of patients, but also how it correlates with resistance to BRAFV600E inhibitory drug. In melanoma, high expression of the BRAFV600E associates with drug resistance to BRAFV600E targeted therapy<sup>112</sup>. Correspondingly, using BRAF expression as a direct assessment tool in consideration it could be a beneficial predictive biomarker especially in the case of patients who are positive for the activating BRAFV600E mutation<sup>223</sup>.

Despite advancements that have been made in the development of small molecules that specifically target this mutation, not all-patient response well to these targeted therapy. In melanoma patients however, where BRAFV600E shows higher in frequency, an 80% response rate was observed in metastatic melanoma patients treated with PLX4032 (a BRAF inhibitor) <sup>224</sup>. Most of those patients who were initially responding to treatment, their tumour eventually relapses and develop resistance within six months period for those treated with a single agent <sup>225,226</sup>. Resistance can result from the re-activation of the MAPK pathway, and combination therapy using both BRAF and MEK inhibitors delayed resistance to nine months in average <sup>227</sup>. In addition, about 10% of colorectal cancers have the BRAFV600E mutation, however, BRAF inhibitors are usually ineffective in these with only; 5% of BRAFV600E positive cases responding to a BRAF inhibitor treatment <sup>143</sup>.

Based on the fact that not every BRAFV600E positive tumour responds to BRAF inhibitor therapy, we are interested in identifying biomarkers for responsiveness to therapy in hope to understand the process involving in the development of resistance to currently available therapies. Therefore, this thesis work has explored two main hypotheses:

Hypothesis 1. An RNA based detection method will provide a quantitative method that can be easily expanded to other genes for characterizing BRAFV600E expression in tumour tissue.

Hypothesis 2. Gene expression and functional differences between sensitive melanoma cells, melanoma cells with acquired resistance, and colorectal cells with inherent resistance will reflect underlying resistance mechanisms and will identify potential targets to overcome resistance.

Therefore, the objectives of the present study are:

Hypothesis 1 (project 1):

- (i) To evaluate the feasibility of obtaining mRNA from formalin-fixed and paraffin-embedded tissue (FFPE) tumour samples for assessing the level of BRAF and BRAFV600E expression;
- (ii) To assess the mRNA expression level of both mutant and WT BRAF in melanoma, colorectal and thyroid FFPE tumour samples;
- (iii) To compare between results from IHC and results obtained by RT-qPCR method;
- (iv) To assess the feasibility of digital droplet PCR as detection method over RT-qPCR;

Hypothesis 2 (project 2):

- (i) To compare the expression level in melanoma cells, resistance melanoma and colorectal cells of genes involved in the MAPK pathway regulation that have been proposed to play a role in the development of resistance to BRAF

inhibitors in melanoma including: total BRAF, EGFR, DUSP4, DUSP6, SPRY1, SPRY2, SPRY4, NOX1, and NOX4;

- (ii) To study what, if any role reactive oxygen species plays in resistance/sensitivity to BRAF inhibitors by comparing melanoma cells, resistant melanoma and colorectal cells;

To answer these questions, a TaqMan based allele-specific RT-qPCR, SYBR™ Green RT-qPCR, and quantitative digital droplet PCR were used to test hypothesis 1. A cell culture based model was used to test cell proliferation (Alamar Blue assay), ROS generation (Amplex Red Assay) and gene expression (SYBR™ Green RT-qPCR) were used to test hypothesis 2.



## **CHAPTER 2 MATERIALS AND METHODS**

### **2.1 CLINICAL SPECIMENS AND CELL CULTURES**

#### **2.1.1 Clinical specimens (Project 1)**

Archival FFPE tissues from 17 patients with melanoma (n=6), papillary thyroid carcinoma (PTC) (n=6), and colorectal cancer (CRC) (n=5) were provided by Dr. Weei-Yuarn Huang from Capital Health, Halifax, Canada. FFPE Tumour specimens were stored in conditions that met the clinical laboratory guideline and aged from a month old up to four years old. In-house naming system was created for easy handling and processing (Table 2, Table 3, and Table 4). IHC staining against mutant BRAFV600E protein using a monoclonal antibody VE1 was performed by Dr. Huang in order to determine mutation status by scoring each in accordance to the proportion of stained tumour cells and scores were ranging from weak (1) to strong (4) (see Table 5, Table 6 and Table 7). Due to limited access to patients' information (Research Ethics Board (REB) protocol), clinicopathological parameters other than BRAFV600E status and tumour grading are unknown at this stage of the project. Further detailed information regarding patients treatment plan, and responsiveness to treatment are undetermined. This research followed the approved protocol and strict guidelines from the Research Ethics Board (REB). Clinicopathological parameters other than BRAFV600E status and tumour grading remain confidential.

**Table 2 Melanoma FFPE samples.**

Cancer	Sample ID	Pooled Samples			Specimen obtained on	How old is the slides	Date Received (at the lab)	RNA		
		S1	S2	S3				Extraction Date	Concentration (ng/µl)	Concentration post DNA digestion (ng/µl)
Melanoma	WH-A_001	A1-1	A1-2	A1-3	2013	Month old	Oct-13	13-12-2013	365.5	145.6
	WH-A_002	A2-1	A2-2	A2-3		Less than year old	17-06-2014	18-06-2014	134	78.6
	WH-A_003	A2-4	A2-5	A2-6		2 year old	Oct-13	13-12-2013	172.1	104.8
	WH-B_001	B1-1	B1-2	B1-3	2011	3 year old	17-06-2014	18-06-2014	450	297.4
	WH-B_002	B2-1	B2-2	B2-3		Year old	Oct-14	13-12-2013	245.2	47.8
	WH-B_003	B2-4	B2-5	B2-6		2 year old	17-06-2014	18-06-2014	85.9	43.4
	WH-C_001	C1-1	C1-2	C1-3	2012	Year old	Oct-13	13-12-2013	56.5	16.9
	WH-C_002	C2-1	C2-2	C2-3		2 year old	17-06-2014	18-06-2014	34.9	27.9
	WH-C_003	C2-4	C2-5	C2-6		Year old	Oct-13	13-12-2013	40.2	53.9
	WH-D_001	D1-1	D1-2	D1-3	2012	2 year old	26-11-2014	9-12-2014	96.7	502.1
	WH-D_002	D2-1	D2-2	D2-3		2 year old	Oct-13	13-12-2013	997.6	502.1
	WH-D_003	D2-4	D2-5	D2-6		3 year old	17-06-2014	18-06-2014	596.3	247.7
	WH-D_101	D2-7	D2-8	D2-9	2011	Year old	Oct-14	13-12-2013	351.1	124.3
	WH-E_001	E1-1	E1-2	E1-3		2 year old	Oct-13	13-12-2013	997.6	502.1
	WH-E_002	E2-1	E2-2	E2-3		3 year old	17-06-2014	18-06-2014	549.2	264.1
	WH-E_003	E2-4	E2-5	E2-6	2012	Year old	Oct-14	13-12-2013	351.1	124.3
	WH-F_001	F1-1	F1-2	F1-3		2 year old	Oct-14	13-12-2013	351.1	124.3
	WH-F_002	F2-1	F2-2	F2-3		2 year old	17-06-2014	18-06-2014	339.4	160.4
WH-F_003	F2-4	F2-5	F2-6					331	180	

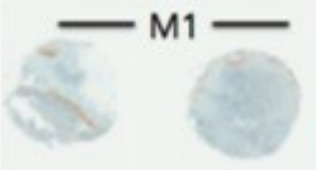
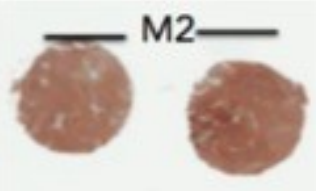
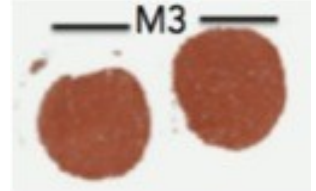
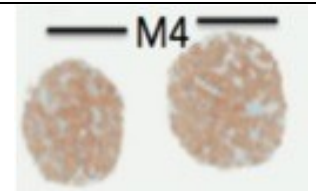
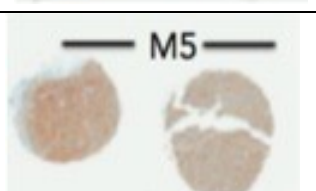
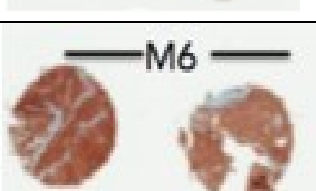
**Table 3 Papillary thyroid cancer FFPE samples.**

Cancer	Sample ID	Pooled Samples			Specimen obtained on	How old is the slides	Date Received (at the lab)	RNA		
		S1	S2	S3				Extraction Date	Concentration (ng/ $\mu$ l)	Concentration post DNA digestion (ng/ $\mu$ l)
Papillary thyroid carcinoma	WH-G_001	G1-1	G1-2	G1-3	2011	3 year old	17-06-2014	19-06-2014	208.5	137.5
	WH-G_002	G1-4	G1-5	G1-6					201.9	113.6
	WH-G_003	G1-7	G1-8	G1-9					289.3	156.4
	WH-H_001	H1-1	H1-2	H1-3	2011	3 year old	17-06-2014	19-06-2014	163.7	85.3
	WH-H_002	H1-4	H1-5	H1-6					186.2	103.9
	WH-H_003	H1-7	H1-8	H1-9					326.3	163.7
	WH-I_001	I1-1	I1-2	I1-3	2010	4 year old	17-06-2014	19-06-2014	516	251.2
	WH-I_002	I1-4	I1-5	I1-6					684.8	320.5
	WH-I_003	I1-7	I1-8	I1-9					656.9	295.1
	WH-J_001	J1-1	J1-2	J1-3	2011	3 year old	17-06-2014	19-06-2014	546.3	327.8
	WH-J_002	J1-4	J1-5	J1-6					395.4	241.4
	WH-J_003	J1-7	J1-8	J1-9					512	325
	WH-K_001	K1-1	K1-2	K1-3	2012	2 year old	17-06-2014	19-06-2014	203.2	120.6
	WH-K_002	K1-4	K1-5	K1-6					237.8	154.4
	WH-K_003	K1-7	K1-8	K1-9					323.7	195.3
	WH-L_001	L1-1	L1-2	L1-3	2011	3 year old	17-06-2014	19-06-2014	32.2	24.6
	WH-L_002	L1-4	L1-5	L1-6					34.8	22.9
	WH-L_003	L1-7	L1-8	L1-9					114.2	56

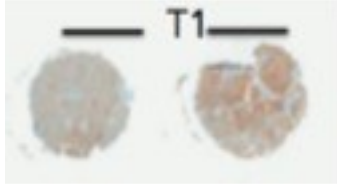
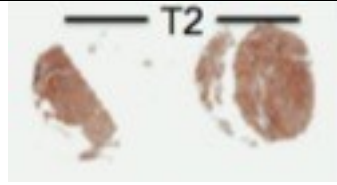
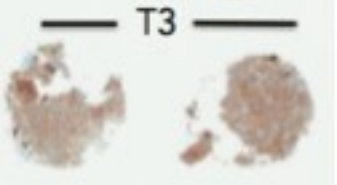
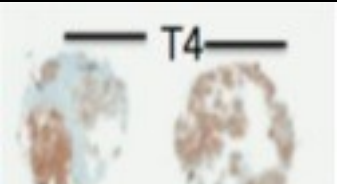
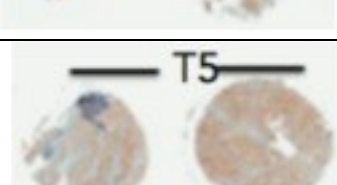
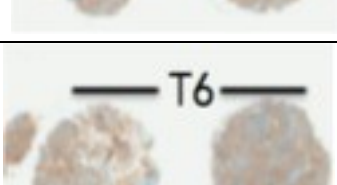
**Table 4 Colorectal cancer FFPE samples.**

Cancer	Sample ID	Pooled Samples			Specimen obtained on	How old is the slides	Date Received (at the lab)	RNA		
		S1	S2	S3				Extraction Date	Concentration (ng/µl)	Concentration post DNA digestion (ng/µl)
Colon Cancer	WH-M_001	M1-1	M1-2	M1-3	2011	3 year old	16-09-2014	30-10-2014	617.6	275.5
	WH-M_002	M1-5	M1-6	M1-7					732	309.1
	WH-M_003	M1-9	M1-10	M1-11					775.3	327.7
	WH-N_001	N1-1	N1-2	N1-3	2012	2 year old	16-09-2014	30-10-2014	315.7	233.5
	WH-N_002	N1-5	N1-6	N1-7					377.4	247.7
	WH-N_003	N1-9	N1-10	N1-11					434.4	301
	WH-O_001	O1-1	O1-2	O1-3	2011	3 year old	16-09-2014	30-10-2014	464.1	346.1
	WH-O_002	O1-5	O1-6	O1-7					386.8	290.7
	WH-O_003	O1-9	O1-10	O1-11					527.2	370.6
	WH-P_001	P1-1	P1-2	P1-3	2013	year old	16-09-2014	30-10-2014	791.8	509.1
	WH-P_002	P1-5	P1-6	P1-7					386.4	276
	WH-P_003	P1-9	P1-10	P1-11					410.3	289.8
	WH-Q_001	Q1-1	Q1-2	Q1-3	2012	2 year old	16-09-2014	30-10-2014	955.1	413
	WH-Q_002	Q1-5	Q1-6	Q1-7					1122.6	489.2
	WH-Q_003	Q1-9	Q1-10	Q1-11					902.5	372.3

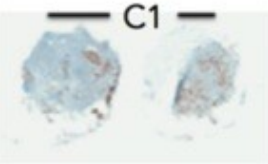
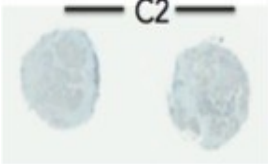
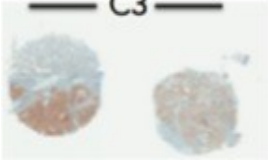
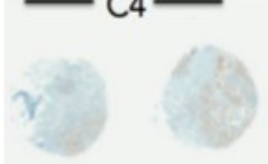
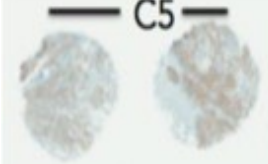
**Table 5 Assessment of V600E BRAF mutant expression in melanoma samples by IHC with monoclonal antibody mutation specific (VE1). IHC staining was assessed by Dr. Huang.**

Cancer	Sample ID	V600E mutant protein / VE1	IHC
Melanoma	A		3
	B		4
	C		3
	D		3
	E		3
	F		4

**Table 6 Assessment of V600E BRAF mutant expression in PTC samples by IHC with monoclonal antibody mutation specific (VE1). IHC staining was assessed by Dr. Huang.**

Cancer	Sample ID	V600E mutant protein / VE1	IHC
Papillary thyroid carcinoma	G		2
	H		4
	I		2
	J		3
	K		3
	L		2

**Table 7 Assessment of V600E BRAF mutant expression in CRC samples by IHC with monoclonal antibody mutation specific (VE1). IHC staining was assessed by Dr. Huang.**

Cancer	Sample ID	V600E mutant protein / VE1	IHC
Colon Cancer	M		3
	N		1
	O		2
	P		0
	Q		1

### 2.1.2 Cell cultures (Project 2)

Two human malignant melanoma cell lines A375 (ATCC<sup>®</sup> CRL-1619<sup>™</sup>), and SK-MEL-28 (ATCC<sup>®</sup> HTB-72<sup>™</sup>) and two human colon cancer cell lines RKO (ATCC<sup>®</sup> CRL-2577<sup>™</sup>), and COLO205 (ATCC<sup>®</sup> CCL-222<sup>™</sup>) were purchased from Cedarlane laboratories (Burlington, ON). All cells were carrying the BRAFV600E mutation. Other characteristic and mutational changes are listed in Table 8. As a result of unexpected difficulties dealing with and getting inconsistent and unsuccessful outcome from SK-MEL-28 (melanoma) and COLO205 (colon cancer), both cell lines were eliminated. Figure 4 displays selection criteria followed when choosing cell lines.

Upon arrival, cells were handled following the manufacture's direction and carried out under strict aseptic condition to reduce potential contaminations. A375 human melanoma cell line (ATCC<sup>®</sup> CRL-1619<sup>™</sup>) was maintained in Dulbecco's Modified Eagle's Medium (DMEM; 4 mM L-glutamine, 4500 mg/L glucose, 1 mM sodium pyruvate, and 1500 mg/L sodium bicarbonate; ATCC<sup>®</sup> 30-2002<sup>™</sup>; (Cedarlane laboratories (Burlington, ON)) supplemented with 10% FBS, 100 U/ml penicillin, and 100 U/ml streptomycin. human colorectal carcinoma cell line RKO (ATCC<sup>®</sup> CRL-2577<sup>™</sup>) was maintained in Eagle's Minimum Essential Medium (EMEM; Earle's Balanced Salt Solution, non-essential amino acids, 2 mM L-glutamine, 1 mM sodium pyruvate, and 1500 mg/L sodium bicarbonate; ATCC<sup>®</sup> 30-2003<sup>™</sup>; (Cedarlane laboratories (Burlington, ON)) supplemented with 10% FBS, 100 U/ml penicillin, and 100 U/ml streptomycin. Complete



**Table 8 Cell lines characteristic and mutational changes.**

ATCC® No.	Name	Tissue	Cell Type	Histology	Tumour Source	Mutant Gene	Genes Sequence	Protein Sequence
CRL-2577	RKO	colon	epithelial	Carcinoma	primary	BRAF	c.1799T>A	p.V600E
						NF1	c.1882delT	p.Y628fs*3
						NF1	c.7022delA	p.N234fs*5
						PIK3CA	c.3140A>G	p.H1047R
CCl-222	COLO 205	colon	epithelial	Adenocarcinoma	metastasis, ascites	BRAF	c.1799T>A	p.V600E
						APC	c.4666_4667insA	p.T1556fs*3
						SMAD4	c.1_667del667	p.?
						TP53	c.308_333>TA	p.Y103_L111>L
CRL-1619	A375	skin	epithelial	malignant melanoma	primary	BRAF	c.1799T>A	p.V600E
						CDKN2A	c.181G>T	p.E61*
						CDKN2A	c.205G>T	p.E69*
HTB-72	SK-MEL-28	skin		malignant melanoma	primary	BRAF	c.1799T>A	p.V600E

## Cell Lines Selection Criteria

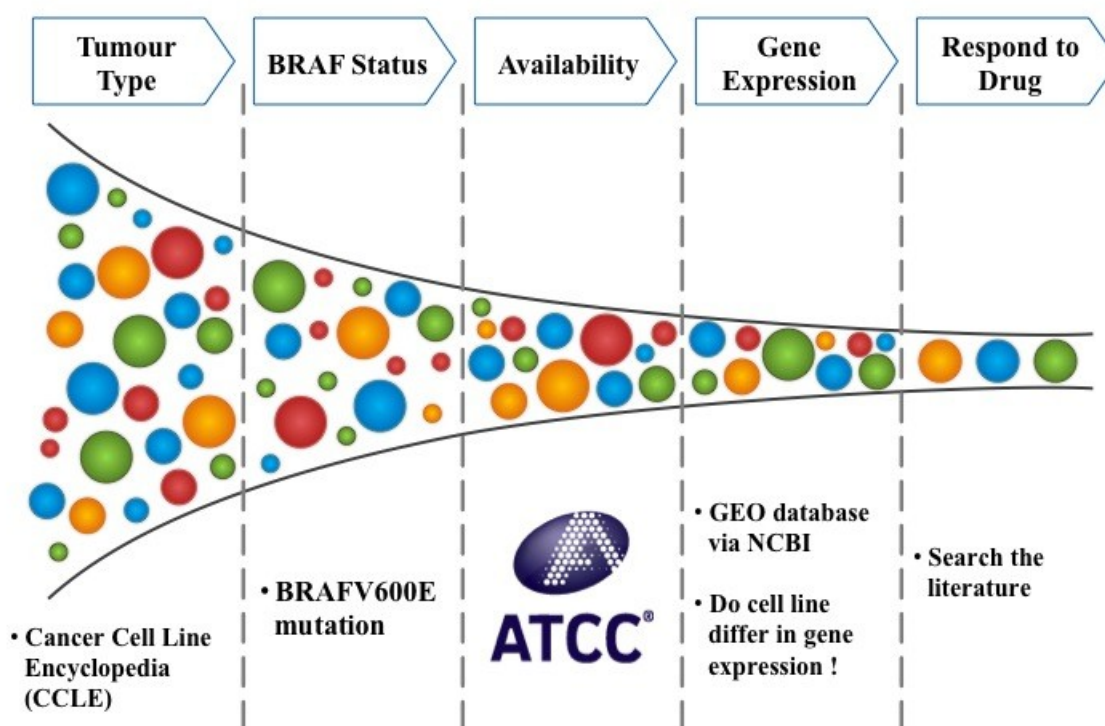


**Figure 4 Processes followed when choosing cell lines.**

The search for cell lines was mostly conducted using online sources that help in identifying possible candidate cell line to establish *in-vitro* model. The search was narrowed down considering these factors: tumour type, BRAF status, availability, gene expression, and finally respond to targeted drug.

growth media was renewed every two to three days and cell were cultured in a humidified atmosphere of 5% CO<sub>2</sub> at 37 °C. For subculture, cell layer was rinsed with PBS before adding 0.5% (w/v) trypsin-EDTA (Sigma Aldrich, Missouri, United States). Since, RKO cells were difficult to detach, they were placed at 37 °C for longer time to facilitate dispersal. Cells ere then either subcultured by dilution or used for experimental purposes.

## 2.2 RNA EXTRACTION

### 2.2.1 FFPE samples

For each case, nine 10- $\mu$ M-thick sections were prepared from FFPE block and placed on a microscope slides. Slides were assessed visually and tumour-contacting areas were circled. Upon arrival, slides were immediately prepared for RNA extraction. RNA was extracted in a manner that ends up in a three different extracted RNA for the same case. Each tube of extracted RNA was collected from three slides. Figure 5 displays samples' allocation.

Before extraction, work area was decontaminated including surface area, Scalpel blade holder, forceps, and tissue storage containers with RNaseZAP in order to terminate any present of RNase and nucleic acid. Each three individual slides (each is 10- $\mu$ M-thick section) were placed into a petri dish and then manual macrodissection was performed using a new, sterile, and disposable scalpel blade. Dissected tissue pieces were immediately placed in a sterile, RNase-free microcentrifuge tube. After each dissection all equipment and work surface were sprayed with RNaseZAP and decontaminated to avoid cross-sample contamination as well as exogenous contamination. Once all samples

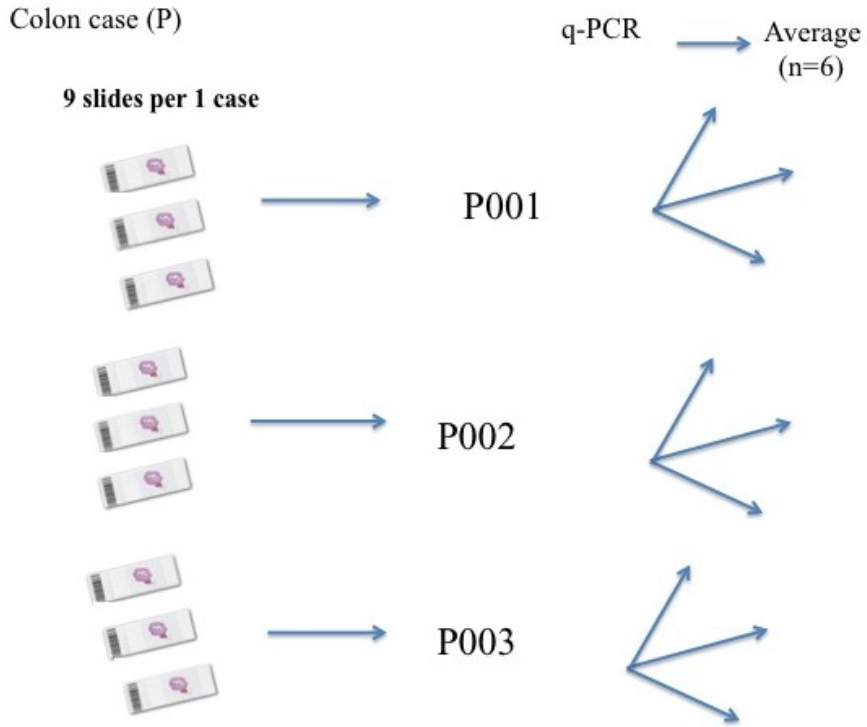


**Figure 5 RNA extraction of FFPE tissue specimens from each patient.**

Nine sets of 10- $\mu$ M-thick FFPE tissue sections were provided on a microscope glass slides. Three pieces of FFPE were then subjected to total RNA extraction using the PureLink™ FFPE Total RNA Isolation Kit (invitrogen, Carlsbad, USA). The end result of extraction is three separate RNA tubes per patient indicated as 001,002, and 003. cDNA is then subjected to experiment assay and run in triplicate (unless otherwise specified) and data are presented as average of six. Colon case (patient ID: P) used as example.

were prepared, total RNA extraction was done using the PureLink™ FFPE Total RNA Isolation Kit (Invitrogen, Carlsbad, USA) following manufacturer's instruction. In short, the procedure started with a melting step where FFPE pieces were deparaffinised using a melting buffer incubated at 72°C for 10 min. Tissue was then lysed using Proteinase K. Digestion step was performed by incubating samples at 60°C until lysis was complete or up to three hours. Centrifugation step was then performed to separate lysed tissue from melted wax. Purification steps were done by adding Binding Buffer (L3) with the addition of ethanol to help in the binding selectivity of RNA molecules to a silica-based membrane that is present in the Spin Cartridge. Before eluting total RNA in RNase-Free Water, Spin Cartridge was washed three times with Washing Buffer (W5) to remove impurities. The amount of RNase-Free Water used for elution may vary and could impact the total yield of total RNA. 40 to 50 µl seemed to produce a good yield of total RNA. Total RNA was collected in RNase-free microcentrifuge tube. Following RNA extraction, either further purification from genomic DNA or determination of the quantity and quality of the isolated RNA was performed. RNA samples were assessed using the NanoDrop 2000 spectrophotometer system (Thermo Scientific), clearly labeled and stored at 80°C.

### 2.2.2 Cell Lines

RNA from cell line was extracted using the QIAshredder kit, and RNeasy Mini Kit (QIAGEN, Venlo, Netherlands) according to the manufacturer's instructions. Briefly, cells were harvested by trypsinization to obtain cell pellet. To that, RTL Buffer containing β-Mercaptoethanol (β-ME); 10 µl of β-ME per 1 ml of RLT Buffer was added (350 µl for up to 5x10<sup>6</sup> pelleted cells and 600 µl for 5x10<sup>6</sup> to 1x10<sup>7</sup>). Cell lysate were

homogenized using the QIAshredder column by centrifugation for 2 min at maximum speed. The homogenized cells were mixed with 70% ethanol (1:1 ratio in volume) and transferred into RNeasy mini spin column and centrifuged for 15 sec at 10000 rpm. RNeasy columns were then washed three times; once with 700µl of Buffer RW1 and twice with 500µl of Buffer RPE. RNA was then eluted in 50µl RNase-free water. Extracted RNA were assessed using the NanoDrop 2000 spectrophotometer system (Thermo Scientific), clearly labeled and stored at 80°C.

## 2.3 REAGENTS

### 2.3.1 Kinase inhibitors

Dabrafenib (GSK2118436), and trametinib (GSK1120212) were obtained from Selleck Chemicals and purchased through Cedarlane laboratories (Burlington, ON). Inhibitors were prepared in stock concentration of 10 mM and 5 mM respectively in  $\geq 99.9\%$  DMSO (Sigma-Aldrich Canada). The compound stock was stored at  $-80^{\circ}\text{C}$ . The working stock solutions were diluted in PBS, kept at  $4^{\circ}\text{C}$  and used within 2 weeks or prepared at the day of the experiment. The final DMSO concentration in all cell culture experiments was at 0.01 % or less.

### 2.3.2 ROS scavenging agents

Diphenyleneiodonium (DPI) (Sigma-Aldrich Canada)<sup>228</sup>; a classical inhibitor of NADPH oxidase, nitric oxide and superoxide, natural plant derived compounds

resveratrol<sup>229,230</sup> and celastrol<sup>231</sup>, and trolox<sup>232</sup>; a vitamin E-based compound were utilized in ROS inhibition.

## 2.4 RNA QUALITY AND QUANTITY ANALYSIS

Experion™ Automated Electrophoresis System (Bio-Rad) was used in the initial determination quality of isolated RNA from FFPE. This system incorporates LabChip based analysis that measures the integrity and concentration of RNA and other molecules such as protein and DNA via performing an automated electrophoresis. This initial quality analysis was performed by a former student of the lab, Michael Mackley<sup>233</sup>. Further assessment of RNA concentration and purity used in this study was accomplished using the NanoDrop 2000 spectrophotometer system (Thermo Scientific).

## 2.5 DNASE I DIGEST TREATMENT

For highly pure RNA exclusive of genomic DNA contamination, extracted RNA was treated with DNase I (Amplification Grade kit, Invitrogen, USA) prior to cDNA synthesis and PCR amplification using DNase I, Amplification Grade kit (Invitrogen, USA). Following manufacture's protocol, RNA samples were always kept on ice except specified otherwise. In an RNase-free microcentrifuge tube, combined 5-8 µl with with amplification grade DNase I (1 µl), and 10x DNase I reaction buffer (1 µl) were combined in RNase-free microcentrifuge tube. Total volume should be 10 µl so if needed, DEPC-treated water can be added to reach the target final volume. Solution mixture was then incubated at RT for 5 to 15 min. Longer incubation could result in RNA hydrolysis

in Mg<sup>++</sup>-manned. Next, 1 µl of 25 mM EDTA was added and incubated at 65°C for 10 min to inactivate the DNase I. Once incubation is done, reaction tubes are centrifuged and placed on ice before performing reverse transcription or stored at -80°C for further usage.

## 2.6 REVERSE TRANSCRIPTION (CDNA SYNTHESIS)

Using the Ready-To-Go™ You-Prime First-Strand Beads kit (GE Healthcare, Little Chalfont, United Kingdom), RNA extracted from FFPE patient tumour samples and RNA extracted from cell lines were reverse transcribed into cDNA, which lacks noncoding regions compared to DNA following manufacture's protocol. The first-strand reaction mix contains the Moloney Murine Leukemia Virus (M-MuLV) reverse transcriptase (75-kDa) beads to produce first strand cDNA. Briefly, in an RNase-free microcentrifuge tube, ddH<sub>2</sub>O was added to 1 µg of RNA to make up to 30 µl and then incubated at 65°C for 10 min followed by 2 min chilling on ice. 0.2 µg/µl of random primers in 3 mM Tris-HCl (pH 7.0), and 0.2 mM EDTA (Invitrogen) was added to the same tube to a final volume of 33 µl. The reaction mixture was thoroughly mixed by gentle vortexing then followed by a quick spin in a microcentrifuge, and then incubated for 60 min at 37°C. Synthesized cDNA was then stored at 4°C for further usage.

## 2.7 PLASMID PREPARATION, PURIFICATION AND QUALITY ANALYSIS

Plasmid vectors containing wild-type BRAF (488 bp) and V600E BRAF mutant sequences were previously constructed by a former student of the lab, Michael Mackley<sup>233</sup>. Vectors containing NOX1 (353 bp)<sup>187</sup> and NOX4<sup>234</sup> sequences were constructed



previously and available in the lab. Vectors containing the following gene sequences were designed and constructed in this study: GUSB (NM\_000181.3; 502 bp), GAPDH (NM\_001289746.1; 96 bp), BRAF (NM\_004333.4; 94 bp), SPRY1 (NM\_001258038.1; 84 bp), SPRY2 (NM\_005842.3; 69 bp), SPRY4 (NM\_001127496.1; 93 bp), DUSP4 (NM\_001394.6; 51 bp), DUSP6 (NM\_000181.3; 70 bp), and EGFR (NM\_005228.3; 84 bp). The TOPO® TA cloning Kit (Invitrogen) was employed to generate plasmid vectors. First, PCR products were produced from a control skin cDNA as template in order to amplify the desired fragment for each gene by primer sets as listed in Table 9. PCR was performed using Biometra® T-gradient thermocycler (Montreal Biotech Inc., Quebec, Canada) in a final volume of 25 µl containing 0.1 µl of Platinum Taq, 2.5 µl of 10x HiFi Buffer, 1 µl of 50 mM MgSO<sub>4</sub>, 0.5 µl of 99.5% 1,2-Propanediol (SIGMA-ALDRICH), 0.5 µl of 10mM dNTP, 0.5 µl of 10 µM forward primer, 0.5 µl of 10 µM reverse primer, 18.4 µl ddH<sub>2</sub>O, and 1 µl cDNA. Thermocycling conditions began with initial denaturation step at 94°C for 3 sec, followed by 35 cycles of 15 seconds denaturation at 94°C, 30 seconds at 60°C for annealing, and 5min at 68°C for extension. PCR products were then assessed using an agarose gel electrophoresis. Bands containing the desired DNA fragments were evaluated by size, excised and purified using QIAquick® Gel Extraction Kit (Qiagen, Venlo, Netherlands) using a microcentrifuge following the manufacturer's instructions. Purified products were cloned into a pCR™2.1-TOPO vector (Invitrogen, Carlsbad, CA) as follows: cloning reaction was first made up into a final volume of 6 µl consisting of 4 µl of purified PCR product, 1 µl salt solution (1.2M NaCl, 0.06M MgCl<sub>2</sub>), and 1 µl vector and incubated for 5min at RT. 2 µl of pCR™2.1-TOPO construct were transformed into One Shot® TOP10 Chemically Competent Escherichia coli (E. coli) cells (Invitrogen) for

**Table 9 List of Primers Used Throughout the Project.**

Gene abbreviation	Gene description	NCBI RefSeq	Bedard Lab ID	Primer designations	Nucleotide sequence or Oligo Sequence (5' - 3') (forward/reverse)	Amplicon length (bp)	Start/Stop	Used for vector	Design tool	Source Reference
BRAF	B-Raf proto-oncogene, serine/threonine kinase	NM_004333.4	2088	BRAF_1681F	GCACAGGGCATGGATTACTT	192	1681/1872			(Mackley, 2014)
BRAF	B-Raf proto-oncogene, serine/threonine kinase	NM_004333.4	2089	BRAF_1872R	GAC TTC TGG TCC CAT CCA C					
BRAF	B-Raf proto-oncogene, serine/threonine kinase	NM_004333.4	2090	BRAF_1548F	CATGGGTAATCCAAAAGC	469	1548/2016	/		(Mackley, 2014)
BRAF	B-Raf proto-oncogene, serine/threonine kinase	NM_004333.4	2091	BRAF_2016R	TCCTGGTCCCAACMAAAA					
BRAF	B-Raf proto-oncogene, serine/threonine kinase	NM_004333.4	2092	BRAF_11799a_Auth	CCACTCATGAGATTCTCTGTAGCTAGACCAAAAT		NA	—		(Mackley, 2014)
BRAF	B-Raf proto-oncogene, serine/threonine kinase	NM_004333.4	2093	BRAF_11799b	ATTTGGTCTAGCTACAGAAATCTCGATGGAGTGG					
BRAF	B-Raf proto-oncogene, serine/threonine kinase	NM_004333.4	2100	BRAF_1535F	GCTATTCCAAAAGCCCAAC	469	1535/2012	/		(Mackley, 2014)
BRAF	B-Raf proto-oncogene, serine/threonine kinase	NM_004333.4	2101	BRAF_2021R	AGGTATCTCTGCCACCAT					
BRAF	B-Raf proto-oncogene, serine/threonine kinase	NM_004333.4	2102	BRAF_1506F	AGGAGTACTAGAAAACACGA	488	1506/1993	/		(Mackley, 2014)
BRAF	B-Raf proto-oncogene, serine/threonine kinase	NM_004333.4	2103	BRAF_1993R	TCCTGGTCCCTGTGTGATGT					
BRAF	B-Raf proto-oncogene, serine/threonine kinase	NM_004333.4	2394	BRAF_1747F	TTCCTATGAGACCTCACAG	88	1747/1815	—		(Mackley, 2014)
BRAF	B-Raf proto-oncogene, serine/threonine kinase	NM_004333.4	2395	BRAF_1815R	TGTTCAAACGTAGTGGGACCC					
GUSB	Glicuronidase beta	NM_00181.3	2570	GUSB_E11_F	ACGATTCCAGGGTTTCAACA	241	1764/2004	—	Primer-BLAST	This study
GUSB	Glicuronidase beta	NM_00181.3	2571	GUSB_E12_R	TCCTCCGAAAAGGACGGCT					
GUSB	Glicuronidase beta	NM_00181.3	2625	GUSB_E11E12_F	GCCATTTCAAGCCCACTCT	502	NA	/	Primer-BLAST	This study
GUSB	Glicuronidase beta	NM_00181.3	2626	GUSB_E11E12_R	GATCCACCTCTGATGTCACTG					
GAPDH	Glyceraldehyde 3-phosphate dehydrogenase	NM_00128746.1	2801	GAPDH_F_NMO	ACTAGCGCTCACTGTTCTC	96	119/214	/	Primer-BLAST	This study
BRAF	B-Raf proto-oncogene, serine/threonine kinase	NM_004333.4	2802	GAPDH_R_NMO	TACBACCAATCCGTTGACTC					
BRAF	B-Raf proto-oncogene, serine/threonine kinase	NM_004333.4	2803	BRAF_F_NMO	TTGGACTGGATCATTTGGA	94	1449/1542	/	GenScript	This study
BRAF	B-Raf proto-oncogene, serine/threonine kinase	NM_004333.4	2804	BRAF_R_NMO	TGCTGAGTGTGAGTGGCTGT					
SPRY1	Sprouty RTK signaling antagonist 1	NM_001258038.1	2806	SPRY1_F_NMO	TGCCTTGAATAAGAACAGC	84	68/151	/	Primer-BLAST	This study
SPRY2	Sprouty RTK signaling antagonist 2	NM_003842.3	2807	SPRY2_F_NMO	ACGGCCGAATGCTTAATG	69	323/391	/	GenScript	This study
SPRY4	Sprouty RTK signaling antagonist 4	NM_00117496.1	2808	SPRY2_R_NMO	TGGCCTCCATCAGGTCTT	93	131/223	/	Primer-BLAST	This study
DUSP4	Dual specificity phosphatase 4	NM_001394.6	2810	SPRY4_F_NMO	GAGTACAGCGCGGCTAA	51	894/944	/	Primer-BLAST	This study
DUSP6	Dual specificity phosphatase 6	NM_00181.3	2812	SPRY4_R_NMO	TTCTAGGGGCTTTGAGGAG	70	868/937	/	Primer-BLAST	This study
EGFR	Epidermal growth factor receptor	NM_005228.3	2814	DUSP4_F_NMO	GCTGTCTAAAAGGCGG	84	2647/2730	/	GenScript	This study
GUSB	Glicuronidase beta	NM_007032.4	2817	DUSP4_R_NMO	AGAATTCTGGGTACTCGGAGG	97		—	GenScript	This study
NOX1	NADPH oxidase 1	NM_007032.4	2818	DUSP6_F_NMO	TCTTACTGGAAGTGGCTT	71		—	Primer-BLAST	This study
NOX4	NADPH oxidase 4	NM_001291926.1	2819	DUSP6_R_NMO	CGTCTAGATTGGTCTCGCAA	97		—	Primer-BLAST	This study
NOX4	NADPH oxidase 4	NM_001291926.1	2827	EGFR-F-84-NMO	THGTTCCGGACACAAAGA					
NOX4	NADPH oxidase 4	NM_001291926.1	2838	EGFR-R-84-NMO	CAAGTAGTCAFGCCCTTTC					
NOX1	NADPH oxidase 1	NM_007032.4	2851	GUSB-97-F	ACGTGGTGGAGAGCTCA					
NOX4	NADPH oxidase 4	NM_001291926.1	2852	GUSB-97-R	TGCCGAGTGAAGATCCCC					
NOX1	NADPH oxidase 1	NM_007032.4	3142	NOX1-F-71-NMO	AGGGGC-ACCTGCT-ATTTT					
NOX4	NADPH oxidase 4	NM_001291926.1	3143	NOX1-R-71-NMO	AGCTGTGGAAAGGTGAGGTT					
NOX4	NADPH oxidase 4	NM_001291926.1	3140	NOX4-F-97-NMO	ACCAGATTGGGGGGAITGT					
NOX4	NADPH oxidase 4	NM_001291926.1	3141	NOX4-R-97-NMO	CAAGAATGTTCCGCACATGG					
NOX4	NADPH oxidase 4		24	h gw k2NOX4F1	GGGGCAAGTTTGTACAAAAAGCAGGCTTCGCCACCAATGGCTGTGCTCGGAGG		NA	/		(Serrander et al., 2007)
NOX1	NADPH oxidase 1		25	h gw NOX4R1	GGGGACCACTTGTACAAAAGAGCTGGGTTTCAGCTGAAAAGACTCTTTATTGTATTC		NA	/		(Whitehouse, 2013)
NOX1	NADPH oxidase 1		26	h gw NOX1F1	GGGGACAAAGTTTGTACAAAAAGCAGGCTTCATGGGAAAACCTGGGTGGTTAAC		NA	/		
NOX1	NADPH oxidase 1		45	h gw NOX1R3	GGGGACCACTTGTACAAAAGAGCTGGGTTTGGGGTTCCTCGGTAATTTTG	353	NA	/		

30 min and then heat shocked at 42°C for 30 sec and transferred on ice. Cells were nourished with 250µl of S.O.C. (Super Optimal broth with Catabolite repression) medium (Cellgro, Virginia, United States). The mixture was then shaken (200 rpm) at 37°C incubator for one hour. From each transformation, 20 and 40µl transformants were spread on a pre-warmed LB agar plates supplemented with kanamycin (50 µg/ml), an antibiotic selecting agent. Plates were incubated overnight at 37°C. Positive resulted bacterial colonies were picked and cultured overnight in 3 ml LB containing 50 µg/ml kanamycin shaking at 37°C incubator. DNA plasmids were isolated from the overnight bacterial culture and purified using the QIAprep Spin Miniprep Kit (Qiagen, Venlo, Netherlands) following the manufacturer's instructions using QIAprep spin columns. Briefly, bacteria cultures were harvested by centrifugation at 8000 rpm at RT for 3 min. Pelleted bacteria cells were then suspended suspended in 250 µl Buffer P1 and transferred into a microcentrifuge tube and 250 µl of Buffer P2 was added and mixed by inverting tube four to six times. 350 µl of Buffer N3 was added and the mixture was centrifuge at 13,000 rpm for 10 min. supernatants were transferred into the QIAprep spin column and centrifuged for an additional 60 sec. Columns were washed with 500µl Buffer PB and washed again with 750µl Buffer PE. Plasmid DNA was eluted in 50µl EB Buffer. Conformation of successful insertion of desired DNA fragment was accomplished utilizing Sanger sequencing using BigDye® (Life Technologies, California, United States), sequencing buffer, and M13 primers provided in the TOPO® TA cloning Kit (Invitrogen). The amplification conditions were 94°C for 2 min, followed by 35 cycles of 94°C for 30 sec; 58°C for 30 sec, 72°C for 45 sec; and a final elongation step for 5 min at 72°C. Prior to sequencing on a 3130xl Genetic Analyzer (Applied Biosystems, California, United States),

the amplified sequencing PCR products were cleaned up using the BigDye® Terminator™ purification kit (Life Technologies, California, United States). Once validated, vectors concentration was measured with NanoDrop 2000 spectrophotometer system (Thermo Scientific). Stock concentration of each vector was equalized at 10 ng/μl, and four dilutions were incorporated (0.1, 0.001, 0.00001, 0.0000001 ng/μl) (Figure 6). This dilution was expanded to ensure linearity and cover a wide range of concentration. The expanded dilutions incorporated 12 dilutions (1, 0.1, 0.01, 0.001, 0.0001, 0.00001, 0.000001, 0.0000001, 0.00000001, 0.000000001, 0.0000000001, 0.00000000001 ng/μl) (Figure 7).

## 2.8 PRIMERS DESIGN

Online tools such as NCBI-Primer-BLAST and GenScript were used in designing primers. Prior to ordering, primers were checked using in-silico PCR tool from University of California, Santa Cruz (UCSC) website. DNA oligos were synthesized by Integrated DNA Technologies (IDT, Coralville, Iowa). To ensure successful amplification, PCR product was subjected to agarose gel electrophoresis. More than ten sets of primers targeting multiple DNA sequence were used either in PCR, qPCR, ddPCR amplification and all are listed in Table 9 on page 48.

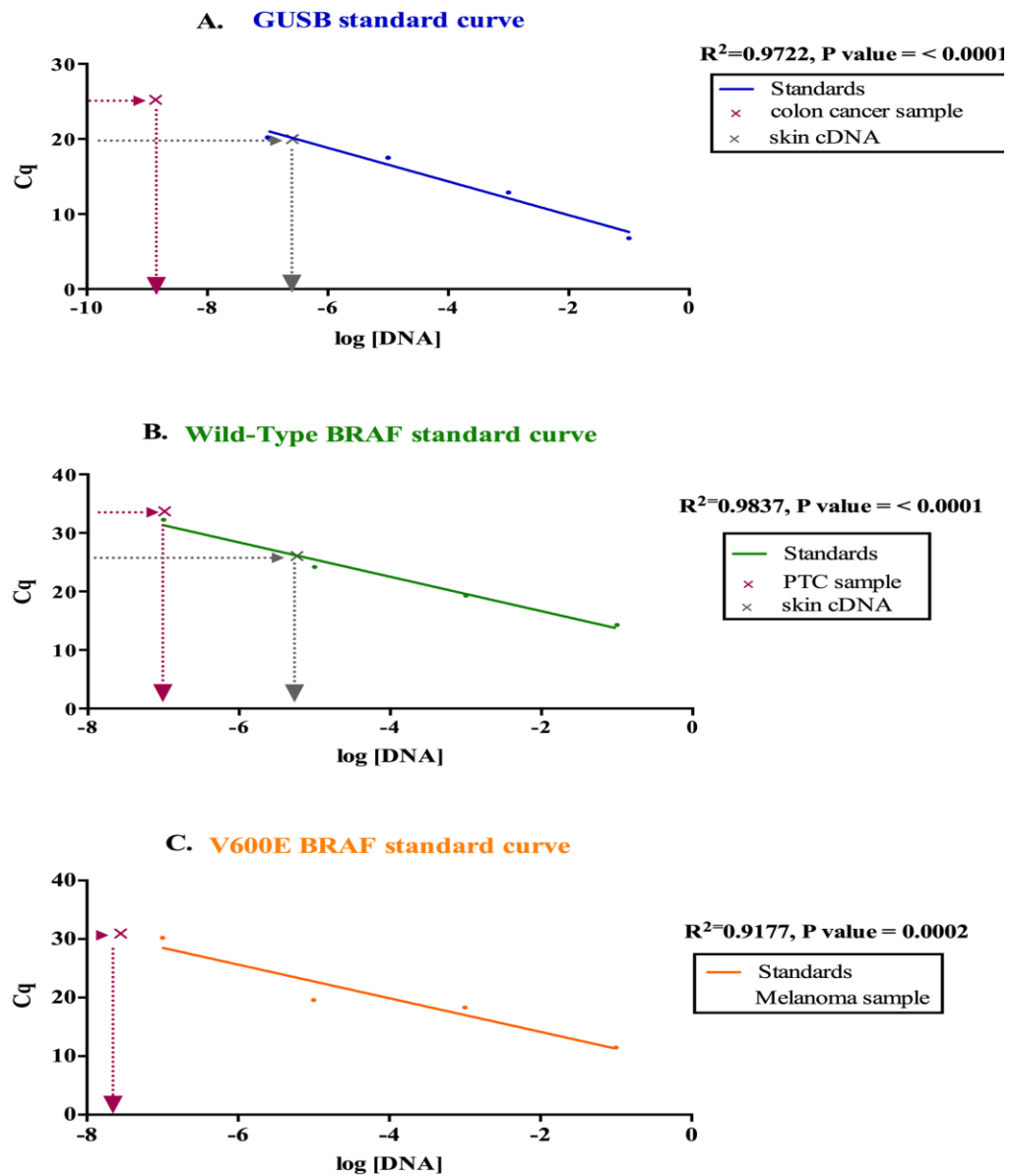
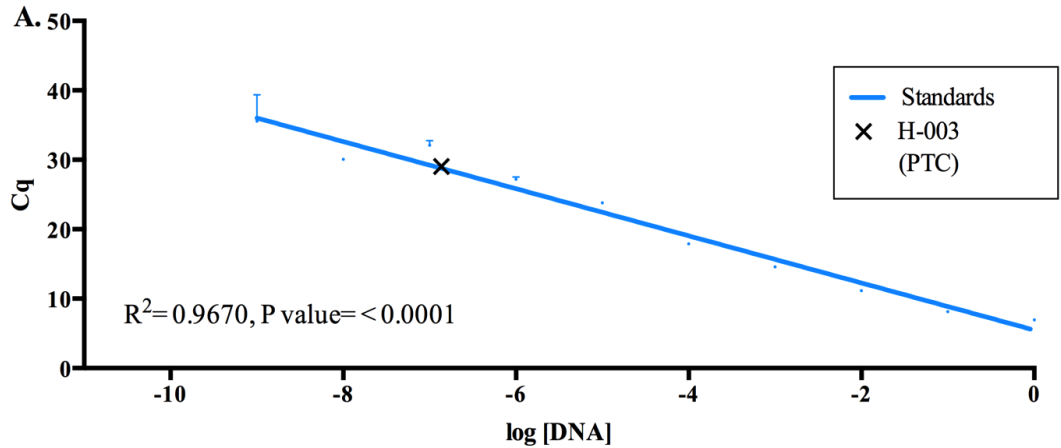


**Figure 6** 10 fold serial dilution of plasmid with known concentration for GUSB as a reference gene, wild-type BRAF, and V600E BRAF.

Standard curves were generated by plotting the quantification cycle (Cq) against log DNA (plasmid DNA or patient cDNA) concentrations; Cq values for samples were then compared with the standard curve to absolutely quantify gene expression. Confidence intervals were determined by linear regression. R2 values for **A.** GUSB =0.9722. **B.** WT BRAF =0.9837. **C.** V600E mutant = 0.9177.

### SPRY2 Expression in PTC Tumour Sample



### SPRY4 Expression in Melanoma Sample

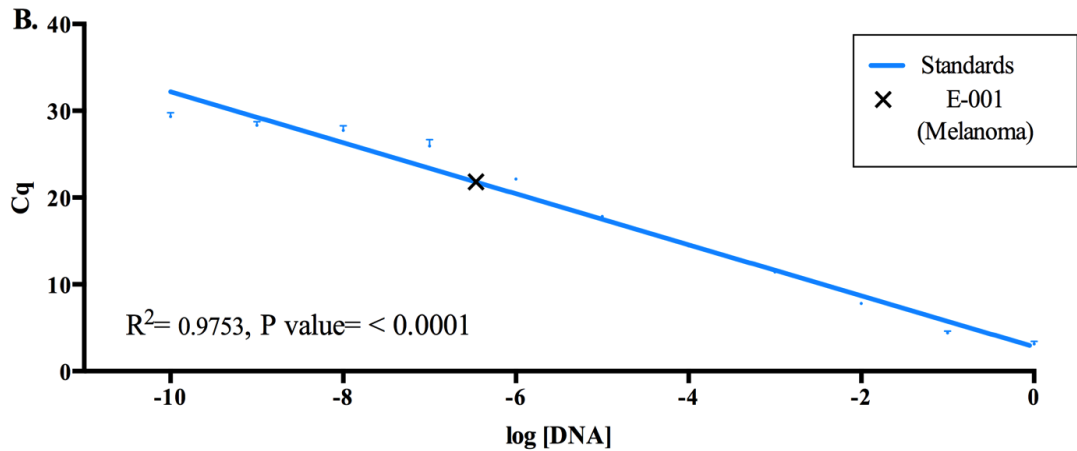


**Figure 7 Representation of standard serial dilution of plasmid with known concentration after expanding the dilution range.**

Standard curves were generated by plotting the quantification cycle (Cq) against log DNA (plasmid DNA or patient cDNA) concentrations; Cq values for samples were then compared with the standard curve to calculate the approximate copy number of our target. Confidence intervals were determined by linear regression.  $R^2$  values for A. SPRY2 = 0.9670. B. SPRY4 = 0.9753. Data were plotted as mean  $\pm$  SD (n=2).

## 2.9 QUANTITATIVE REVERSE TRANSCRIPTASE POLYMERASE CHAIN REACTION (RT-QPCR)

The Rotor-Gene Q real-time PCR detection system (QIAGEN) allows us to monitor the amplification of a target DNA sequence in real time meaning the amplification of a target is observed after each PCR cycle. This attained by measuring the fluorescent emitted from the amplified sequence. The number of cycles required to detect a real signal referred to as the quantification cycle ( $C_q$ ) as recommended by The Minimum Information for Publication of Quantitative Real-Time PCR Experiments (MIQE) guidelines<sup>235</sup> and the Real-Time PCR Data Markup Language (RDML)<sup>236</sup>, but also previously known as  $C_t$  (cycle threshold),  $C_p$  (crossing point), and TOP (take-off point). The lower the  $C_q$  value, the greater the amount of target within the sample. Target can be quantified either using a standard curve to determine the approximate copy number of our target of interest in unknown samples or semi-quantified relative to reference gene (normalizer)<sup>237,238</sup> that constitutively expressed in normal and patho-physiological condition.

When using a standard curve<sup>239</sup>,  $C_q$  values of standard curves were used to determine the approximate copy number of our target on interest in unknown samples. To generate a standard curve,  $C_q$  values were plotted against the log standard concentrations. The  $C_q$  values from the samples were then used to quantity of gene expression by interpolation from the regression line of the standard curve (see Figure 6 on page 51, and Figure 7 on page 52 for demonstration).

For semi-quantitative real-time PCR, a reference gene was used and noted here, an presumption was made that the experimental conditions would not altered the expression level of the selected reference gene. Thus, the expression of the target gene of interest is reported relative to the expression of the normalizer (reference gene). One approach to obtain this is by using the  $2^{-\Delta\Delta CT}$  method described by Livak and Schmittgen<sup>240</sup>. This method compares the quantification cycle or the Ct values in the experiment condition relative to the control condition.  $\Delta Ct$  for both conditions; relative and control, can be accomplished by subtracting the Ct values of a reference gene from the Ct value of a target of interest. Following these subtractions, two to the power of the negative value of  $-\Delta\Delta CT$  is calculated to obtain the relative fold change of expression.

### 2.9.1 TaqMan based RT-qPCR Assay

This technique utilizes a fluorescent dyes probes that can be measured during amplification at each cycle of the reaction. TaqMan probes are one of the probes that designed to have higher specificity for quantitative PCR. This method was introduced back in the 1990s<sup>241</sup> and then developed by two clinical analytical company (Roche molecular diagnostic and Applied biosystems). The TagMan probes involve the addition of fluorescent labels to the interest target sequence. There are two labels attach to the probe, a reporter dye at one end and a quencher dye at the other end. When amplification of the target has happened, the reporter dye will cleave and then emit fluoresce. The machine then is measuring the fluorescence that being emitted as a direct evaluating tool to the target. In addition, this technique has been shown to obtain reliable and consistent results, even with older archived tissues such as FFPE tissue samples<sup>242</sup>. This actually



shows potential in using this assay not only for testing this assay, but also in applying it in pooled tissues samples for future experiments.

The development of a TaqMan-based RT-qPCR assay that was capable to distinguish between BRAF WT and BRAFV600E was initiated in the lab by Michael Mackley (see <sup>233</sup> for detailed). The assay comprised primers designed to amplify a 192 bp fragment that encompassed the V600E mutation, along with two TaqMan probes; a yellow fluorescent probe specific for the mutant and a green fluorescent probe specific for the wild-type sequence. The assay was validated using known ratios of vectors containing the sequence for the wild-type and mutant. Figure 8 outlines the general steps that have been followed in the assessment of this assay.

### 2.9.2 SYBR Green based RT-qPCR Assay

Unlike TaqMan chemistry, SYBR® Green I dye fluorescence when bound to the double-stranded product and signals increase as more products are being amplified. In addition, there is no need for probe. PCR was performed using the Rotor-Gene Q real-time PCR detection system (QIAGEN) in a final volume of 10µl containing 5µl 2x SYBR Green Mix for RotorGene, 2.5µl primers at 250 nM, and 2.5µl cDNA. Real-time thermal cycling program was as follow; 94°C for 10 min; 40 cycles of (95 °C, 10 sec; 60 °C, 15 sec; and 72 °C, 30 sec) acquiring to cycling A on Green; followed by a melting ramp from 72 to. 95°C, with a 90 sec hold on the first step of the ramp (72°C) and and 5 sec holds on all subsequent temperatures.

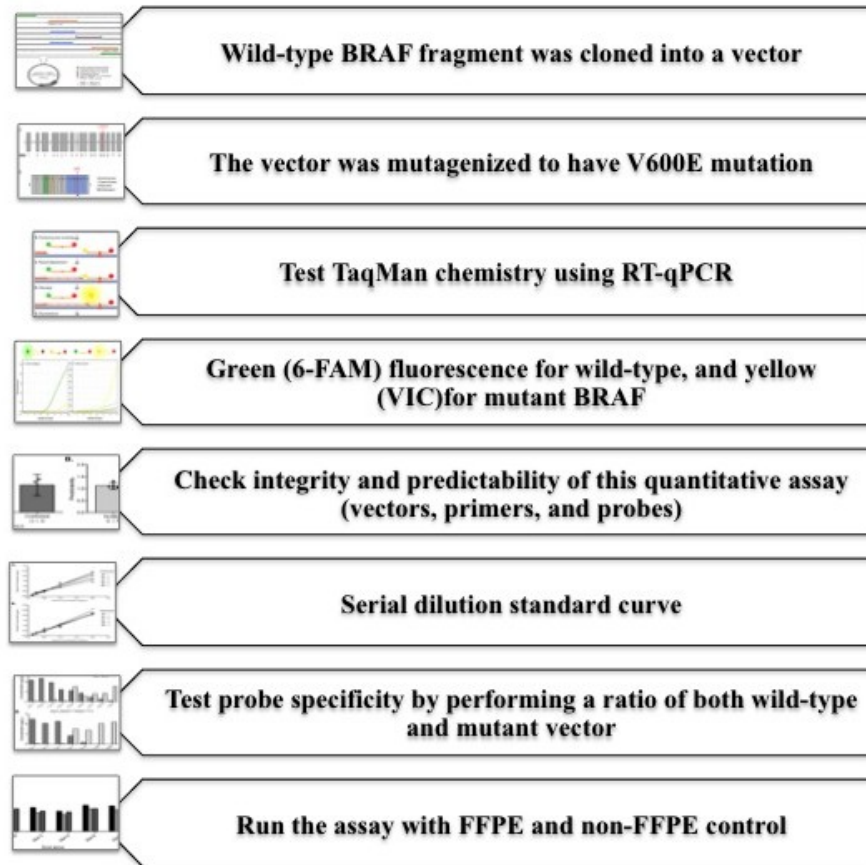


**Figure 8 Steps followed in the development and assessment of a TaqMan-based RT-qPCR assay.**

### 2.9.3 Quantitative Digital Droplet PCR

Quantitative digital droplet PCR (qddPCR) is a recent method that has the potential to precisely quantifying the copy number of nucleic acid target present in a sample. Digital droplet PCR share similar concept to regular PCR, the only difference is that in ddPCR the reaction is broken up into little nano liter (nl) sized droplet prior to thermocycling. The original number of DNA target is calculated from a Poisson distribution where some droplets have no template (negative) and some droplets have template (positive). To circumvent the possibility of the present of more than one template in a single droplet, Poisson-based 95% confidence intervals statistics are employed to calculate the absolute copy number of particular target present in a sample. The anticipated result per droplet is either 0 or +1. Our study utilized DNA binding-dye chemistry using the Bio-Rad's QX100™ Droplet Digital™ PCR (ddPCR™) system, previously known as QuantaLife Droplet Digital PCR. The droplets that contain the template will fluorescence due to the presence of EvaGreen dye. A uniplex absolute quantification (ABS) experiment was done following these essential steps. First, cDNA optimization was performed to determine the optimal starting DNA material. Next, primers annealing temperature optimization was accomplished by performing a thermal gradient PCR ranged from 62 °C to 55 °C using pooled cDNA from FFPE samples as template. Primers designed to amplify a 94 bp BRAF fragment and a 97 bp GUSB fragment are listed in Table 9 on page 48. The optimal annealing temperature for BRAF and GUSB primers was determined at 56.5°C based on the clear separation of positive and negative bands at this temperature (see Figure 9 and Figure 10).

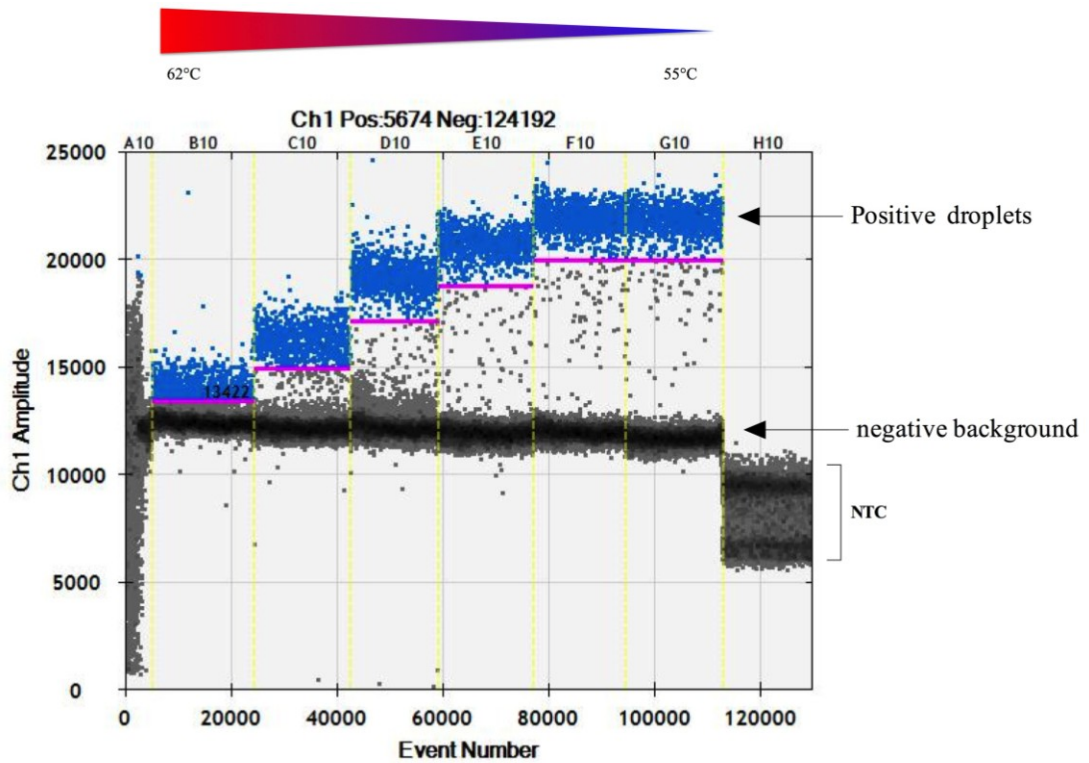


**Figure 9 A graphical representation of the fluorescence amplitudes of droplets detected.**

A thermal gradient PCR ranged from 62 °C to 55 °C was applied to determine the optimal annealing temperature for BRAF and GUSB primers using the QX200 ddPCR EvaGreen supermix . Pooled cDNA from FFPE samples were used as template. Dashed yellow lines separate between experiment wells and different annealing temperature. Data were visualised in channel 1 amplitude, negative background droplets in black, positive droplets represented in blue were determined by setting a single-well threshold (indicated by the pink line). Distinguishable separations between positive and negative droplets were improved as the annealing temperature become more and more suitable for the primers. We determined 56.5 °C was an optimal annealing temperature (well F10).

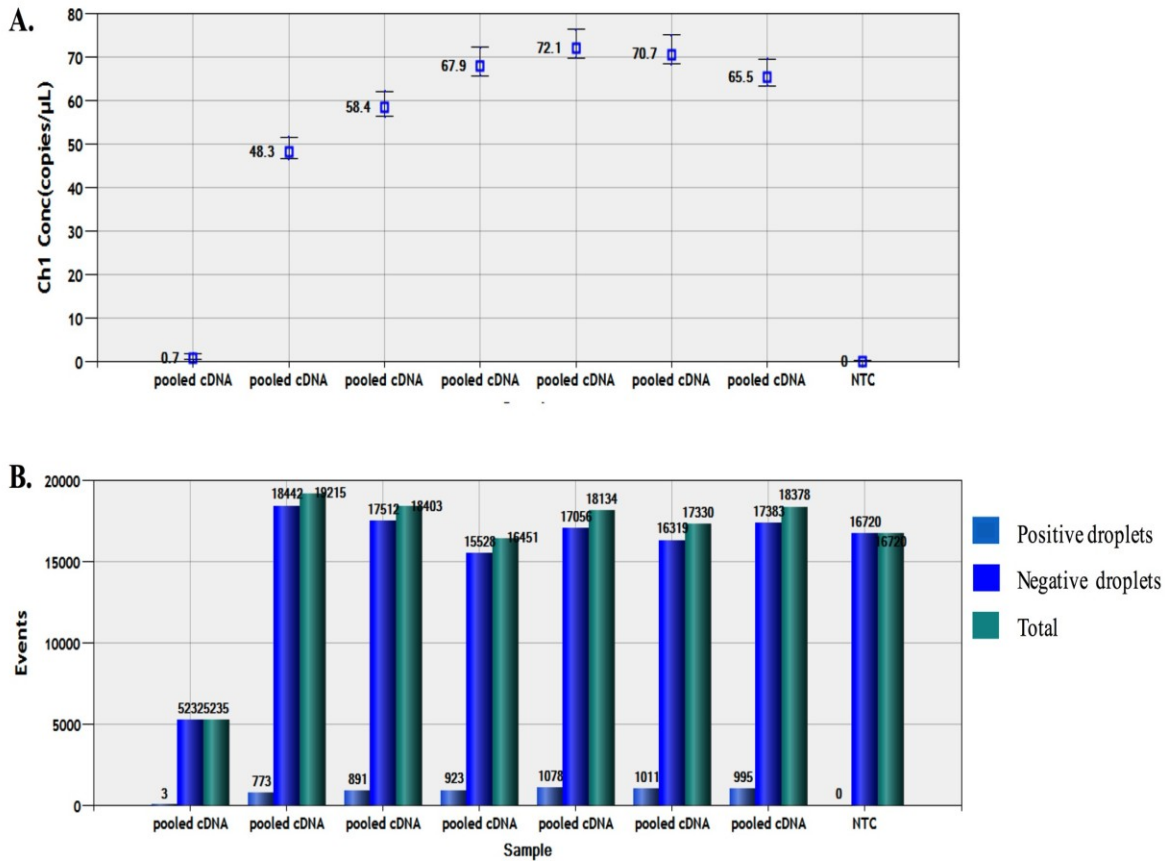


**Figure 10 QuantaSoft software (BioRad) data output.**

Viewing Concentration (copies/μl) and event data from BRAF optimizing annealing temperature experiments. **A.** An absolute quantification of BRAF as determined after reading droplets from each reaction tubes. Error bars indicate Poisson 95% confidence limits. **B.** Number of droplet events counted per sample. Three bars per sample viewing positive, negative droplets, and total events count in a sample. 12 000 events or more indicates a successful generated droplets.

A ddPCR reaction mix was prepared by first combined the BioRad QX200™ ddPCRTM EvaGreen Supermix, final primer concentration of 0.1  $\mu$ M, cDNA, and ddH<sub>2</sub>O to a total volume of 20  $\mu$ l. Prior to PCR thermocycling, reactions are thoroughly mixed by vortexing to obtain nice Poisson distribution. A water-in-oil approach was used to enable partitioned samples into 20 000 droplets using the QX200 droplet generator. Once prepared, samples were loaded into the sample wells of disposable droplet generator cartridge (Bio-Rad). A volume of 65  $\mu$ l of QX200 droplet generation oil for EvaGreen assays (Bio-Rad) was loaded to the oil well and then droplet are generated using the QX200 droplet generator (Bio-Rad). Consequently, a cloudy and vague mixture is formed. Once droplets are generated, samples were collected carefully to avoid shearing and transferred to a 96-well PCR plate for PCR amplification within an hour (before droplets starting to diffuse together). Droplet PCR amplification to end-point was performed on the BioRad C1000 Touch™ Thermal Cycler with the following cycling conditions: 90°C for 5 min; 50 cycles of 95°C for 3 sec, 56.5°C for 1 min, 72°C for 3 sec; 4°C for 5 min; 90°C for 5 min; and finally an infinite hold at 10°C. After amplification, the plate was then transferred to a droplet reader (QX200 droplet reader, BioRad) where the fluorescence intensity of droplets was read individually on channel 1 (FAM). In addition, the detector also assessed the quality of each droplet; detecting the size and shape of droplets as well as automatically eliminating droplets that did not meet the quality metric. Data was visualized and analyzed using the QuantaSoft software (Bio-Rad, CA, USA) as the absolute quantification of a starting copy number of target DNA is reported in Copies/ $\mu$ l. Figure 9 on page 58 and Figure 10 on page 59 illustrate different

viewing options obtained from QuantaSoft software Non specific products can be eliminated from the analysis by visualization of fluorescence amplitude and adjusting the threshold to capture only true positive droplets (Figure 11).

## 2.10 CELL VIABILITY ASSAY

Cell viability was assessed using AlamarBlue® (AB) assay where cell metabolic activity was measured by the amount of fluorescence emitted by living cells. AB is a flurometric and colorimetric assay that measures the oxidation-reduction (REDOX) indicator. In response to the addition of resazurin to the growth medium viable growing cell convert this dark blue non-fluorescent form dye into a red fluorescent reduced form resorufin (Figure 12). In this study, fluorescence measurement were collected at 350 nm excitation wavelengths and 590 nm emission wavelengths using the Infinite M200 Pro microplate reader (Tecan Group Ltd., Männedorf, Switzerland).

## 2.11 AMPLEX RED ASSAY

Detection of hydrogen peroxide ( $H_2O_2$ ) was obtained employing Amplex Red® fluorescence assay (AmR). In the presence of horse radish peroxidase (HRP), AmR oxidized by  $H_2O_2$  is subsequently converting AmR into highly fluorescent resorufin that can be detected colorimetrically or fluorometrically.

The stock concentration for reagents needed for this assay was as follow: 10 mM Amplex Red in DMSO (Invitrogen Canada Inc., Burlington, ON), 500 U/ml horse radish

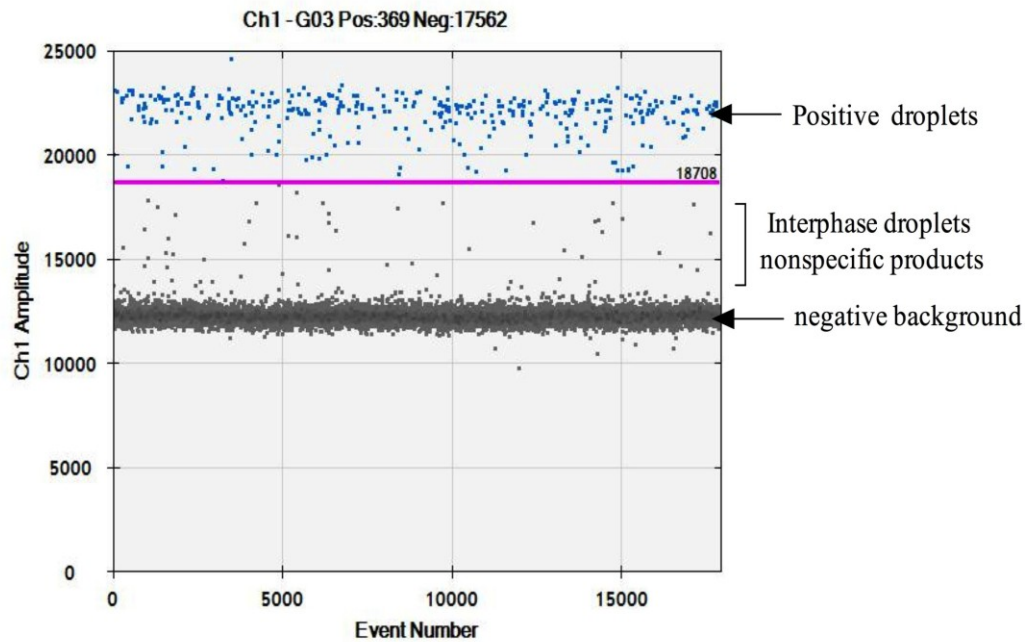


**Figure 11 A graphical representation of the intermediate droplets “rain”.**

Example of data output from RT-ddPCR uniplex assay for BRAF absolute quantification copies/ $\mu$ l using the QX200 ddPCR EvaGreen supermix. Sample E-002-melanoma used in this illustrative figure. Data were visualized in channel 1 amplitude, negative background droplets in black, positive droplets represented in blue and determined by setting a single-well threshold (indicated by the pink line) and interphase (“rain”) that fall between positive and negative bands represent nonspecific products.



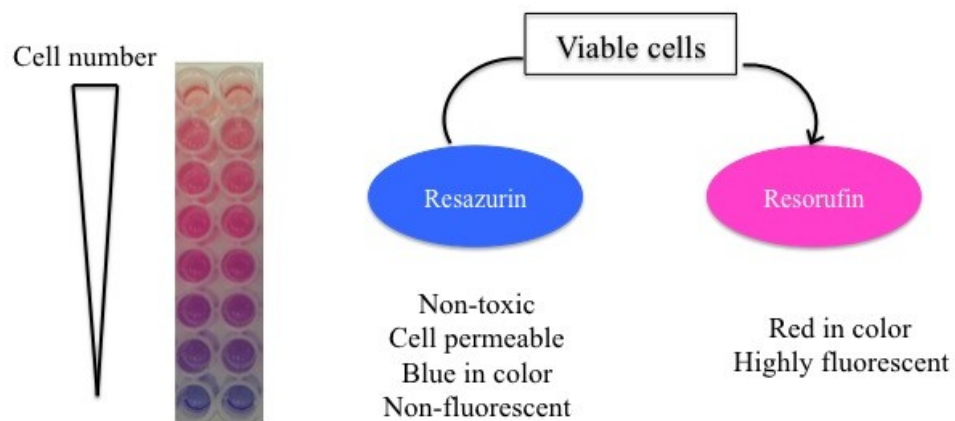


**Figure 12 Alamar Blue assay principle.**

Relative cytotoxicity of agents tested in this study was determined by AlamarBlue (AB) assay. This ready-to-use assay reagent assesses cells health via reduction-oxidation indicator that changes in response to cellular metabolic reduction. Viable cells continuously convert resazurin into resorufin increasing the overall fluorescence in experiment wells (graphical abstract on the right). The image on the left represents cell viability examination for cell serial dilution incubated with 10% AB reagent for 2 hours at 37°C. it can be seen that the higher the number of viable cells present, the more resazurin converted to resorufin.

peroxidase in PBS (HRP) (Sigma-Aldrich Canada, Oakville, ON), and 100 mM H<sub>2</sub>O<sub>2</sub> in water (Fisher Scientific Ltd., Napean, ON). Hank's Buffered Salt Solution ++ solution contains 0.137 M NaCl, 5.4 mM KCl, 0.25 mM Na<sub>2</sub>HPO<sub>4</sub>, 0.44 mM KHPO<sub>4</sub>, 1.3 mM CaCl<sub>2</sub>, 1% Glucose (w/v), 1.0 mM MgSO<sub>4</sub>, and 4.2 mM NaHCO<sub>3</sub> was used in Amplex Red assay.

Cells were collected and washed with HBSS prepared freshly on the day of experiment once, then resuspended cells at 500,000/ml in HBSS. 100 µl cell suspensions (50,000 cells) were plated in each well of a 96-well plate. Subsequently, a 100 µl of master mix containing 25 µM Amplex Red and 0.005 U/ml HRP was added to each well. Serial standard dilutions of H<sub>2</sub>O<sub>2</sub> ranged from 0 nM to 5000 nM was prepared freshly with each experiment as standards (Figure 13). Fluorescence was measured at 37°C every two minutes for 30 cycles with excitation at 530 nm and emission at 590 nm using the Infinite M200 Pro microplate reader (Tecan Group Ltd., Männedorf, Switzerland). The concentration of H<sub>2</sub>O<sub>2</sub> corresponding to a given fluorescence value was determined from detection of fluorescence in a serial dilution of H<sub>2</sub>O<sub>2</sub> standards. The rate of H<sub>2</sub>O<sub>2</sub> production by cells was measured as the increase in peroxide concentration (nM) per second. Values of nM/well (200 µl; 50,000 cells) is then converted into picomoles (pmols) and then into pmol/hr/10<sup>4</sup> cells.

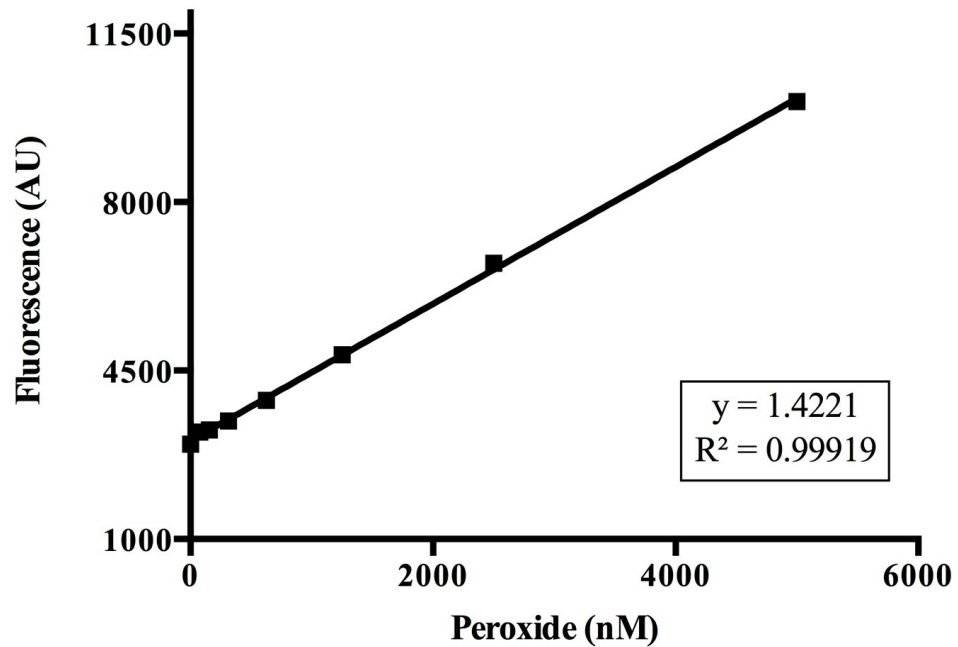


**Figure 13 Representative Standard curve of peroxide.**

Serial dilutions of H<sub>2</sub>O<sub>2</sub> standards (5000 nM to 0 nM) prepaid in duplicate. Fluorescence was measured at 37°C every two minutes for 30 cycles with excitation at 530 nm and emission at 590 nm using the Infinite M200 Pro microplate reader (Tecan Group Ltd., Männedorf, Switzerland). Confidence intervals were determined by linear regression ( $R^2=0.999$ ).

## 2.12 STATISTICAL ANALYSIS

Experiments were conducted using a minimum of three technical replicates and data were reported as mean  $\pm$  standard deviation, unless otherwise specified. Statistical analysis was performed using GraphPad Prism™ Software version 6.0 h for Mac OS X 10.8.5 (GraphPad Software, Inc, California, USA). Data were analysed using a T-test, linear regression, or two-way ANOVA with repeated or non-repeated measure, followed by Dunnett's or Sidak's multiple comparisons test. Values were considered to be statistically significant when  $p < 0.05$  as follow: \*  $p < 0.05$ ; \*\*,  $p < 0.01$ ; \*\*\*,  $p < 0.001$ ; \*\*\*\*,  $p < 0.0001$ .

## CHAPTER 3 RESULTS

### 3.1 PROJECT 1: UTILIZATION OF RT-QPCR AND DDPCR IN THE DETECTION OF BRAF IN PATIENT'S TUMOUR SAMPLES

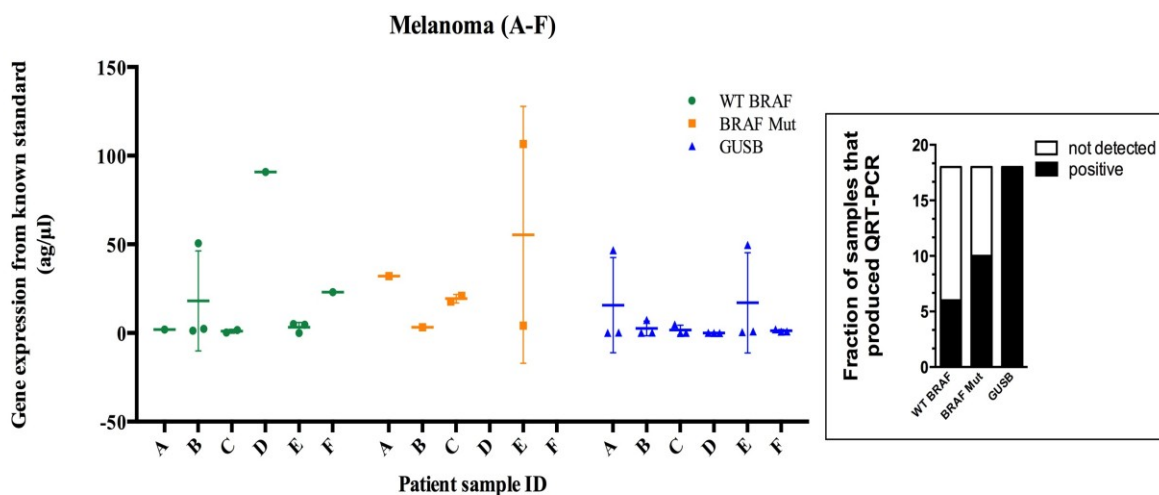
#### 3.1.1 Assessment of a TaqMan-based RT-qPCR method and ddPCR method in detecting BRAF expression in FFPE tumour samples

To evaluate whether a quantitative reverse transcriptase PCR (RT-qPCR) based method could be used to specifically examine the BRAFV600E expression in tumour using RNA extracted from FFPE samples, we utilized a TaqMan-based RT-qPCR assay developed in the lab by Michael Mackley<sup>233</sup>. Because multiple tissue types, and tissues with multiple cell types were being used, and also because the tissue samples and extracted RNA might vary in quality, we opted to include in our assay a standard curve using a vector with known concentration for each gene to allow us to determine the approximate copy number quantification of our gene of interest. For this, Wild type BRAF, V600E BRAF mutants and reference gene GUSB DNA sequences were inserted into plasmid vector (pCR™2.1-TOPO vector), separately. Serial dilutions for each vector were assayed in triplicate by q-PCR. The technical replicates for each of the vectors at all dilutions examined were highly concordant with one another, and demonstrated linearity over a wide range of concentrations.

However the reproducibility of the results from cDNA samples prepared from the FFPE extracted RNA was less satisfactory. Six melanomas (A-F), six PTC (G-L), and

five CRC samples (M-Q), each representing an individual patient, were tested using the Taq-Man assay as described above. For each of these 17 cases, three separate RNA extractions were performed, leading to 51 cDNA samples. Each of these was measured three times. Figure 14, Figure 15 and Figure 16 show gene expression (ag/ $\mu$ l) of WTBRF, BRAFMut, and reference gene GUSB in melanoma, PTC and colon respectively. The variability in technical replicates for three replicate measurements on each of these 51 samples was summarized in the tables within Figure 14, Figure 15 and Figure 16, illustrating mean and standard deviation. The normalizer gene GUSB was detected in all 51 samples. However, for both the BRAF and BRAF mutant, the results were un-interpretable. No BRAF WT was detected in 21/51 samples, and BRAF mutant was undetectable in 34/51 measurements. In some samples no gene expression could be detected in all three replicates, which may indicate low or no gene expression. However, there were many samples where one or two of the three replicates led to a detectable signal. Thus the performance of the RT-qPCR on cDNA prepared from FFPE RNA was highly variable and unreliable.

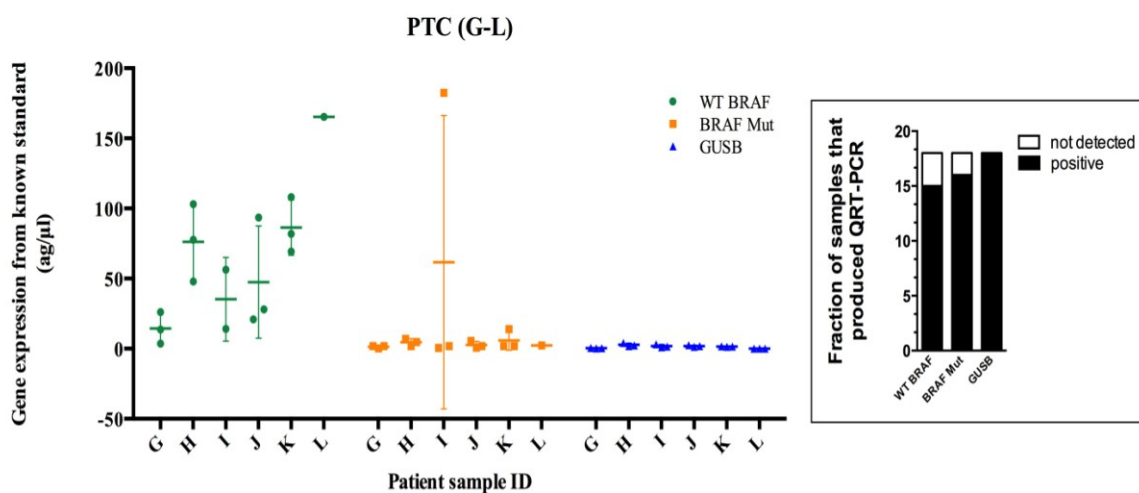
Results from immunohistochemical (IHC) staining of the BRAFV600E protein were available from each of the 17 individuals. Each slide was graded by pathologist Dr. Huang. There was no correlation between the IHC score and the level of BRAF mutant mRNA detected by RT-qPCR (Figure 17).



	BRAF WT			BRAF Mut			GUSB		
	Mean	SD	N	Mean	SD	N	Mean	SD	N
A	2.004160		1	32.062200		1	15.700800	26.819670	3
B	18.072990	28.179600	3	3.199540		1	2.582768	4.176796	3
C	0.972699	1.081337	2	19.350100	2.351130	2	1.619126	2.725679	3
D	90.855600		1				0.041691	0.068528	3
E	3.217044	2.792886	3	55.418180	72.435760	2	17.019750	28.267280	3
F	23.037600		1				1.271272	0.646112	3

**Figure 14 Gene expression (ag/μl) from FFPE melanoma patients' samples as determined from known standard serial dilution curve.**

Upper left: Gene expression (ag/μl) of WT BRAF, BRAF Mut, and reference gene GUSB in technical replicates on same isolated RNA. Individual points represent replicates, horizontal bar represents the mean, with vertical bar representing the standard deviation (n=0-3). Upper right: Bar graph representing the fraction of samples detected by RT-qPCR. Lower panel: Table summarizing the average for each melanoma case with mean, SD, and number of samples where RT-qPCR signals were detected.

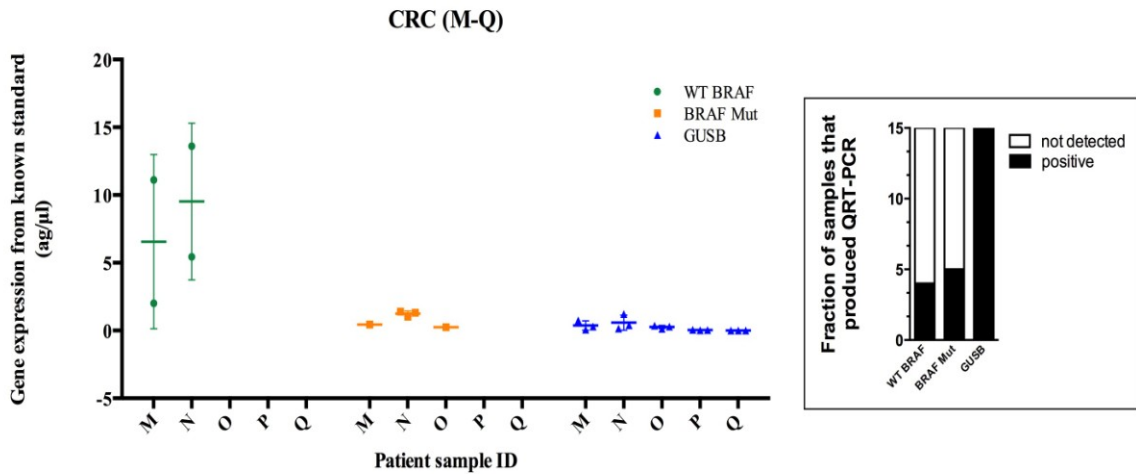


	BRAF WT			BRAF Mut			GUSB		
	Mean	SD	N	Mean	SD	N	Mean	SD	N
<b>G</b>	14.475000	11.237460	3	1.321667	0.980055	3	0.424500	0.148030	3
<b>H</b>	76.183330	27.606260	3	4.553333	2.553240	3	2.738333	1.198722	3
<b>I</b>	35.250000	29.839910	2	61.638000	104.671800	3	1.871833	1.123763	3
<b>J</b>	47.468330	39.985720	3	2.709000	2.552043	3	1.878333	0.613440	3
<b>K</b>	86.366680	19.750020	3	5.926667	6.991712	3	1.497833	0.168802	3
<b>L</b>	165.235000		1	2.235000		1	0.017640	0.009555	3

**Figure 15 Gene expression (ag/μl) from FFPE PTC patients' samples as determined from known standard serial dilution curve.**

Upper left: Gene expression (ag/μl) of WT BRAF, BRAF Mut, and reference gene GUSB in technical replicates on same isolated RNA. Individual points represent replicates, horizontal bar represents the mean, with vertical bar representing the standard deviation (n=0-3). Upper right: Bar graph representing the fraction of samples detected by RT-qPCR. Lower panel: Table summarizing the average for each melanoma case with mean, SD, and number of samples where RT-qPCR signals were detected.





	BRAF WT			BRAF Mut			GUSB		
	Mean	SD	N	Mean	SD	N	Mean	SD	N
M	6.561710	6.432395	2	0.438978		1	0.371683	0.347710	3
N	9.521925	5.776178	2	1.244450	0.198671	3	0.584500	0.559656	3
O				0.247406		1	0.266633	0.114346	3
P							0.036667	0.018858	3
Q							0.004599	0.005147	3

**Figure 16 Gene expression (ag/μl) from FFPE colorectal cancer patients' samples as determined from known standard serial dilution curve.**

Upper left: Gene expression (ag/μl) of WT BRAF, BRAF Mut, and reference gene GUSB in technical replicates on same isolated RNA. Individual points represent replicates, horizontal bar represents the mean, with vertical bar representing the standard deviation (n=0-3). Upper right: Bar graph representing the fraction of samples detected by RT-qPCR. Lower panel: Table summarizing the average for each melanoma case with mean, SD, and number of samples where RT-qPCR signals were detected.

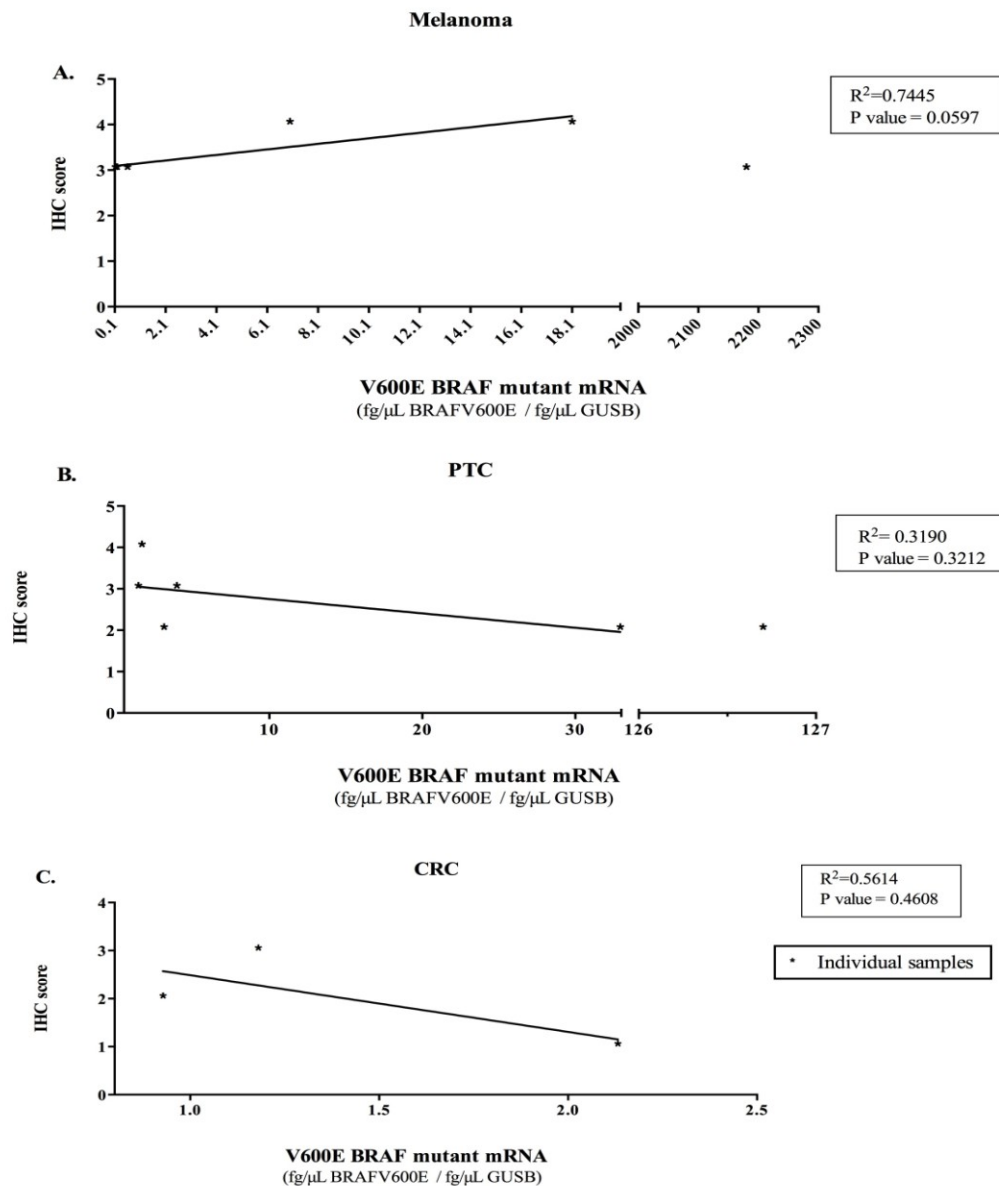


**Figure 17 Correlation between V600E BRAF mutant protein expression from IHC score and V600E BRAF mutant mRNA expression from QRT-PCR.**

Normalized concentrations (fg/μl) of V600E BRAF mutant to the concentration of a reference gene GUSB (fg/μl) were plotted against the subjective score (0 - 4) obtained from IHC. Correlation analysis of 95% confidence interval of a linear regression was determined.  $R^2$  values for **A.** Melanoma = 0.7445. **B.** PTC = 0.3190. **C.** Colorectal cancer = 0.5614.

The lack of consistency within the replicates on the same cDNA samples despite the very high level of concordance within the vector standard curves led to the consideration that RNA degradation or the presence of contaminants carried over from the FFPE might be interfering with the PCR amplification, or that probes were failing to distinguish between the WT and mutant BRAF. In an effort to overcome this, we assessed two additional detection methods: quantitative reverse transcriptase PCR (RT-qPCR) using SYBR green, and digital droplet PCR (ddPCR). A smaller fragment of BRAF (94 bp) was targeted to circumvent poor RNA quality that is often degraded in FFPE sample. The smaller fragment was not designed to achieve mutational specificity, rather examining the ability of detecting total BRAF expression from FFPE samples.

Unlike RT-qPCR, digital droplet PCR requires only that an amplicon within any given droplet be amplified to a detectable level within the complete program, but is not sensitive to whether reaching that threshold takes 10 or 30 cycles. The quantification is based on the fraction of droplets that contain a detectable signal within a sample. Thus this assay is likely to be more resistant to variability introduced by impurities in the FFPE extraction. Indeed, ddPCR demonstrated less variability within each sample compared to RT-qPCR (Figure 18). BRAF was detected in 46/51 with ddPCR, and 45/51 with qPCR. Sample (Q, CRC case) did not amplify with qPCR but was detected in ddPCR in all three replicates  $0.691 \pm 0.647$  copies/ $\mu$ l (mean $\pm$ SD), suggesting a more sensitive method for detecting low-abundant target See supplementary Table A 1 and Table A 2.

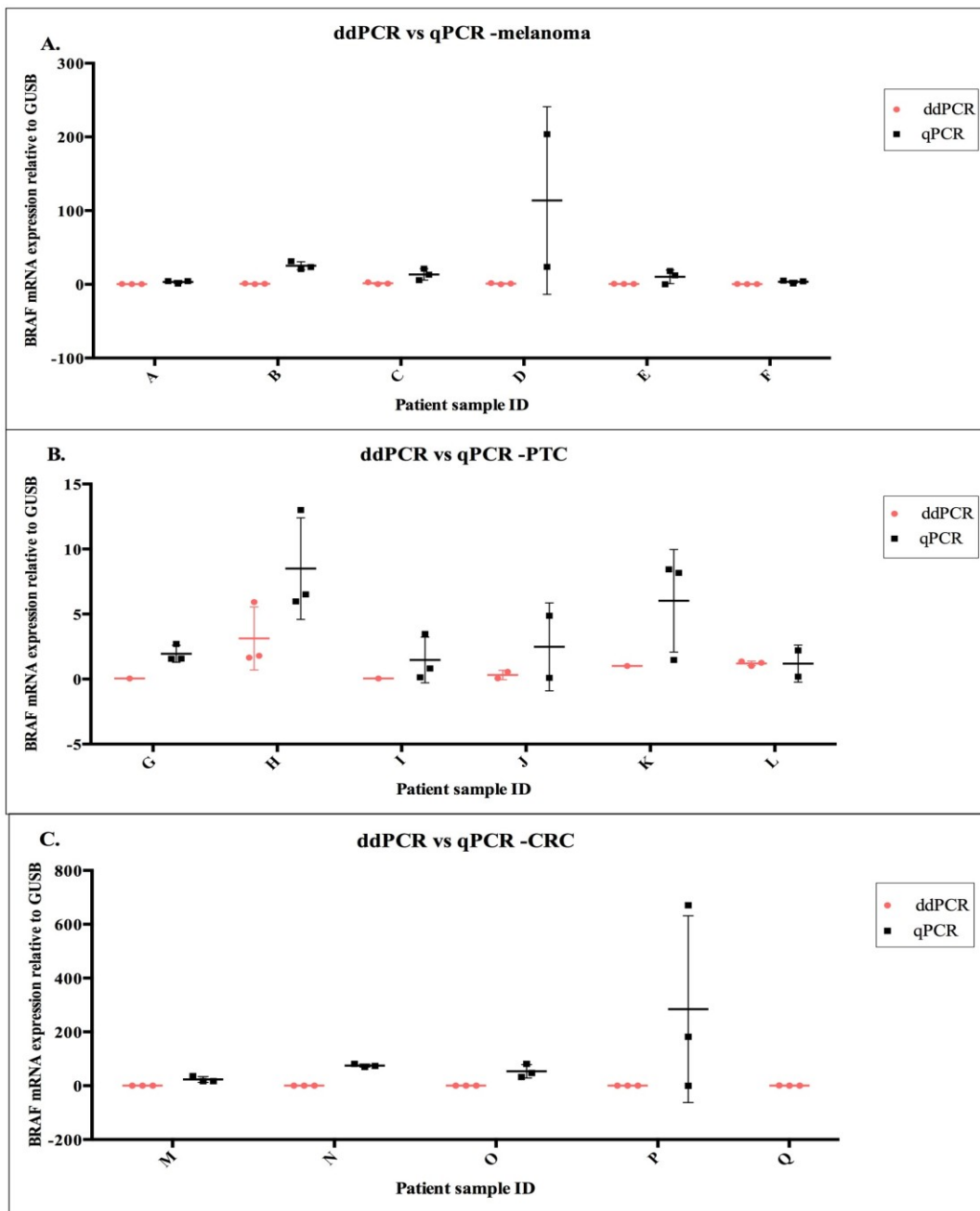


**Figure 18 Comparison between quantitative reverse transcriptase PCR (RT-qPCR) and digital droplet PCR (ddPCR) in detecting BRAF expression from FFPE samples.**

BRAF mRNA expression relative to reference gene GUSB assessed in **A.** Melanoma. **B.** PTC. **C.** CRC. Using ddPCR (circle) and RT-qPCR (square). Each point represents replicate measurements; bar represents the mean and standard deviation.

## 3.2 PROJECT 2: UTILIZATION OF CELL CULTURE BASED MODEL TO INVESTIGATE THE UNDERLYING MECHANISMS AND POTENTIAL TARGETS TO OVERCOME RESISTANCE

Many different mechanisms have been proposed to explain the development of resistance to BRAF targeted therapy. Most of this research has focused on melanoma, which often are initially responsive to therapy, but ultimately relapse with a resistant form of cancer. Only a small percent of positive BRAFV600E colon cancers are responsive to therapy even initially. Understanding what features distinguish these responsive colorectal cancers from other colorectal cancers might help find ways to identify responsive patients, find mechanisms to prevent the development of resistance, and develop tools to convert resistant tumours into sensitive ones.

We were interested in comparing melanoma and colorectal cancers in terms of the changes that occur in response to BRAF inhibitor treatment, and the changes that occur during the development of resistance to that treatment. We started by searching for possible cell lines to use in establishing an *in-vitro* model to investigate resistance to BRAF inhibitory treatment.

The Cancer Cell Line Encyclopaedia (CCLE) website was used to select cells based on the primary site (large intestine and skin) and histology (carcinoma, adenocarcinoma and malignant melanoma), then narrowed to cells harbouring the BRAFV600E mutation. Of these, we compared gene expression among cell lines accessible via ATCC (American

Type Culture Collection) and included in the GEO (Gene Expression Omnibus) dataset derived from a study of expression profiling by array on 947 human cancer cell lines (PMID: 22460905; GEO accession: GSE36133)<sup>243</sup>. Twenty-six melanoma cell lines carried the V600E mutation in the BRAF gene, including but not limited to, Malme-3, IGR-37, A2058, MDA-MB-435S, A375, SK-MEL-28, SK-MEL-1, and C32; while only six colon cancer cell lines carried the V600E mutation COLO205, SNU-C5, RKO, LS411N, COLO201, CL-34, and SW1417. We assessed the level of gene expression for a set of candidate genes that had previously been associated with the development of resistance to BRAF inhibition: BRAF, DUSP4, DUSP6, SPRY1, SPRY2, SPRY 4, and EGFR by utilizing the GEO online database at The National Center for Biotechnology Information (NCBI). The level of gene expression varied among both melanoma and colon cancer cell lines, in particular for the MAPK pathway regulator genes DUSP4, SPRY1, and SPRY4 (Figure 19 A, B).

It was not possible from the database or from the literature to confidently assess, which cell lines would be responsive and which would be resistant to therapy. The vast majority studies on BRAF mutation and resistance were conducted on melanoma but data were lacking other types of cancer including colon. In addition, there were disagreements in labeling cells' response to treatment as the same cell lines were identified as being sensitive in one paper but resistant with another study. There were not obvious expression differences among the genes associated with resistance that clearly showed a pattern difference between colon and melanoma cells.

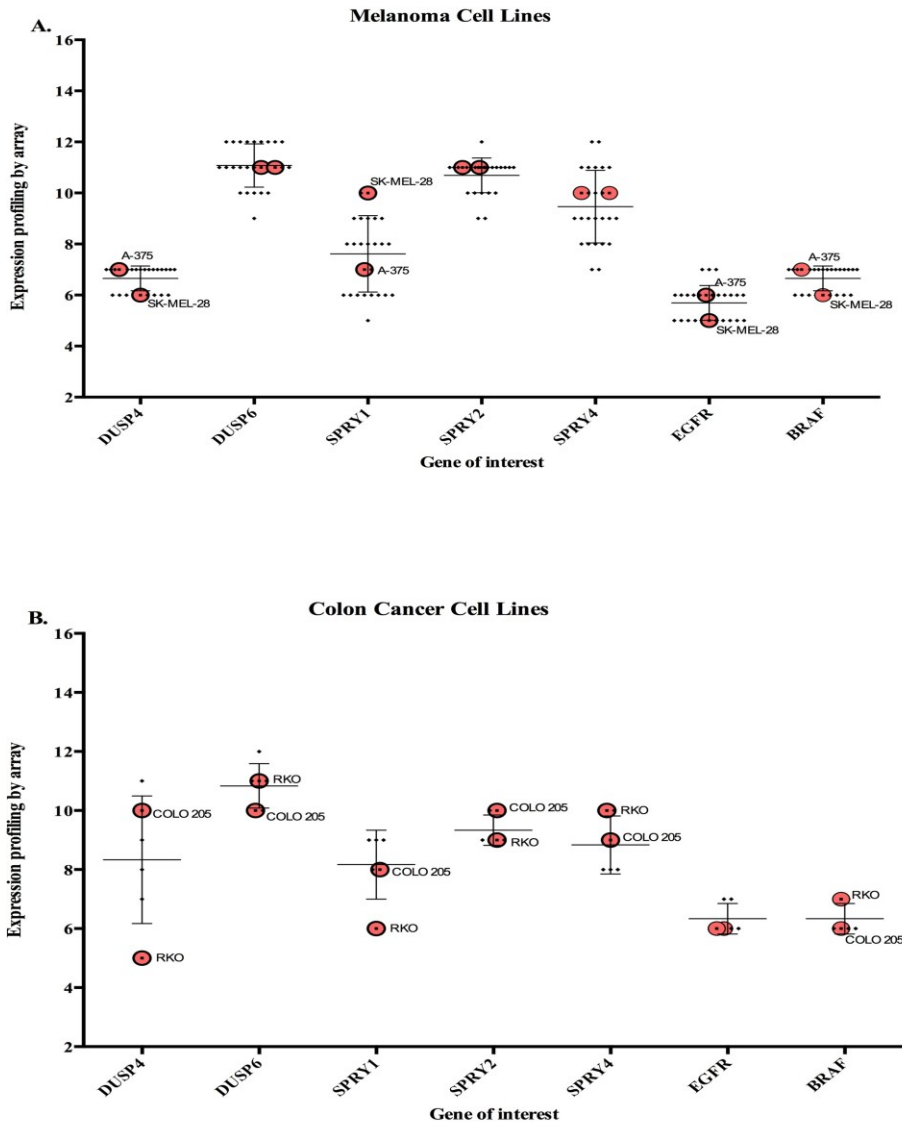


**Figure 19 Cell Lines gene expression as obtained from available online expression profiling study.**

Expression data from the Cancer Cell Line Encyclopedia demonstrating expression profiling for the MAPK pathway regulators (DUSPs and SPRYs family proteins), EGFR and BRAF. Data were plotted in a scatter graph, “Expression by array” on the y-axis against “Gene of interest” on the x-axis. Columns represent different genes and within each column individual cell line is presented as dot. Selected cell lines for this study are highlighted. **A.** 26 human Melanoma cell lines. **B.** Six human colon cancer cell lines.

Cell lines were therefore selected to try to capture melanomas and colorectal cancer cells that showed differences among our selected genes of interest. The following cell lines were selected A375 (human malignant melanoma), SK-MEL-28 (human malignant melanoma), COLO205 (human colorectal adenocarcinoma), RKO (human colon carcinoma); additional characteristics are listed in Table 8 on page 39.

Due to technical challenges, insufficient data was obtained for two of the selected cell lines: COLO205 (colon), and SK-MEL-28 (melanoma) due to time limitation for the current study. COLO205 cells were difficult to handle given their culture properties as they consist of mixed cell (adherent and suspension). By the end of the treatment course (establishing drug resistance) SK-MEL-28 cells were lost due to contamination during the establishment of resistance.

Establishing the *in-vitro* model started by investigating the cytotoxicity of BRAF inhibitor. The BRAF inhibitor (dabrafenib) was effective at inhibiting the growth of A375 melanoma cells (Figure 20), however RKO colon carcinoma cells were relatively insensitive to this treatment (Figure 21). A375 melanoma cells displayed an EC50 value of  $20.9 \text{ nM} \pm 13.7 \text{ nM}$ , calculated using a sigmoidal dose response with a fixed maximum (100%) and fixed minimum (0%) (Figure 20). With the RKO colon cells, even the highest concentrations tested did not fully inhibit growth (Figure 21). To estimate the half-maximal effect, EC50 value, curves were constructed with only the maximum was fixed at 100%, and the minimum was not constrained. Under this model, the calculated EC50 values fell in the range 80 to 400 nM.



### naïve A375

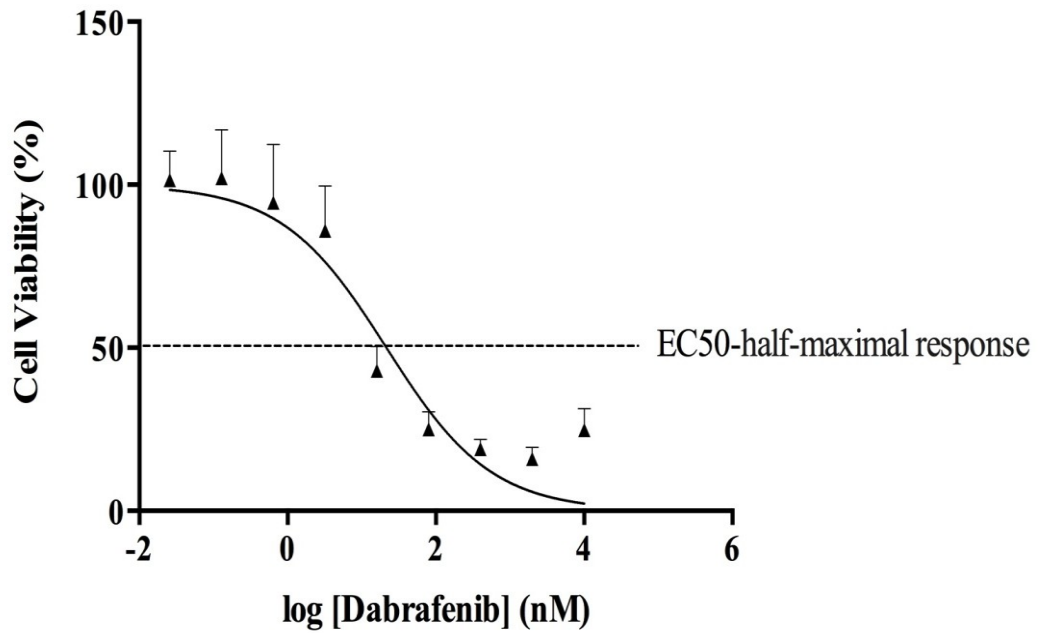


**Figure 20 Cytotoxicity effect of BRAF inhibitor (dabrafenib) on A375 melanoma cells.**

Dose-response curve for A375 melanoma cells expressing BRAFV600E. Cells were treated with increasing concentration of dabrafenib for 72 hr in Sextuplicate. Cell viability was calculated relative to the vehicle control (0.1% DMSO). Data are represented as mean  $\pm$  SD from three independent experiments (n=3).

## naïve RKO

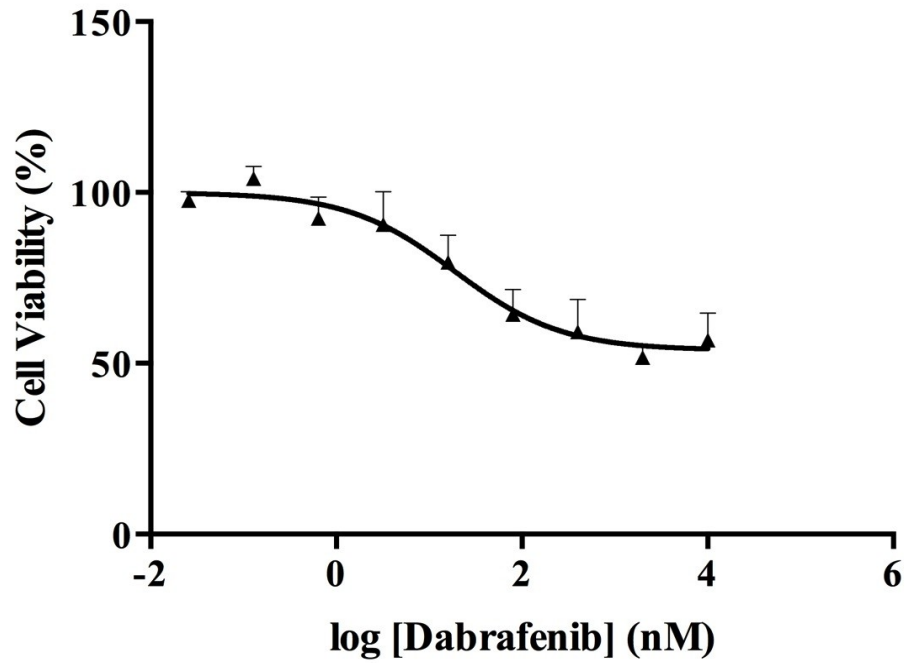


**Figure 21 Cytotoxicity effect of BRAF inhibitor (dabrafenib) on RKO colon carcinoma.**

Dose-response curve for RKO colon carcinoma cells expressing BRAFV600E. Cells were treated with increasing concentration of dabrafenib for 72 hr in Sextuplicate. Cell viability was calculated relative to the vehicle control (0.1% DMSO). Data are represented as mean  $\pm$  SD from three independent experiments (n=3).

We next established dabrafenib-resistant cell lines in culture. A375 and RKO were treated with 20.9 and 239.6 nM dabrafenib respectively for 21 -31 days. We confirmed the resistance status for both cell types by comparing the concentration-response curves of naïve to resistant cells treated with dabrafenib for 72 hours. Melanoma cells displayed a shift in the EC50 value from 21 nM (naïve A375) to 420 nM (Resistant-A375) (Figure 22). Although the RKO cells were relatively insensitive to dabrafenib initially, they also become more insensitive to dabrafenib (Figure 23).

We thereafter set out to assess the impact of dabrafenib treatment in melanoma versus colon carcinoma cells by looking at the differences in expression of genes associated with the development of BRAF inhibitor resistance. In resistant A375 compared to naïve cells, six genes were down-regulated DUSP4, DUSP6, SPRY4, BRAF, NOX1, and NOX4 in a range from 0.009- to 0.17-fold; while only three genes SPRY1, SPRY2, and EGFR demonstrated up-regulation with fold change > 6.1, 3.3, and 11, respectively (Figure 24, and supplementary Figure A 1). Resistant RKO cells exhibited increases in the same genes as R-A375 melanoma cells (Figure 25, and supplementary Figure A 1).

We next examined the effect of combining MEK inhibitor (trametinib) with BRAF inhibitor (dabrafenib) on cytotoxicity. Both naïve A375 and RKO cells were sensitive to for 72 hour treatment with trametinib (Figure 26; A and B respectively). We identified a single dose of trametinib (1nM) approximately the half-maximal response and suitable for both cell lines. Naïve cells (A375, RKO) and resistant cells (R-A375, R-RKO) were then

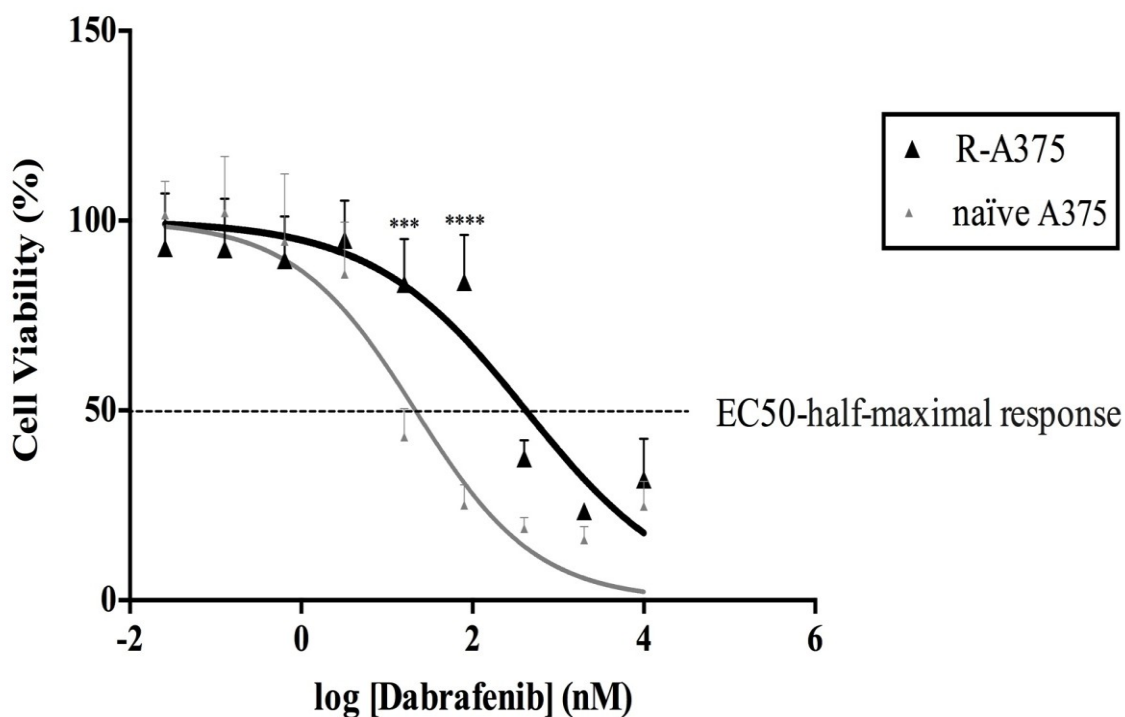


**Figure 22 Comparison of cytotoxicity effect of BRAF inhibitor (dabrafenib) on naïve and resistance A375 melanoma cells.**

Normalized cell viability values relative to the vehicle control (0.1% DMSO) as determined by AlamarBlue assay for naïve A375 (gray line with small triangle symbol) and established dabrafenib-resistance (R-A375) cells (dark line with large triangle symbol). Cells were seeded at density of  $3 \times 10^4$  cells/ml in 96 well culture plate and incubated at 37°C, 5% CO<sub>2</sub> with increasing concentration of dabrafenib for 72 hours. Dotted line across the 50% indicates the half-maximal response as determined from sigmoidal dose-response curve. Data are represented as mean  $\pm$  SD from three independent experiments (n=3). Asterisks indicate significant differences between naïve and resistance cells (Two-way ANOVA, Sidak's multiple comparisons test).

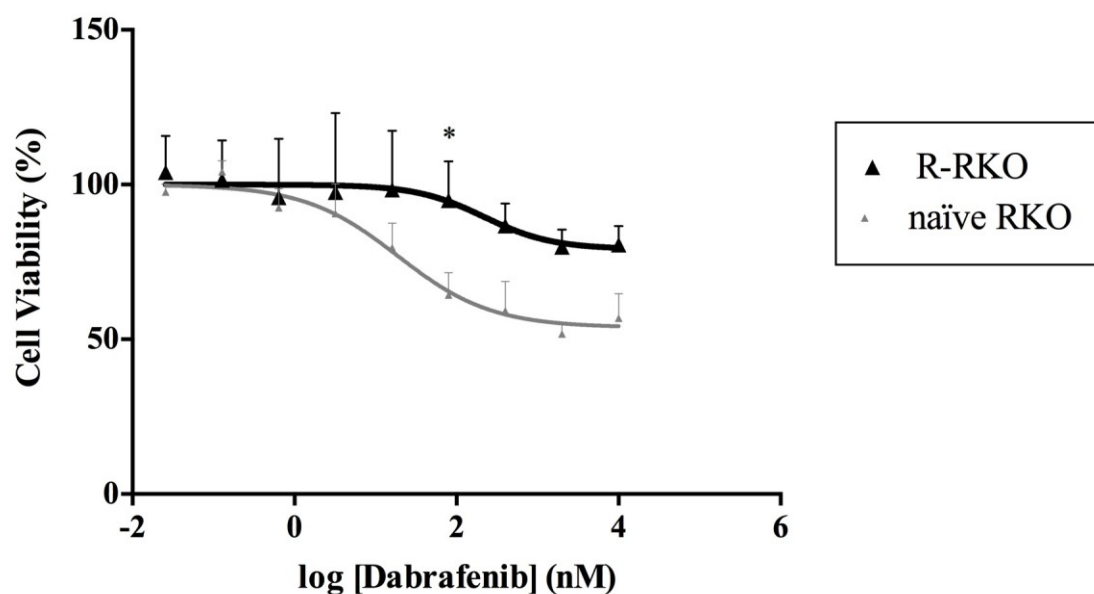


**Figure 23 Comparison of cytotoxicity effect of BRAF inhibitor (dabrafenib) on naïve and resistance RKO colon carcinoma.**

Normalized cell viability values relative to the vehicle control (0.1% DMSO) as determined by AlamarBlue assay for naïve RKO (gray line with small triangle symbol) and established dabrafenib-resistance (R-RKO) cells (dark line with large triangle symbol). Cells were seeded at density of  $3 \times 10^4$  cells/ml in 96 well culture plate and incubated at 37°C, 5% CO<sub>2</sub> with increasing concentration of dabrafenib for 72 hours. Data are represented as mean  $\pm$  SD from three independent experiments (n=3). An asterisk indicates significant differences between naïve and resistance cells (Two-way ANOVA, Sidak's multiple comparisons test).

### A375 resistant cells

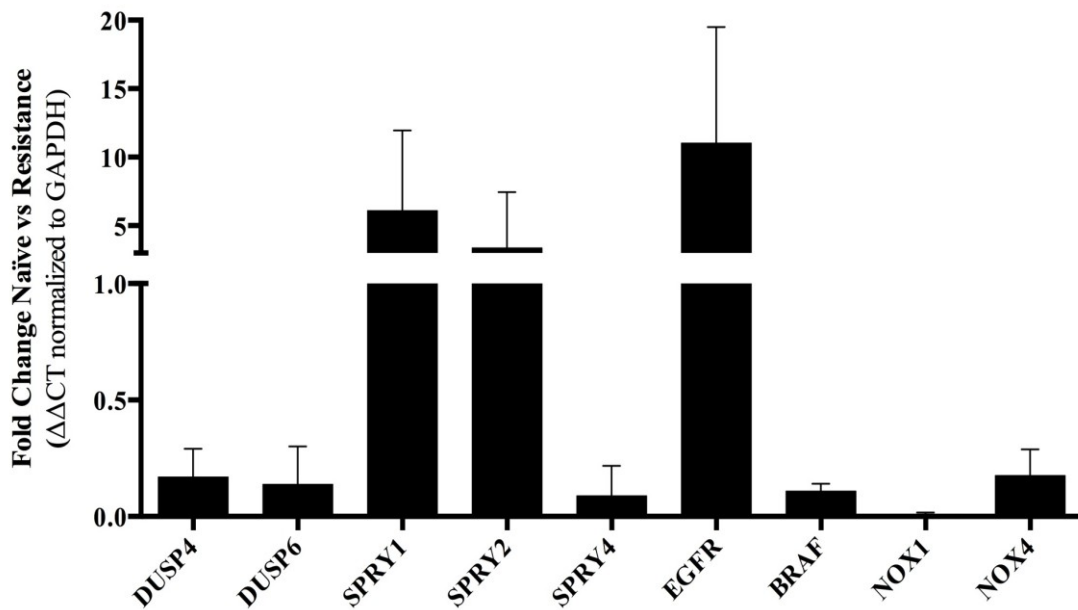


**Figure 24 Effect of dabrafenib treatment on gene expression.**

Bar graph showing the mean  $\pm$  SD (n=2,3) in  $\Delta\Delta C_t$  values of fold change between mRNA expression between naïve and resistance A375 melanoma cells. Fold change in expressions was calculated using  $2^{-\Delta\Delta C_t}$  assuming 100% efficiency.

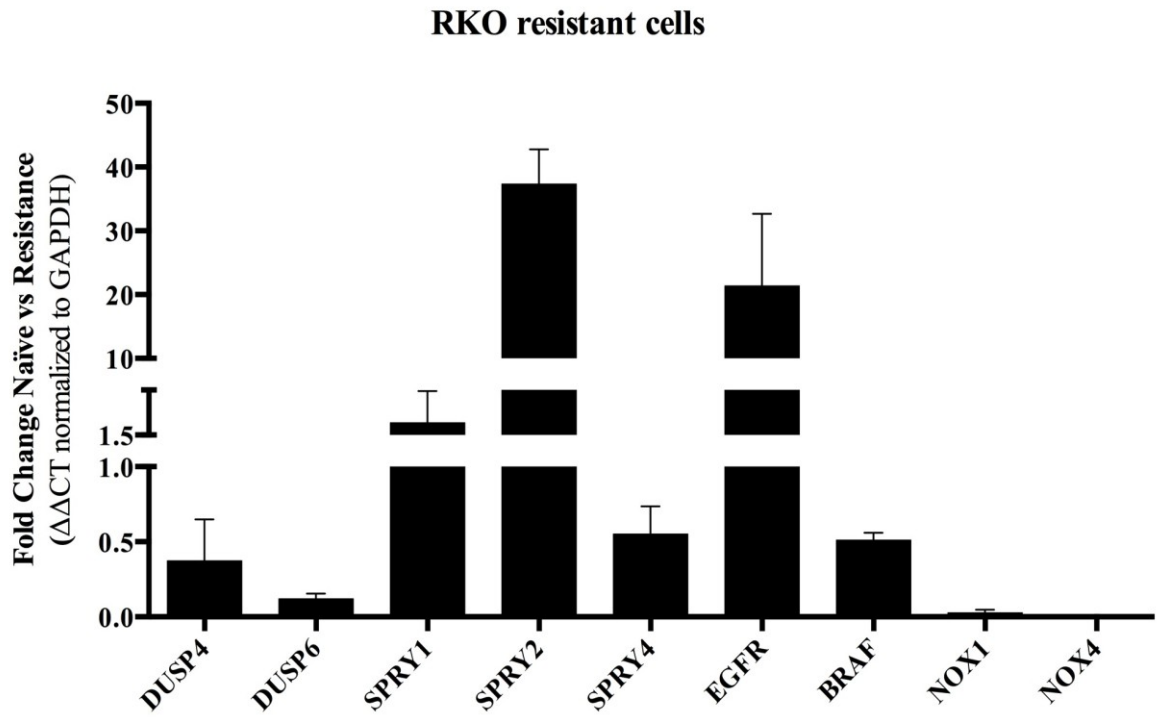


**Figure 25 Effect of dabrafenib treatment on gene expression.**

Bar graph showing the mean  $\pm$  SD (n=2,3) in  $\Delta\Delta C_t$  values of fold change between mRNA expression between naïve and resistance RKO colon carcinoma cells. Fold change in expressions was calculated using  $2^{-\Delta\Delta C_t}$  assuming 100% efficiency.

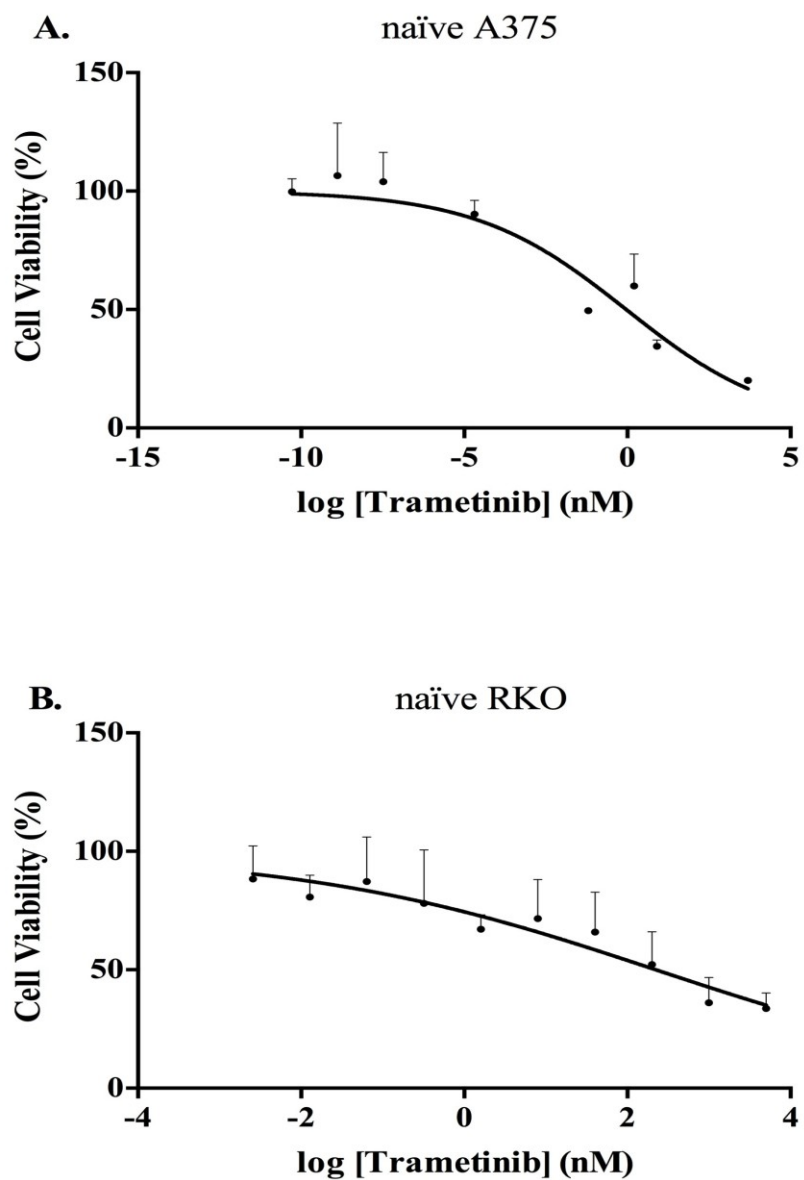


**Figure 26 Cytotoxicity effect of MEK inhibitor (trametinib) on naïve A375 melanoma and RKO.**

Dose-response curve for **A.** A375 melanoma cells (n=2). **B.** RKO colon carcinoma (n=3). Cells were treated with increasing concentration of trametinib for 72 hr in Sextuplicate. Cell viability was calculated relative to the vehicle control (0.1% DMSO). Data are represented as mean  $\pm$  SD from three independent experiments.



treated for 72 hours with a range of concentrations of dabrafenib with and without the presence of trametinib at 1nM. Our results indicate that combination therapy of BRAF inhibitor plus MEK inhibitor has improved the potency of BRAF inhibitor not only in naïve cells but also in dabrafenib-resistance cells (Figure 27 and Figure 28). The results thus obtained are compatible with what have been seen in clinical studies<sup>99,154,226,244</sup>.

Changes in reactive oxygen species generation have been observed in both melanoma and colon cancer development. The impact of treatment on ROS generation, or the impact of ROS generation on the development of resistance has received relatively little attention. We therefore assessed the effect of dabrafenib treatment on ROS generation, what if any effect the development of resistance had on ROS generation, and what if any effect ROS inhibition had on sensitivity to BRAF inhibition.

We examined the cytotoxicity of resveratrol, a plant-derived polyphenolic phytoalexin along with ROS scavenging activity<sup>229</sup>; Diphenyleneiodonium (DPI) a classical inhibitor of NADPH oxidase<sup>228</sup>; and celastrol<sup>231</sup>; a plant derived compound that inhibits NOX enzymes. Naïve cells (A375, RKO) and resistance cells (R-A375, R-RKO) were treated with three different concentrations that evident to have inhibitory effects (1, 5, and 10  $\mu$ M) of resveratrol, DPI, and celastrol with a vehicle control (1% DMSO). Cell toxicity was measured using Alamar Blue assay. DPI and celastrol were very toxic even with the lowest dose of 1  $\mu$ M (Supplementary Figure A 2). Resveratrol on the other hand stimulated cell growth. However, resveratrol was eliminated due to its multiple modes of action.

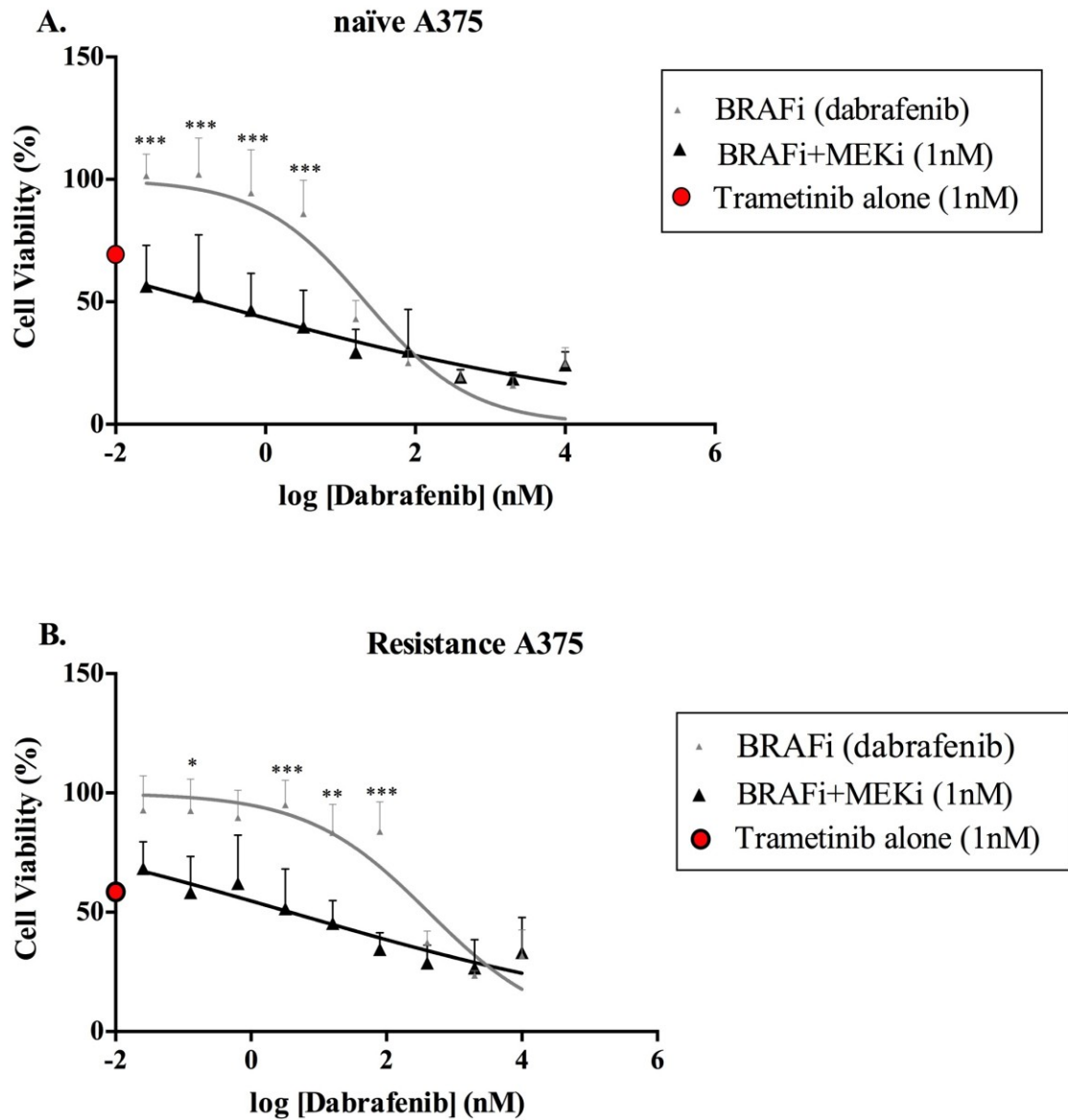


**Figure 27 Enhanced dabrafenib (BRAF inhibitor) potency after combination with trametinib (MEK inhibitor).**

A375 naïve and resistance cells were treated for 72 hours with increasing doses of dabrafenib with and without the presence of trametinib. Cell viability was calculated relative to the vehicle control (0.1% DMSO). **A.** naïve A375. **B.** Resistance-A375. Data are represented as mean  $\pm$  SD from three independent experiments (n=3). Asterisks indicate significant differences (Two-way ANOVA, Sidak's multiple comparisons test).

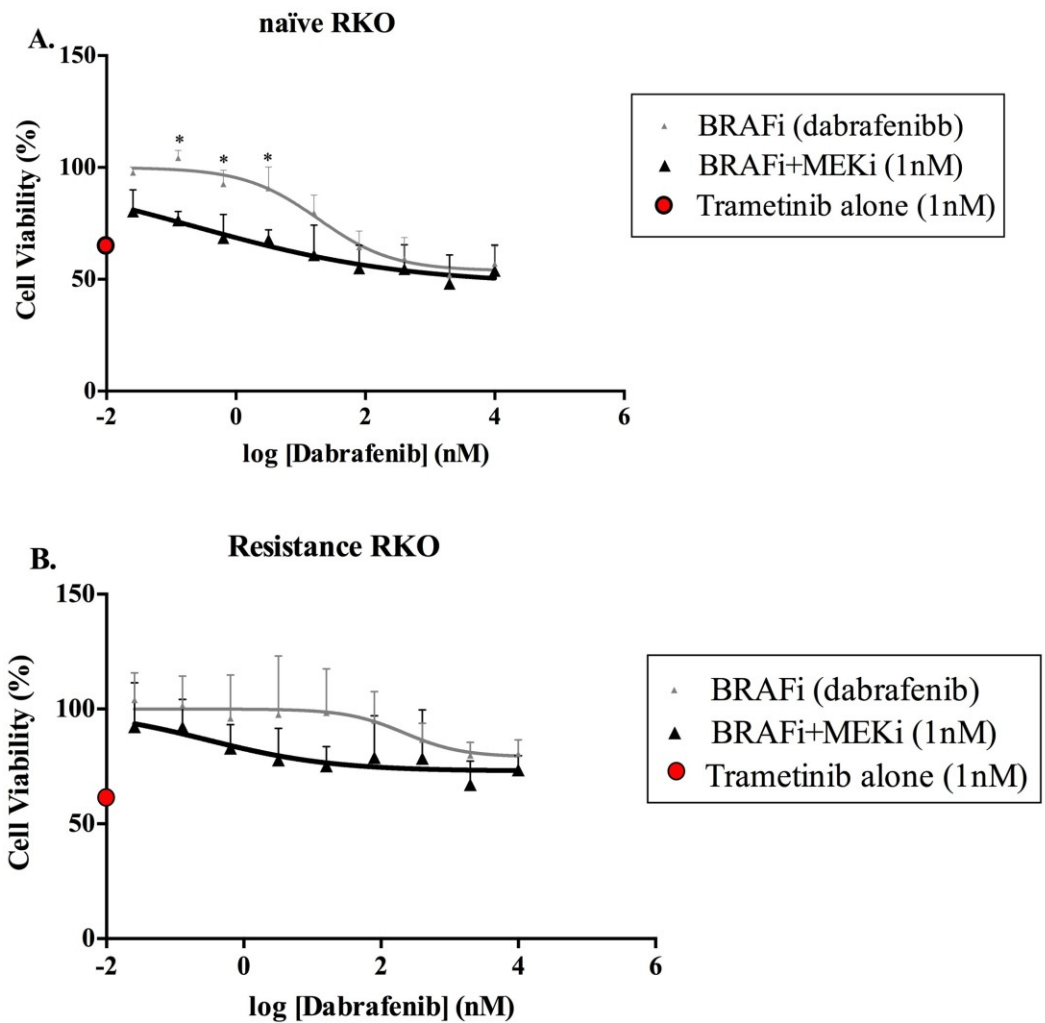


**Figure 28 Enhanced dabrafenib (BRAF inhibitor) potency after combination with trametinib (MEK inhibitor).**

RKO naïve and resistance cells were treated for 72 hours with increasing doses of dabrafenib with and without the presence of trametinib. Cell viability was calculated relative to the vehicle control (0.1% DMSO). **A.** Naïve RKO. An asterisk indicates significant (Two-way ANOVA, Sidak's multiple comparisons test). **B.** Resistance- RKO. No significant differences were noted (Two-way ANOVA, Sidak's multiple comparisons test). Data are represented as mean  $\pm$  SD (n=3).

We next selected an agent with ROS scavenging activity, trolox, a vitamin E analog<sup>232</sup>. Toxicity of trolox was examined on A375 melanoma cells at three different concentrations 1mM, 100, and 10  $\mu$ M alone and with the presence of BRAF inhibitor, dabrafenib and then cell viability was evaluated using Alamar Blue assay (Supplementary Figure A 2). Trolox treatment was not toxic to cells compared to the other agents that we tested. Experiments were then undertaken to confirm that the cells in fact do generate ROS and trolox treatment decreased the level of ROS. Cells were treated for 48 hours with trolox at 25, 50, 250  $\mu$ M and 1mM. Hydrogen peroxide ( $H_2O_2$ ) was detected in naïve cells A375, and R-A375 (Figure 29) and in naïve RKO, and R-RKO (Figure 30). Trolox treatment displayed concentration-dependent effect on scavenging ROS that evident by decline in  $H_2O_2$  production compared to no treatment control. Since 1mM trolox was most effective in decreasing ROS generation, and was not toxic, this concentration was selected.

Short-term treatment of resistant A375 melanoma cells with dabrafenib did not lead to a detectable change in ROS generation (Figure 31). In RKO cells on the other hand, particularly after cells acquired resistance, dabrafenib treatment led to an increase in ROS generation (Figure 32). As anticipated, trolox treatment reduced ROS generation in naïve and resistance cells. Nonetheless, an unexpected finding was the higher ROS production in resistance RKO colon carcinoma cell lines under the condition of combining BRAF inhibitor with trolox compared to trolox alone (Figure 32).

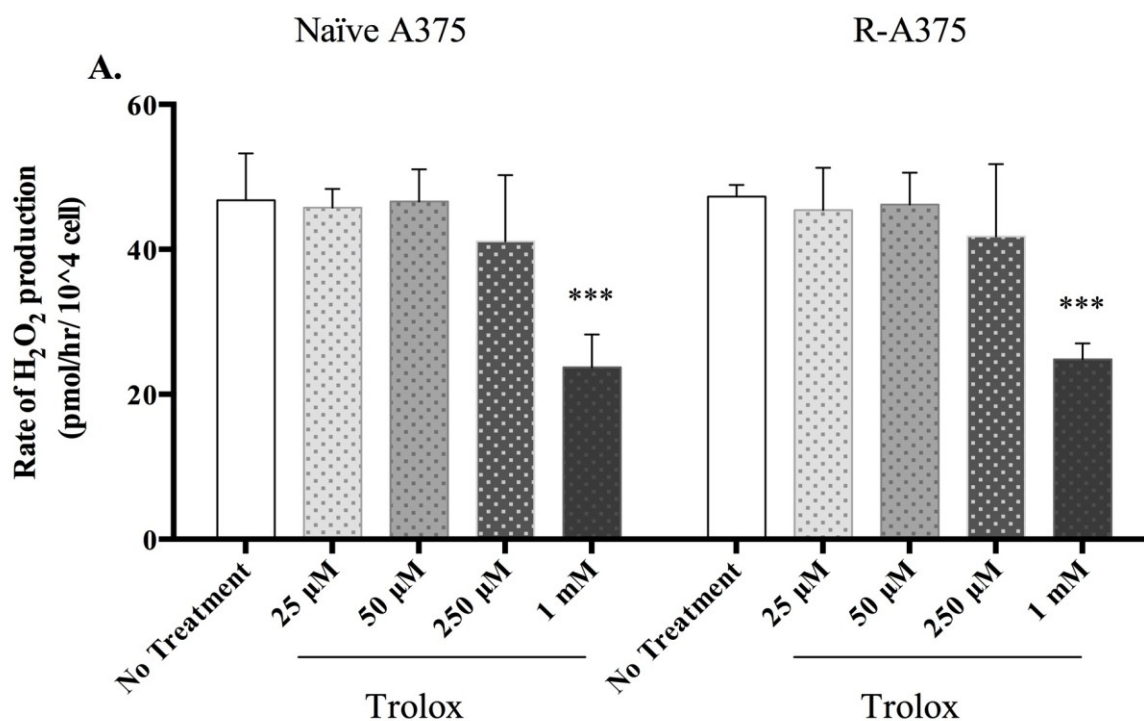


**Figure 29 Concentration-dependent effect of trolox on scavenging ROS in A375 naïve and resistance cells.**

The rate of H<sub>2</sub>O<sub>2</sub> productions was measured using AmplexRed assay in naïve and resistance A375 melanoma cells. Fluorescence was measured using the Infinite M200 Pro microplate reader (Tecan Group Ltd., Männedorf, Switzerland) at 37°C every two minutes for 30 cycles with excitation at 530 nm and emission at 590 nm. Asterisks indicate significant differences from no treatment control (Two-way ANOVA, Dunnett's multiple comparisons test). Bars indicate mean standard deviation (n=3).

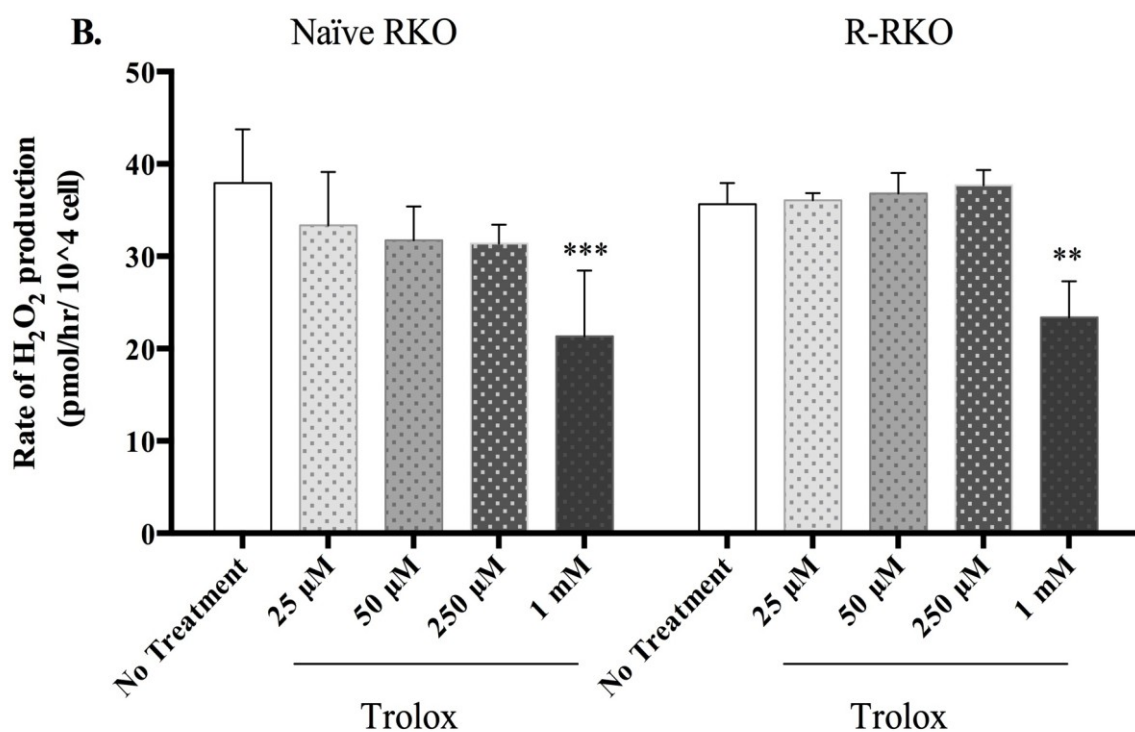


**Figure 30 Concentration-dependent effect of trolox on scavenging ROS in RKO naïve and resistance cells.**

The rate of H<sub>2</sub>O<sub>2</sub> productions was measured using AmplexRed assay in naïve and resistance RKO colorectal cancer cells. Fluorescence was measured using the Infinite M200 Pro microplate reader (Tecan Group Ltd., Männedorf, Switzerland) at 37°C every two minutes for 30 cycles with excitation at 530 nm and emission at 590 nm. Asterisks indicate significant differences from no treatment control (Two-way ANOVA, Dunnett's multiple comparisons test). Bars indicate mean standard deviation (n=3).

### A375 melanoma cells

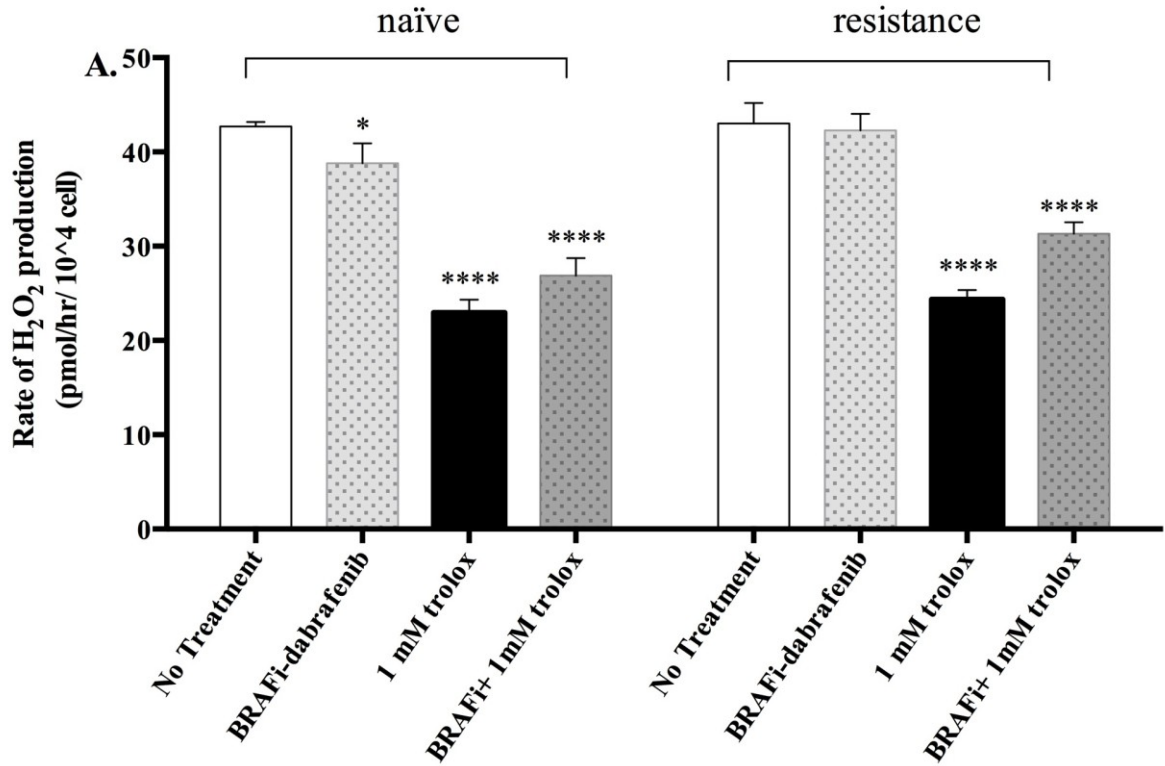


**Figure 31 Evaluation of Reactive Oxygen Species (ROS) productions in A375 melanoma cells.**

Detection and measurement of ROS generation in naïve A375 melanoma cell (left bars) and in resistance A375 (right bars). The rate of H<sub>2</sub>O<sub>2</sub> was calculated from H<sub>2</sub>O<sub>2</sub> standard curve. Asterisks indicate significant differences from no treatment control (Two-way ANOVA, Dunnett's multiple comparisons test). Data were presented as mean and error bar indicate standard deviation (n=3).

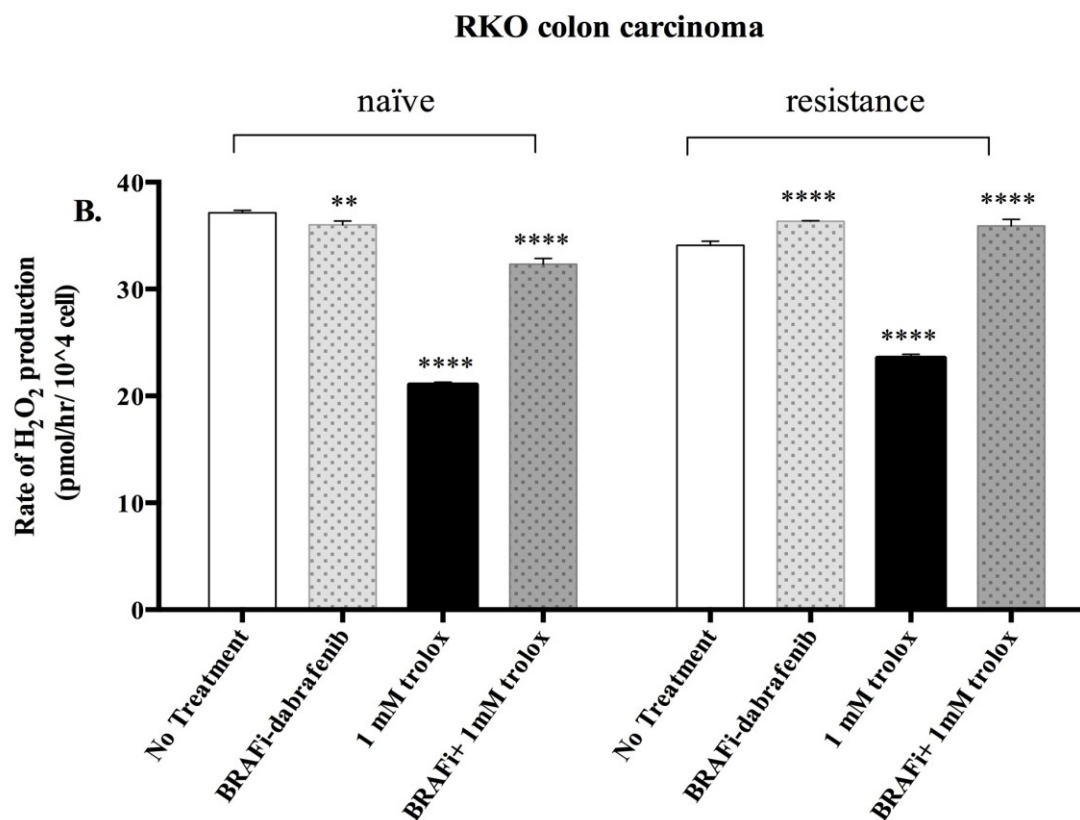


**Figure 32 Evaluation of Reactive Oxygen Species (ROS) productions in RKO colon carcinoma cells.**

Detection and measurement of ROS generation in naïve RKO colon carcinoma cell (left bars) and in resistance RKO (right bars). The rate of H<sub>2</sub>O<sub>2</sub> was calculated from H<sub>2</sub>O<sub>2</sub> standard curve. Asterisks indicate significant differences from no treatment control (Two-way ANOVA, Dunnett's multiple comparisons test). Data were presented as mean and error bar indicate standard deviation (n=3).



We next examined whether scavenging ROS alters the sensitivity to BRAF inhibition. Cell viability was examined with increasing concentrations of dabrafenib in the presence or absence of trolox. The addition of trolox shifted the curve to the left indicating an enhanced in the potency of BRAF inhibitor trolox for both A375 (Figure 33) and RKO cells (Figure 34). Trolox alone shifted the curve down, suggesting some decrease in viability from the presence of trolox. However, comparing the individual EC50 values obtained for A375 cells, the results suggested that for naïve cells, trolox reduced sensitivity to dabrafenib treatment, but in the resistant cells this was not observed (Figure 35, A). Although not significant, there was a trend towards resistant cells displaying increased sensitivity to dabrafenib in the presence of trolox (Figure 35, B).

Similar results were obtained from RKO colon carcinoma cells (Figure 34). As RKO cells failed to produce sigmoidal concentration-response curves, we fit the data using linear curves (Figure 36). We compared the slopes of the cell viability with increasing concentration of BRAF inhibitor alone to the slope in the presence of trolox. The results demonstrate that in resistant RKO cells, the addition of trolox improves dabrafenib toxicity.

### A375 melanoma cells

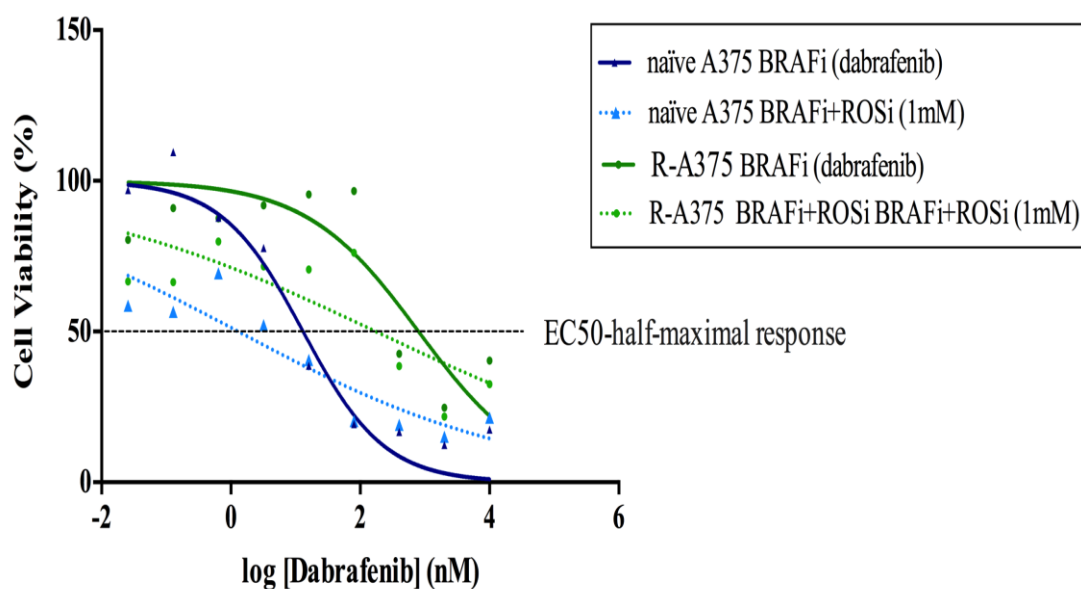


**Figure 33 Representative curves comparing the cytotoxicity effect of BRAF inhibitor (dabrafenib) alone and in combination with trolox.**

A375 naïve and resistance cells were treated for 72 hours with increasing doses of dabrafenib with and without the presence of trolox at 1mM. Cell viability was calculated relative to the vehicle control (0.1% DMSO). Solid lines represent dabrafenib treatment (BRAFi) and dotted lines represent combination strategy of dabrafenib plus trolox. (n=1).

### RKO colon carcinoma

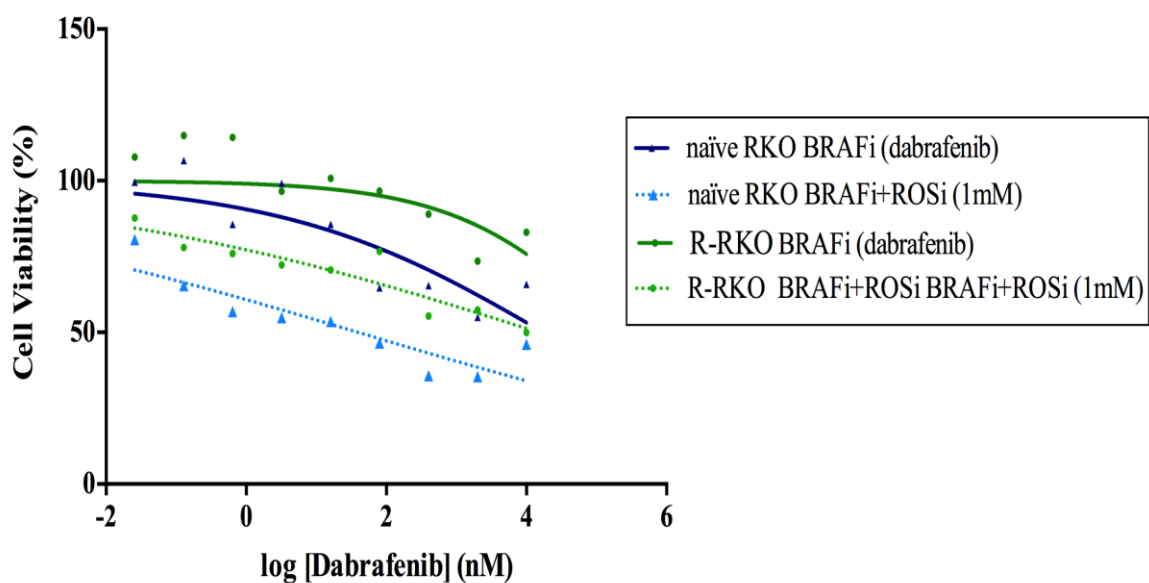


**Figure 34 Representative curves comparing the cytotoxicity effect of BRAF inhibitor (dabrafenib) alone and in combination with trolox.**

RKO naïve and resistance cells were treated for 72 hours with increasing doses of dabrafenib with and without the presence of trolox at 1mM. Cell viability was calculated relative to the vehicle control (0.1% DMSO). Solid lines represent dabrafenib treatment (BRAFi) and dotted lines represent combination strategy of dabrafenib plus trolox. (n=1).

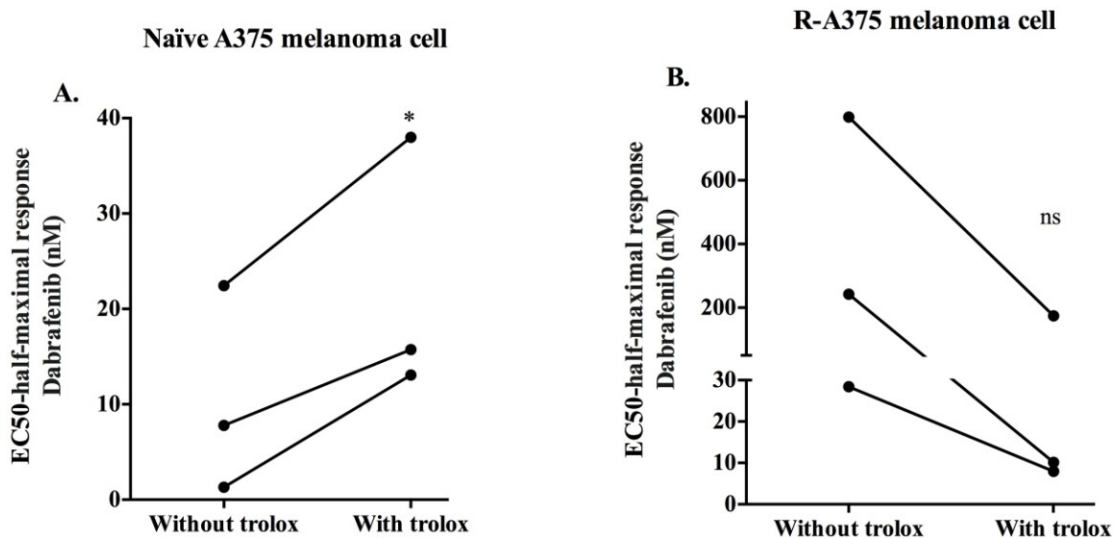


**Figure 35 EC50-half-maximal response comparison in naïve and resistance A375 melanoma cells.**

EC50 values for naïve and resistance A375 melanoma cells after treatment with increasing concentration of dabrafenib and/or dabrafenib plus trolox from 3 independent experiments. **A.** An asterisk indicates significant differences between dabrafenib alone (without trolox) compared to when combined with trolox (Paired, two tailed T-test). **B.** No significant differences were noted (Paired, two tailed T-test).

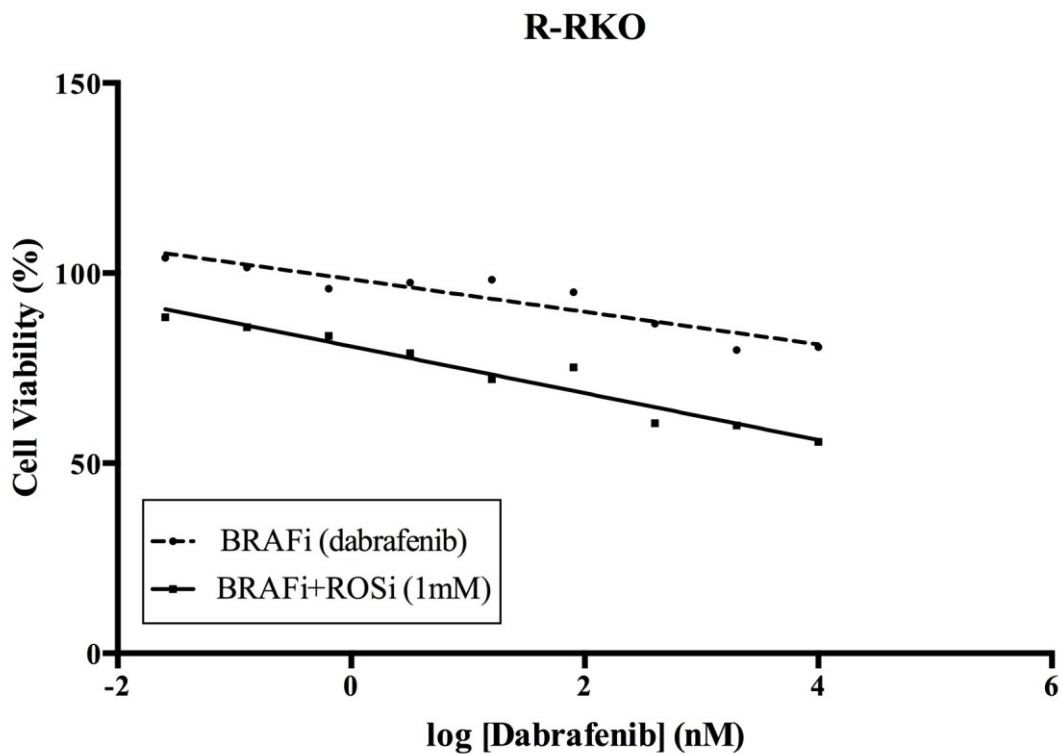


**Figure 36 Linear regression curve comparisons in naïve and resistance RKO colon carcinoma cells.**

Linear regression analysis for naïve and resistance RKO cells after treatment with increasing concentration of dabrafenib (n=3) and/or dabrafenib plus trolox (n=2). Confidence intervals were determined by linear regression. R2 values for BRAFi (dabrafenib) =0.8654. BRAFi+ROSi (trolox) =0.9435. The slope was  $-4.284 \pm 0.6386$  for BRAFi (dabrafenib) and  $-6.156 \pm 0.5692$  for BRAFi+ROSi (trolox). Data were plotted as mean.

## CHAPTER 4      DISCUSSION

### 4.1 PROJECT 1

Current clinical methods used in the detection of BRAFV600E positive tumour include IHC and sequencing of tumour DNA. IHC is very sensitive in detecting the BRAFV600E mutation. However, IHC is not an ideal assay to assess the level of expression. It is interpreted subjectively based on the color intensity of the stain on the slides. Generally slides are categorized using a scoring system based on intensity of staining and the percentage cells that stain, however as there is no standardized guidelines for interpreting IHC results<sup>245</sup> the results may vary between individual pathologists and between labs.

On the other hand, IHC staining does have some advantages over DNA based tests. DNA based tests could detect the presence of the mutation, but say nothing about in which cells the mutation is present, nor to what extent the mutant protein is being expressed. The VE1 antibody used in IHC specifically recognizes the mutant BRAFV600E protein<sup>93</sup>, and permits the visualization of the distribution and localization of the mutant protein expression within the tissue and cells<sup>246</sup>. One advantage of seeing the distribution is that can distinguish between situations where a few cells express a lot of the mutant protein or where all cells express a little.

One of the aims of this project was to consider the feasibility and utility of using an RNA based assay that could potentially offer an easier, less expensive, quantitative test

that provides information on the level of expression of mutant BRAF. In addition, an RNA test could be easily expanded to follow other functionally relevant changes that occur at different stages in the progression and treatment of the disease. Therefore, ultimately, the goal is to provide a test that could be used to improve diagnosis, but also be extended to provide information about prognosis and response to therapy.

Detection of mRNA expression in FFPE tumour specimens could be a valuable tool given their substantial availability as the most common archived specimen. Despite limitation such as loss of RNA integrity as a result of FFPE processing and/or storage conditions, continuous progress has been made in improving strategies in RNA isolation<sup>247,248</sup> and assay design<sup>249</sup>. A study by Kokkat *et al.*<sup>250</sup> revealed that there were no significant differences found when comparing the quality and quantity of macromolecules extracted from FFPE stored for over 12 years to fresh FFPE block. Another study by Kashofer *et al.*<sup>251</sup> examined the effect of different fixation methods on the variability of RT-qPCR performance and identified that measuring cDNA synthesis efficiency could overcome negative impact of crosslinking of RNA introduced by formaldehyde fixation<sup>252</sup>. We have considered the consequence of this fixation method as the RNA isolation technique employed proteinase K that is able to liberate RNA from crosslinked protein and nucleic acid. This digestion step was performed while incubating samples at 60°C allowing for breakdown of actual crosslinks. Particular attention is also paid to RNA fragmentation as we addressed by two ways: cDNA generation was performed using random primers so that amplification was not limited to the poly A tail at the 3' end of a transcript, and amplicon length was shortened.

The first detection method used in this study was developed previously in the lab by Michael Mackley<sup>233</sup> and displayed mutational specificity employing a TaqMan- allele-specific chemistry when applied to different ratios of a mixtures of vectors with and without the mutation. However, when applied here to cDNA from FFPE samples, the results obtained showed high variability both between samples obtained from the same slide, and within the same RNA sample when processed 3 times.

One possible explanation for the variability might be contamination of non-tumour cells within samples. It is impossible to get a sample that is 100% tumour and there is always the possibility of 10-20% contamination resulting in variation. This differences in the cellular makeup could include other cell type including inflammatory cells, and stromal cells affecting the overall changes in the relative level of BRAF expression that reflect different cell populations rather than different disease status. To avoid this difficulty, it is necessary to adopt a new technology such as cell-isolation method where a 100% purity of isolate specific tumour cell avoiding tumour heterogeneity<sup>253</sup>, or use a cell-type specific gene in order to estimate and quantify the level of contamination looking for instance at vascular cells, inflammatory cells, or fibroblast cells.

The extent of variability within a given sample measured multiple times suggests a technical problem with the assay. Some possible explanations for this include pipetting errors, variability of the PCR cycle, a problem with the PCR amplification, or a problem with the probes distinguishing between the mutant and the wildtype transcript in the FFPE samples. We developed an assay approach that used pipetting volumes of 2.5 µl or more at all steps, and this along with the close agreement of the replicates on the standard



curves argues against pipetting errors the main source of the variability. We can also disregard well-to-well variability in this study because the Rotor-Gene Q real-time PCR detection system operates in rotary format allowing samples to move through the same optics and thermoregulation, so all wells should be the same. One possible explanation for this might be the length of the amplified product (192 bp) being not suitable for FFPE samples. Typical amplicon lengths for RNA extracted from FFPE is 100 bp<sup>254</sup>. To address this we designed primers to amplify a shorter fragment. However, a good design for a shorter fragment that would still work with the TaqMan probes was not found. Further, as one of the possible issues was with the probes distinguishing between the mutant and wildtype, we opted for a more simplified approach using a portion of BRAF distant from the mutation to evaluate digital droplet PCR. We also opted to compare the method to a SYBR green based approach, a fluorescent dye that binds to double-stranded DNA. This approach, while it has the potential to be less specific than TaqMan, offers the advantage over TaqMan of providing independent way of assessing the accuracy of the amplified product by looking at the melt curve rather than the shape of the amplification plot.

Other mutational specific technique would be a good candidate for this purpose is the multiplex ligation-dependent probe amplification (MLPA) detection method<sup>255</sup>. This method has the potential to discriminate known point mutations as in BRAFV600E. The feasibility of this method in assessing the presence of the BRAFV600E mutation in DNA extracted from FFPE of melanoma tumours has been demonstrated by Lake, et al.<sup>256</sup>.

We were aiming to compare the potential utility of droplet digital PCR (ddPCR) over quantitative reverse transcriptase PCR (RT-qPCR). In qPCR we are looking at how many cycles it takes for the amount of fluorescent product to reach a threshold value ( $C_q$ ). On the other hand, ddPCR is an end point measurement where fragments are dispersed into individual droplets for the PCR reaction to take place, and in the end we check each droplet to see whether it fluoresces or not. Thus the assay is less sensitive to differences in primer efficiency, or inhibitory factors that might slow the rate of amplification in some samples. As long as the fragment can be amplified eventually, the droplets will produce a signal.

Based on our assessment of these two detection methods, it can be concluded that despite possibly poor RNA quality, the gene expression could be measured from RNA extracted from FFPE tumour specimens. While the data did not directly assess the optimal amplicon length, our results support an approach of designing amplicons less than 100 bp. Droplet digital PCR was superior to RT-qPCR as it resulted in better agreement between reads and is able to detect low copy number target. It provides the absolute copies/ $\mu$ l directly without the need for generating a standard curve. The visualization of signal amplitude and the distinct separation between positive and negative signals makes it easier to exclude droplets without an amplified product and other interfering signals resulting from primer dimers represented as interphase drops. In TaqMan based RTqPCR, primer dimers and non-specific amplifications may give me  $C_q$  values that may not be easily distinguished from real signals. In SYBR green based PCR, these can be detected from melt curve analysis, but one cannot detect if amplification

proceeded slowly due to contaminants, which is not an issue in ddPCR. Another significant advantage of ddPCR is the reduced requirement for technical replicates unless the total events number of positive and negative was less than 12000 events, as each reaction in ddPCR is partitioned into 20,000 nano liter (nl) sized droplets for single amplification events. This is particularly significant factor when only small amount of samples are available. Two of the key elements to performing successful ddPCR are; primer optimization and cDNA dilution. Since ddPCR work best with very low copy number target (samples that produce C<sub>q</sub> values of 25 and higher with qPCR), a high concentration of target in a sample could result in lack in a distinguishable separation between positive and negative amplitude signals<sup>257</sup>. Thus, it can be concluded from our results that both RT-qPCR and RT-ddPCR are theoretically suitable for detecting the mRNA transcript from FFPE samples. For our purpose as we are assessing degraded, poor quality RNA ddPCR provided the potential of measuring the absolute copies present. Droplet digital PCR has been used successfully for a number of applications such as quantifying the PML-RARA transcript in acute promyelocytic leukemia offering a valuable predicting factor for providing optimal patients management<sup>258</sup>. This technique has been also utilized in designing improved treatment strategy in resistance tumour by identifying biomarkers that accompany the development of resistance in relapsed patients<sup>259</sup>.

While the methods worked well for detecting total BRAF, we did not then compare the methods for distinguishing the mutant from the wild type. Both SYBR green and ddPCR based methods exist for this purpose. Based on the superior performance of the

ddPCR based method, the next step for this project would be to test the ability of ddPCR to quantify BRAFV600E in tumour samples and compare these results to the IHC scoring. The other future direction for this project is to apply the RT-ddPCR based method of quantifying mRNA from FFPE samples to assess the relationship between BRAFV600E expression, as well as other candidate biomarker genes in a larger cohort of melanoma, thyroid and colorectal cancer patients where clinical outcome data is available to assess the predictive value of these as markers for response to therapy, relapsing disease, metastasis and overall survival.

## 4.2 PROJECT 2

The major impediment to successful targeted treatment for cancer is the development of resistance. Like other forms of cancer, BRAF-driven tumours are prone to becoming resistant to therapies that initially work well. For instance, despite the remarkable initial antitumor activity of available targeted drugs in BRAFV600E positive melanoma patients, patients often relapse and these tumours are usually no longer responsive to treatment. What is worse is that in many cancer types that share the exact same BRAFV600E mutation, these tumours do not respond well even to the initial treatment with targeted therapies. In 95% of positive BRAFV600E CRC patients, there is little or no response to targeted inhibitor therapy<sup>110,144</sup>. However, 5% of these patients do respond, and one of the long-term goals of this project is to identify biomarkers for these 5% of patients that could benefit. This may also help in identifying potential mechanisms that could be manipulated to increase responsiveness in other CRC tumours.

We opted for a hypothesis-driven approach where specific genes of interest were cherry-picked based on proposed mechanisms of resistance described in the literature. From this we aimed to look at functional differences between melanoma and colon cancer, and more specifically, between resistant and responsive tumours. This would identify markers to recognize responsive tumours, and potentially point the way towards mechanisms to convert resistant tumours into sensitive ones. Factors such as existing treatment strategies, clinical studies on tumour biopsies from patients, and genome-wide studies featuring mechanisms of resistance were considered before moving forward with

this research. Our established *in-vitro* dabrafenib-resistant cell lines displayed increases in the EC50 values, and also exhibited changes in expression in resistance-associated genes compared to the naïve cell lines. Among the seven selected potential biomarkers, three genes (EGFR, SPRY1, and SPRY2) were overexpressed in both melanoma and colon dabrafenib-resistant cells. Incomplete inhibition of the MAPK signalling pathway despite elevation in expression of negative-feedback regulators that are able to limit MAPK activity is one of the BRAFV600E signatures. As our dabrafenib-resistant cell lines model revealed, our results thus agreed to some extent that negative regulator of MAPK pathway may play a role in the development of resistance. These findings are in agreement with previous studies that hypothesized the involvement of these genes in the development of drug resistance<sup>127,260</sup>. It has been proposed that SPRYs proteins can act both as “tumour suppressors” and as “tumour promoters”<sup>150</sup>. In 18% and 60 % biopsies from patients with resistant BRAF-mutant melanoma and colorectal cancer respectively, there is a high level of activated EGFR<sup>110</sup>. Our results were consistent with this, as our dabrafenib-resistant cell lines displayed an elevated EGFR expression. These findings are not conclusive and they do not rule out that other mechanisms may also be involved in developing resistance in our *in-vitro* model. Furthermore, although the RKO colorectal cell line was already quite resistant to dabrafenib, the fold increase expression of EGFR was still very high after the prolonged exposure.

An alternative approach to finding genes associated with resistance would have been to have measured genome-wide expression where we have a chance to look at all genes indiscriminately and see the effect of treatment on gene expression changes. While a

genome wide unbiased approach can yield many potential candidates, there is also the challenge of finding meaningful data with multiple comparisons and biological variability. Important factors can be missed, nevertheless, genome-wide approaches have been a route that certainly has led to benefits especially in identifying biomarkers<sup>261,262</sup>. In breast cancer for example this approach has been contributed to our knowledge about the genetic etiology of the disease<sup>263,264</sup>. HER2 for instance is a very successful example that predicts response to trastuzumab treatment illustrating the important of finding such markers in other type of cancer<sup>265,266</sup>.

In addition to a search for biomarkers, we also investigated what if any role ROS may play in determining sensitivity to BRAF inhibitory drugs. There is an ongoing discussion about the involvement of ROS in the progression of melanomas and colorectal cancer<sup>195-201</sup>. The originality of our research lies in the fact that we compare the effect of manipulation ROS in BRAFV600E mutated melanoma and colon carcinoma. To our knowledge, this is the first study to examine combined BRAF and ROS inhibition, as compared with BRAF inhibition alone, in naïve and resistant melanoma and colorectal cancer cell lines. The activity of H<sub>2</sub>O<sub>2</sub> was measured by AmplexRed assay in naïve and resistant melanoma and colon cancers after treatment with dabrafenib, trolox, and combined dabrafenib and trolox. In most cases, the presence of trolox, as expected, led to reduction in the amount of ROS detected. However the resistant colon cancer cells demonstrated quite an unexpected result as under the condition of combined dabrafenib and trolox, ROS generation increased compared to the trolox alone. The reason for this is not clear. One possibility is that dabrafenib interferes with trolox's ability to scavenge

ROS, however, arguing against this is the observation that the effect was not as pronounced in the melanoma cell line. Another possible explanation is that the presence of dabrafenib treatment altered the cell-cell connections in the colon cancer, and interfered with the ability of trolox to enter the colon cancer cells. One solution to address this is to see whether the elevation in ROS is the presence of dabrafenib plus trolox is cell number sensitive. As colon cancer cells have a rapid growth rate and demonstrated loss of contact inhibition that result in multilayer of growing cells, we could try to treat cells when they are floating free by trypsinizing prior to administering the trolox.

The effect of trolox on dabrafenib cytotoxicity was evaluated using a cell viability assay. Our results describe for the first time how inhibiting ROS may restore the sensitivity of resistant cells to BRAF inhibitors. Our studies did not determine the underlying mechanism for this. Reactivation of the MAPK pathway accounts for the majority of acquired resistance to BRAF targeted therapy<sup>104</sup>. This reactivation occurs primarily through phosphorylation events<sup>267</sup>. Cancer cells have elevated level of ROS that has the tendency to turn off phosphatases to allow phosphorylation to occur<sup>268-270</sup>. Blocking ROS may allow re-activation of these phosphatases, and permit the de-phosphorylation and deactivation of proteins in the pathway.

So far the significance of these findings are not clear. Multiple questions are still unanswered such as whether trolox treatment in fact alters the phosphorylation status of proteins involved in the MAPK pathway. Further research will be needed to address this question, such as analysis of the cell lysates and employing a western blot technique to



provide a visualization and characterisation of the phosphorylation status of the signalling proteins involve in the MAPK pathway. Future work should also consider examining the expression of NOX family of NADPH oxidases as they contribute greatly to the generation of ROS.

### 4.3 LIMITATIONS AND STRENGTHS

One of the strengths of the present study is the use of histologically confirmed tumour samples obtained from biopsies from clinical samples for three different tumour types. Studies based solely on isolating DNA or RNA from biopsies run the risk that up to 20% of biopsy samples may contain no tumour tissue at all. Although the long term goal of the study is to identify methods to quantify differences in gene expression of BRAF and other relevant genes, the patient FFPE tissue collections available for this part of the study were authorized only for anonymous studies. Due to consent restrictions on this particular study and time limitations for collecting a larger cohort we could not reach our initial plan and test if the markers would be useful in predicting outcomes. It would be interesting in the future to determine the expression level of genes associated with resistance in these samples and perhaps to link this expression profile back to clinical outcomes or responsiveness to treatment. As for the detection methods investigated in the present study there were some limitations to either method. Even though we tried to follow the MIQE guidelines: minimum information for publication of quantitative real-time PCR experiments and quantitative digital PCR experiments<sup>235,236,271</sup>, there was one important aspect of this guidelines that we did not met which is the use of more than two reference genes to normalize our data. The initial plan was to use two reference gene

GUSB and GAPDH, nonetheless, at some stage either one did not show stability and normalized data with the one that shows to be more stable across our samples. This can be avoided by careful examination to more than five candidate reference genes to indicate which genes displayed the highest stability across the three tissue types being investigated. The stability of the candidate reference targets could be verified further using geNorm<sup>272,273</sup>; an algorithm based tool. For ddPCR method, limitations include machine accessibility and the fact that there is a minimum required sample per run. The cost per sample is highly dependent on whether the number of samples is a multiple of 8.

The development of resistance in the cell model allow us to investigate and compare some novel aspects of BRAF inhibitor resistance, including the role that ROS play in resistance, and differences between colon cancer and melanoma. However, limitations of the work included a great deal of variability in the cell behaviour, including to the DMSO vehicle alone, that led to many of the experiments being un-interpretable. The resulting low number of successful replicates means that caution must be taken in drawing conclusions. However, the results do suggest that further work in this area is warranted.

#### 4.4 CONCLUSION

Unfortunately, cancer is a life threatening disease that does and will continue to affect many individuals. Being a scientist allows us to appreciate that even bad things happen for a reason. But beyond that, as scientists we have the opportunity to use this understanding to change the course of events.

Regarding the cancer causing effects of the BRAF mutation, it is being used as helpful marker to guide treatment. In the future, studies with attention to long-term outcomes using a wider array of cell lines may give a better insight into useful biomarkers to characterize tumour responsiveness to treatment. Studies comparing the differences between resistant and responsive melanomas and colorectal tumours may guide our ability to prevent or reverse resistance. Studies into the role of reactive oxygen species in resistance may point towards co-treatment options using readily available and safe antioxidant products.

## REFERENCES

- 1 Asad. *Surah 46. Al-Ahqaf, Ayah 15*, <<http://www.alim.org>> (2017).
- 2 Bromfield, G. *et al.* Canadian Cancer Statistics 2015. (Canadian Cancer Society, Toronto, ON, 2015).
- 3 Mery, L. *et al.* Canadian Cancer Statistics 2014. (Canadian Cancer Society, Toronto, ON, 2014).
- 4 Corn, P. G. & El - Deiry, W. S. Derangement of growth and differentiation control in oncogenesis. *Bioessays* **24**, 83-90 (2002).
- 5 Lane, D. How cells choose to die. *Nature* **414**, 25, 27, doi:10.1038/35102132 (2001).
- 6 Becker, W. M., Kleinsmith, L. J., Hardin, J. & Raasch, J. *The world of the cell*. Vol. 6 (Benjamin Cummings San Francisco, 2003).
- 7 Friedberg, E. C., Walker, G. C. & Siede, W. *DNA repair and mutagenesis*. (American Society for Microbiology (ASM), 1995).
- 8 Hanahan, D. & Weinberg, R. A. The hallmarks of cancer. *Cell* **100**, 57-70 (2000).
- 9 Hanahan, D. & Weinberg, R. A. Hallmarks of cancer: the next generation. *cell* **144**, 646-674 (2011).
- 10 Duffy, M. J. & Crown, J. A personalized approach to cancer treatment: how biomarkers can help. *Clinical chemistry* **54**, 1770-1779 (2008).
- 11 Mankoff, D. A. & Dehdashti, F. Imaging tumor phenotype: 1 plus 1 is more than 2. *Journal of Nuclear Medicine* **50**, 1567-1569 (2009).

- 12 Dowsett, M. & Dunbier, A. K. Emerging biomarkers and new understanding of traditional markers in personalized therapy for breast cancer. *Clinical Cancer Research* **14**, 8019-8026 (2008).
- 13 Dellaire, G. in *Biology on the Cutting Edge: Concepts, Issues, and Canadian Research Around the Globe* (eds S.L. Gillies & S. Hewitt) 55-61 (Pearson Education Canada, 2010).
- 14 Zebisch, A. & Troppmair, J. Back to the roots: the remarkable RAF oncogene story. *Cellular and Molecular Life Sciences CMLS* **63**, 1314-1330 (2006).
- 15 Ikawa, S. *et al.* B-raf, a new member of the raf family, is activated by DNA rearrangement. *Molecular and cellular biology* **8**, 2651-2654 (1988).
- 16 Sithanandam, G. *et al.* B-raf and a B-raf pseudogene are located on 7q in man. *Oncogene* **7**, 795-799 (1992).
- 17 Barnier, J. V., Papin, C., Eychène, A., Lecoq, O. & Calothy, G. The mouse B-raf gene encodes multiple protein isoforms with tissue-specific expression. *Journal of Biological Chemistry* **270**, 23381-23389 (1995).
- 18 Storm, S., Cleveland, J. & Rapp, U. Expression of raf family proto-oncogenes in normal mouse tissues. *Oncogene* **5**, 345-351 (1990).
- 19 Storm, S., Brennscheidt, U., Sithanandam, G. & Rapp, U. raf oncogenes in carcinogenesis. *Critical reviews in oncogenesis* **2**, 1-8 (1989).
- 20 Eychene, A. *et al.* Quail neuroretina c-Rmil (B-raf) proto-oncogene cDNAs encode two proteins of 93.5 and 95 kDa resulting from alternative splicing. *Oncogene* **7**, 1315-1323 (1992).

- 21 Wellbrock, C., Karasarides, M. & Marais, R. The RAF proteins take centre stage. *Nature Reviews Molecular Cell Biology* **5**, 875-885 (2004).
- 22 Human Protein Atlas. *Tissue expression of BRAF*, <<http://www.proteinatlas.org/ENSG00000157764-BRAF/tissue>> (2017).
- 23 Davies, H. *et al.* Mutations of the BRAF gene in human cancer. *Nature* **417**, 949-954 (2002).
- 24 Ascierto, P. A. *et al.* The role of BRAF V600 mutation in melanoma. *J Transl Med* **10**, 85 (2012).
- 25 Santarpia, L., Lippman, S. M. & El-Naggar, A. K. Targeting the MAPK-RAS-RAF signaling pathway in cancer therapy. *Expert opinion on therapeutic targets* **16**, 103-119 (2012).
- 26 Cantwell-Dorris, E. R., O'Leary, J. J. & Sheils, O. M. BRAFV600E: implications for carcinogenesis and molecular therapy. *Molecular cancer therapeutics* **10**, 385-394 (2011).
- 27 Wangari-Talbot, J. & Chen, S. Genetics of melanoma. *Frontiers in genetics* **3** (2012).
- 28 Cohen, Y. *et al.* BRAF mutation in papillary thyroid carcinoma. *Journal of the National Cancer Institute* **95**, 625-627 (2003).
- 29 Xing, M. BRAF mutation in thyroid cancer. *Endocrine-related cancer* **12**, 245-262 (2005).
- 30 Yuen, S. T. *et al.* Similarity of the phenotypic patterns associated with BRAF and KRAS mutations in colorectal neoplasia. *Cancer research* **62**, 6451-6455 (2002).

- 31 Pollock, P. M. *et al.* High frequency of BRAF mutations in nevi. *Nature genetics* **33**, 19-20 (2002).
- 32 Yazdi, A. S. *et al.* Mutations of the BRAF gene in benign and malignant melanocytic lesions. *Journal of Investigative Dermatology* **121**, 1160-1162 (2003).
- 33 Garnett, M. J. & Marais, R. Guilty as charged: B-RAF is a human oncogene. *Cancer cell* **6**, 313-319 (2004).
- 34 Wan, P. T. *et al.* Mechanism of activation of the RAF-ERK signaling pathway by oncogenic mutations of B-RAF. *Cell* **116**, 855-867 (2004).
- 35 Hoeflich, K. P. *et al.* Oncogenic BRAF is required for tumor growth and maintenance in melanoma models. *Cancer Res* **66**, 999-1006, doi:10.1158/0008-5472.can-05-2720 (2006).
- 36 Uribe, P., Wistuba, II & Gonzalez, S. BRAF mutation: a frequent event in benign, atypical, and malignant melanocytic lesions of the skin. *The American Journal of dermatopathology* **25**, 365-370 (2003).
- 37 Pollock, P. M. *et al.* High frequency of BRAF mutations in nevi. *Nature genetics* **33**, 19-20 (2003).
- 38 Patton, E. E. *et al.* BRAF mutations are sufficient to promote nevi formation and cooperate with p53 in the genesis of melanoma. *Current Biology* **15**, 249-254 (2005).
- 39 Roberts, P. & Der, C. Targeting the Raf-MEK-ERK mitogen-activated protein kinase cascade for the treatment of cancer. *Oncogene* **26**, 3291-3310 (2007).

- 40 Chappell, W. H. *et al.* Ras/Raf/MEK/ERK and PI3K/PTEN/Akt/mTOR inhibitors: rationale and importance to inhibiting these pathways in human health. *Oncotarget* **2**, 135 (2011).
- 41 Wada, T. & Penninger, J. M. Mitogen-activated protein kinases in apoptosis regulation. *Oncogene* **23**, 2838-2849 (2004).
- 42 Rapp, U. *et al.* Structure and biological activity of v-raf, a unique oncogene transduced by a retrovirus. *Proceedings of the National Academy of Sciences* **80**, 4218-4222 (1983).
- 43 Obaid, N., Bedard, K. & Huang, W.-Y. Strategies for Overcoming Resistance in Tumours Harboring BRAF Mutations. *International Journal of Molecular Sciences* **18**, 585 (2017).
- 44 Robinson, M. J. & Cobb, M. H. Mitogen-activated protein kinase pathways. *Current opinion in cell biology* **9**, 180-186 (1997).
- 45 Keshet, Y. & Seger, R. in *MAP Kinase Signaling Protocols* 3-38 (Springer, 2010).
- 46 Niault, T. S. & Baccarini, M. Targets of Raf in tumorigenesis. *Carcinogenesis* **31**, 1165-1174 (2010).
- 47 Papin, C., Denouel-Galy, A., Laugier, D., Calothy, G. & Eychène, A. Modulation of kinase activity and oncogenic properties by alternative splicing reveals a novel regulatory mechanism for B-Raf. *Journal of Biological Chemistry* **273**, 24939-24947 (1998).
- 48 Marshall, C. Specificity of receptor tyrosine kinase signaling: transient versus sustained extracellular signal-regulated kinase activation. *Cell* **80**, 179-185 (1995).



- 49 Perrimon, N. The torso receptor protein-tyrosine kinase signaling pathway: an endless story. *Cell* **74**, 219-222 (1993).
- 50 Kolch, W. Meaningful relationships: the regulation of the Ras/Raf/MEK/ERK pathway by protein interactions. *Biochem. J* **351**, 289-305 (2000).
- 51 Troppmair, J. *et al.* Ras controls coupling of growth factor receptors and protein kinase C in the membrane to Raf-1 and B-Raf protein serine kinases in the cytosol. *Oncogene* **7**, 1867-1873 (1992).
- 52 Vojtek, A. B., Hollenberg, S. M. & Cooper, J. A. Mammalian Ras interacts directly with the serine/threonine kinase Raf. *Cell* **74**, 205-214 (1993).
- 53 Bermudez, O., Pagès, G. & Gimond, C. The dual-specificity MAP kinase phosphatases: critical roles in development and cancer. *American Journal of Physiology-Cell Physiology* **299**, C189-C202 (2010).
- 54 Rubin, C. *et al.* Sprouty fine-tunes EGF signaling through interlinked positive and negative feedback loops. *Current biology* **13**, 297-307 (2003).
- 55 Kato, K. *et al.* Phosphorylation of  $\alpha$ B-crystallin in mitotic cells and identification of enzymatic activities responsible for phosphorylation. *Journal of Biological Chemistry* **273**, 28346-28354 (1998).
- 56 Therrien, M. *et al.* KSR, a novel protein kinase required for RAS signal transduction. *Cell* **83**, 879-888 (1995).
- 57 Keller, E. T., Fu, Z. & Brennan, M. The role of Raf kinase inhibitor protein (RKIP) in health and disease. *Biochemical pharmacology* **68**, 1049-1053, doi:10.1016/j.bcp.2004.04.024 (2004).

- 58 Park, S., Yeung, M. L., Beach, S., Shields, J. M. & Yeung, K. C. RKIP downregulates B-Raf kinase activity in melanoma cancer cells. *Oncogene* **24**, 3535-3540 (2005).
- 59 Brummer, T. *et al.* Functional analysis of the regulatory requirements of B-Raf and the B-RafV600E oncoprotein. *Oncogene* **25**, 6262-6276 (2006).
- 60 Eblen, S. T. *et al.* Mitogen-activated protein kinase feedback phosphorylation regulates MEK1 complex formation and activation during cellular adhesion. *Mol Cell Biol* **24**, 2308-2317 (2004).
- 61 Anderson, N. *et al.* Raf-1 is a potential substrate for mitogen-activated protein kinase in vivo. *Biochemical Journal* **277**, 573-576 (1991).
- 62 Dougherty, M. K. *et al.* Regulation of Raf-1 by direct feedback phosphorylation. *Molecular cell* **17**, 215-224 (2005).
- 63 Brummer, T., Naegele, H., Reth, M. & Misawa, Y. Identification of novel ERK-mediated feedback phosphorylation sites at the C-terminus of B-Raf. *Oncogene* **22**, 8823-8834 (2003).
- 64 Sturgill, T. W., Ray, L. B., Erikson, E. & Maller, J. L. Insulin-stimulated MAP-2 kinase phosphorylates and activates ribosomal protein S6 kinase II. (1988).
- 65 Mukhopadhyay, N. K. *et al.* An array of insulin-activated, proline-directed serine/threonine protein kinases phosphorylate the p70 S6 kinase. *Journal of Biological Chemistry* **267**, 3325-3335 (1992).
- 66 Wang, L., Gout, I. & Proud, C. G. Cross-talk between the ERK and p70 S6 kinase (S6K) signaling pathways. MEK-dependent activation of S6K2 in

- cardiomyocytes. *The Journal of biological chemistry* **276**, 32670-32677, doi:10.1074/jbc.M102776200 (2001).
- 67 Camps, M. *et al.* Catalytic activation of the phosphatase MKP-3 by ERK2 mitogen-activated protein kinase. *Science (New York, N.Y.)* **280**, 1262-1265 (1998).
- 68 Marchetti, S. *et al.* Extracellular signal-regulated kinases phosphorylate mitogen-activated protein kinase phosphatase 3/DUSP6 at serines 159 and 197, two sites critical for its proteasomal degradation. *Molecular and cellular biology* **25**, 854-864 (2005).
- 69 Masuda, K., Shima, H., Katagiri, C. & Kikuchi, K. Activation of ERK induces phosphorylation of MAPK phosphatase-7, a JNK specific phosphatase, at Ser-446. *Journal of Biological Chemistry* **278**, 32448-32456 (2003).
- 70 Ozaki, K., Miyazaki, S., Tanimura, S. & Kohno, M. Efficient suppression of FGF-2-induced ERK activation by the cooperative interaction among mammalian Sprouty isoforms. *Journal of cell science* **118**, 5861-5871, doi:10.1242/jcs.02711 (2005).
- 71 Hacohen, N., Kramer, S., Sutherland, D., Hiromi, Y. & Krasnow, M. A. sprouty encodes a novel antagonist of FGF signaling that patterns apical branching of the *Drosophila* airways. *Cell* **92**, 253-263 (1998).
- 72 Alvarez, E. *et al.* Pro-Leu-Ser/Thr-Pro is a consensus primary sequence for substrate protein phosphorylation. Characterization of the phosphorylation of c-myc and c-jun proteins by an epidermal growth factor receptor threonine 669 protein kinase. *Journal of Biological Chemistry* **266**, 15277-15285 (1991).

- 73 Arnaud, M., Crouin, C., Deon, C., Loyaux, D. & Bertoglio, J. Phosphorylation of Grb2-associated binder 2 on serine 623 by ERK MAPK regulates its association with the phosphatase SHP-2 and decreases STAT5 activation. *The Journal of Immunology* **173**, 3962-3971 (2004).
- 74 Langlois, W. J., Sasaoka, T., Saltiel, A. R. & Olefsky, J. M. Negative feedback regulation and desensitization of insulin-and epidermal growth factor-stimulated p21ras activation. *Journal of Biological Chemistry* **270**, 25320-25323 (1995).
- 75 Andreozzi, F. *et al.* Activation of the hexosamine pathway leads to phosphorylation of insulin receptor substrate-1 on Ser307 and Ser612 and impairs the phosphatidylinositol 3-kinase/Akt/mammalian target of rapamycin insulin biosynthetic pathway in RIN pancreatic  $\beta$ -cells. *Endocrinology* **145**, 2845-2857 (2004).
- 76 Balaban, R. S., Nemoto, S. & Finkel, T. Mitochondria, oxidants, and aging. *Cell* **120**, 483-495, doi:10.1016/j.cell.2005.02.001 (2005).
- 77 Saal, S. K. G. & Parsons, R. Is the small heat shock protein  $\alpha$ B-crystallin an oncogene? *The Journal of clinical investigation* **116**, 30-32 (2006).
- 78 Cruzalegui, F. H., Cano, E. & Treisman, R. ERK activation induces phosphorylation of Elk-1 at multiple S/TP motifs to high stoichiometry. *Oncogene* **18**, 7948-7957 (1999).
- 79 Murphy, L. O., MacKeigan, J. P. & Blenis, J. A network of immediate early gene products propagates subtle differences in mitogen-activated protein kinase signal amplitude and duration. *Molecular and cellular biology* **24**, 144-153 (2004).

- 80 Morton, S., Davis, R. J., McLaren, A. & Cohen, P. A reinvestigation of the multisite phosphorylation of the transcription factor c - Jun. *The EMBO journal* **22**, 3876-3886 (2003).
- 81 Milne, D., Campbell, D., Caudwell, F. & Meek, D. Phosphorylation of the tumor suppressor protein p53 by mitogen-activated protein kinases. *Journal of Biological Chemistry* **269**, 9253-9260 (1994).
- 82 Yeh, P. Y. *et al.* Phosphorylation of p53 on Thr55 by ERK2 is necessary for doxorubicin-induced p53 activation and cell death. *Oncogene* **23**, 3580-3588 (2004).
- 83 Biswas, S. C. & Greene, L. A. Nerve growth factor (NGF) down-regulates the Bcl-2 homology 3 (BH3) domain-only protein Bim and suppresses its proapoptotic activity by phosphorylation. *Journal of Biological Chemistry* **277**, 49511-49516 (2002).
- 84 Allan, L. A. *et al.* Inhibition of caspase-9 through phosphorylation at Thr 125 by ERK MAPK. *Nature cell biology* **5**, 647-654 (2003).
- 85 Scheid, M. P., Schubert, K. M. & Duronio, V. Regulation of Bad phosphorylation and association with Bcl-xL by the MAPK/Erk kinase. *Journal of Biological Chemistry* **274**, 31108-31113 (1999).
- 86 Garnovskaya, M. N. *et al.* Mitogen-induced rapid phosphorylation of serine 795 of the retinoblastoma gene product in vascular smooth muscle cells involves ERK activation. *Journal of Biological Chemistry* **279**, 24899-24905 (2004).

- 87 Yang, X. & Gabuzda, D. Mitogen-activated protein kinase phosphorylates and regulates the HIV-1 Vif protein. *Journal of Biological Chemistry* **273**, 29879-29887 (1998).
- 88 Tsavachidou, D. *et al.* SPRY2 is an inhibitor of the ras/extracellular signal-regulated kinase pathway in melanocytes and melanoma cells with wild-type BRAF but not with the V599E mutant. *Cancer Res* **64**, 5556-5559, doi:10.1158/0008-5472.can-04-1669 (2004).
- 89 Pratilas, C. A. & Solit, D. B. Targeting the mitogen-activated protein kinase pathway: physiological feedback and drug response. *Clinical Cancer Research* **16**, 3329-3334 (2010).
- 90 Edlundh-Rose, E. *et al.* NRAS and BRAF mutations in melanoma tumours in relation to clinical characteristics: a study based on mutation screening by pyrosequencing. *Melanoma research* **16**, 471-478 (2006).
- 91 Arcila, M., Lau, C., Nafa, K. & Ladanyi, M. Detection of KRAS and BRAF mutations in colorectal carcinoma roles for high-sensitivity locked nucleic acid-PCR sequencing and broad-spectrum mass spectrometry genotyping. *The Journal of Molecular Diagnostics* **13**, 64-73 (2011).
- 92 Lamy, A. *et al.* Metastatic colorectal cancer KRAS genotyping in routine practice: results and pitfalls. *Modern pathology* **24**, 1090-1100 (2011).
- 93 Capper, D. *et al.* Assessment of BRAF V600E mutation status by immunohistochemistry with a mutation-specific monoclonal antibody. *Acta neuropathologica* **122**, 11-19 (2011).

- 94 Adackapara, C. A., Sholl, L. M., Barletta, J. A. & Hornick, J. L.  
Immunohistochemistry using the BRAF V600E mutation - specific monoclonal antibody VE1 is not a useful surrogate for genotyping in colorectal adenocarcinoma. *Histopathology* **63**, 187-193 (2013).
- 95 Uguen, A. *et al.* NRAS(Q61R), BRAF(V600E) immunohistochemistry: a concomitant tool for mutation screening in melanomas. *Diagnostic Pathology* **10**, doi:10.1186/s13000-015-0359-0 (2015).
- 96 Robert, C. *et al.* Improved overall survival in melanoma with combined dabrafenib and trametinib. *The New England journal of medicine* **372**, 30-39, doi:10.1056/NEJMoa1412690 (2015).
- 97 Chapman, P. B. *et al.* Improved survival with vemurafenib in melanoma with BRAF V600E mutation. *The New England journal of medicine* **364**, 2507-2516, doi:10.1056/NEJMoa1103782 (2011).
- 98 Gibney, G. T., Messina, J. L., Fedorenko, I. V., Sondak, V. K. & Smalley, K. S. Paradoxical oncogenesis--the long-term effects of BRAF inhibition in melanoma. *Nature reviews. Clinical oncology* **10**, 390-399, doi:10.1038/nrclinonc.2013.83 (2013).
- 99 Corcoran, R. B. *et al.* in *ASCO Annual Meeting Proceedings*. 3517.
- 100 Hatzivassiliou, G. *et al.* RAF inhibitors prime wild-type RAF to activate the MAPK pathway and enhance growth. *Nature* **464**, 431-435, doi:10.1038/nature08833 (2010).

- 101 Heidorn, S. J. *et al.* Kinase-dead BRAF and oncogenic RAS cooperate to drive tumor progression through CRAF. *Cell* **140**, 209-221, doi:10.1016/j.cell.2009.12.040 (2010).
- 102 Poulidakos, P. I., Zhang, C., Bollag, G., Shokat, K. M. & Rosen, N. RAF inhibitors transactivate RAF dimers and ERK signalling in cells with wild-type BRAF. *Nature* **464**, 427-430, doi:10.1038/nature08902 (2010).
- 103 Oberholzer, P. A. *et al.* RAS mutations are associated with the development of cutaneous squamous cell tumors in patients treated with RAF inhibitors. *Journal of Clinical Oncology* **30**, 316-321 (2012).
- 104 Alcala, A. M. & Flaherty, K. T. BRAF inhibitors for the treatment of metastatic melanoma: clinical trials and mechanisms of resistance. *Clin Cancer Res* **18**, 33-39, doi:10.1158/1078-0432.ccr-11-0997 (2012).
- 105 Rizos, H. *et al.* BRAF inhibitor resistance mechanisms in metastatic melanoma: spectrum and clinical impact. *Clinical cancer research : an official journal of the American Association for Cancer Research* **20**, 1965-1977, doi:10.1158/1078-0432.CCR-13-3122 (2014).
- 106 Johnson, D. B. *et al.* Acquired BRAF inhibitor resistance: A multicenter meta-analysis of the spectrum and frequencies, clinical behaviour, and phenotypic associations of resistance mechanisms. *Eur J Cancer* **51**, 2792-2799, doi:10.1016/j.ejca.2015.08.022 (2015).
- 107 Nazarian, R. *et al.* Melanomas acquire resistance to B-RAF(V600E) inhibition by RTK or N-RAS upregulation. *Nature* **468**, 973-977, doi:10.1038/nature09626 (2010).



- 108 Long, G. V. *et al.* Increased MAPK reactivation in early resistance to dabrafenib/trametinib combination therapy of BRAF-mutant metastatic melanoma. *Nature communications* **5**, 5694, doi:10.1038/ncomms6694 (2014).
- 109 Wagle, N. *et al.* Dissecting therapeutic resistance to RAF inhibition in melanoma by tumor genomic profiling. *Journal of clinical oncology : official journal of the American Society of Clinical Oncology* **29**, 3085-3096, doi:10.1200/jco.2010.33.2312 (2011).
- 110 Corcoran, R. B. *et al.* EGFR-mediated re-activation of MAPK signaling contributes to insensitivity of BRAF mutant colorectal cancers to RAF inhibition with vemurafenib. *Cancer discovery* **2**, 227-235, doi:10.1158/2159-8290.cd-11-0341 (2012).
- 111 Hoogstraat, M. *et al.* Detailed imaging and genetic analysis reveal a secondary BRAF(L505H) resistance mutation and extensive inpatient heterogeneity in metastatic BRAF mutant melanoma patients treated with vemurafenib. *Pigment cell & melanoma research* **28**, 318-323, doi:10.1111/pcmr.12347 (2015).
- 112 Wagenaar, T. R. *et al.* Resistance to vemurafenib resulting from a novel mutation in the BRAFV600E kinase domain. *Pigment Cell Melanoma Res* **27**, 124-133, doi:10.1111/pcmr.12171 (2014).
- 113 Poulikakos, P. I. *et al.* RAF inhibitor resistance is mediated by dimerization of aberrantly spliced BRAF(V600E). *Nature* **480**, 387-390, doi:10.1038/nature10662 (2011).

- 114 Raaijmakers, M. I. *et al.* Co-existence of BRAF and NRAS driver mutations in the same melanoma cells results in heterogeneity of targeted therapy resistance. *Oncotarget* **7**, 77163-77174, doi:10.18632/oncotarget.12848 (2016).
- 115 Danysh, B. P. *et al.* Long-term vemurafenib treatment drives inhibitor resistance through a spontaneous KRAS G12D mutation in a BRAF V600E papillary thyroid carcinoma model. *Oncotarget* **7**, 30907-30923, doi:10.18632/oncotarget.9023 (2016).
- 116 Ahronian, L. G. *et al.* Clinical Acquired Resistance to RAF Inhibitor Combinations in BRAF-Mutant Colorectal Cancer through MAPK Pathway Alterations. *Cancer discovery* **5**, 358-367, doi:10.1158/2159-8290.CD-14-1518 (2015).
- 117 Johannessen, C. M. *et al.* COT drives resistance to RAF inhibition through MAP kinase pathway reactivation. *Nature* **468**, 968-972, doi:10.1038/nature09627 (2010).
- 118 Montagut, C. *et al.* Elevated CRAF as a potential mechanism of acquired resistance to BRAF inhibition in melanoma. *Cancer Res* **68**, 4853-4861, doi:10.1158/0008-5472.can-07-6787 (2008).
- 119 Grbovic, O. M. *et al.* V600E B-Raf requires the Hsp90 chaperone for stability and is degraded in response to Hsp90 inhibitors. *Proc Natl Acad Sci U S A* **103**, 57-62, doi:10.1073/pnas.0609973103 (2006).
- 120 da Rocha Dias, S. *et al.* Activated B-RAF is an Hsp90 client protein that is targeted by the anticancer drug 17-allylamino-17-demethoxygeldanamycin. *Cancer Res* **65**, 10686-10691, doi:10.1158/0008-5472.can-05-2632 (2005).

- 121 Maloney, A., Clarke, P. A. & Workman, P. Genes and proteins governing the cellular sensitivity to HSP90 inhibitors: a mechanistic perspective. *Curr Cancer Drug Targets* **3**, 331-341 (2003).
- 122 Acquaviva, J. *et al.* Overcoming acquired BRAF inhibitor resistance in melanoma via targeted inhibition of Hsp90 with ganetespib. *Mol Cancer Ther* **13**, 353-363, doi:10.1158/1535-7163.mct-13-0481 (2014).
- 123 Paraiso, K. H. *et al.* The HSP90 inhibitor XL888 overcomes BRAF inhibitor resistance mediated through diverse mechanisms. *Clin Cancer Res* **18**, 2502-2514, doi:10.1158/1078-0432.ccr-11-2612 (2012).
- 124 Wang, H., Lu, M., Yao, M. & Zhu, W. Effects of treatment with an Hsp90 inhibitor in tumors based on 15 phase II clinical trials. *Molecular and clinical oncology* **5**, 326-334, doi:10.3892/mco.2016.963 (2016).
- 125 Solit, D. B. *et al.* Phase II trial of 17-allylamino-17-demethoxygeldanamycin in patients with metastatic melanoma. *Clinical cancer research : an official journal of the American Association for Cancer Research* **14**, 8302-8307, doi:10.1158/1078-0432.CCR-08-1002 (2008).
- 126 Pacey, S. *et al.* A Phase II trial of 17-allylamino, 17-demethoxygeldanamycin (17-AAG, tanespimycin) in patients with metastatic melanoma. *Investigational new drugs* **30**, 341-349, doi:10.1007/s10637-010-9493-4 (2012).
- 127 Pratilas, C. A. *et al.* (V600E)BRAF is associated with disabled feedback inhibition of RAF-MEK signaling and elevated transcriptional output of the pathway. *Proc Natl Acad Sci U S A* **106**, 4519-4524, doi:10.1073/pnas.0900780106 (2009).

- 128 Spagnolo, F., Ghiorzo, P. & Queirolo, P. Overcoming resistance to BRAF inhibition in BRAF-mutated metastatic melanoma. *Oncotarget* **5**, 10206-10221, doi:10.18632/oncotarget.2602 (2014).
- 129 Chung, J., Grammer, T. C., Lemon, K. P., Kazlauskas, A. & Blenis, J. PDGF- and insulin-dependent pp70S6k activation mediated by phosphatidylinositol-3-OH kinase. *Nature* **370**, 71-75, doi:10.1038/370071a0 (1994).
- 130 Sun, C. *et al.* Reversible and adaptive resistance to BRAF(V600E) inhibition in melanoma. *Nature* **508**, 118-122, doi:10.1038/nature13121 (2014).
- 131 Shi, H., Kong, X., Ribas, A. & Lo, R. S. Combinatorial treatments that overcome PDGFRbeta-driven resistance of melanoma cells to V600EB-RAF inhibition. *Cancer Res* **71**, 5067-5074, doi:10.1158/0008-5472.can-11-0140 (2011).
- 132 Villanueva, J. *et al.* Acquired resistance to BRAF inhibitors mediated by a RAF kinase switch in melanoma can be overcome by cotargeting MEK and IGF-1R/PI3K. *Cancer Cell* **18**, 683-695, doi:10.1016/j.ccr.2010.11.023 (2010).
- 133 Wilson, T. R. *et al.* Widespread potential for growth-factor-driven resistance to anticancer kinase inhibitors. *Nature* **487**, 505-509, doi:10.1038/nature11249 (2012).
- 134 Straussman, R. *et al.* Tumour micro-environment elicits innate resistance to RAF inhibitors through HGF secretion. *Nature* **487**, 500-504, doi:10.1038/nature11183 (2012).
- 135 Shi, H. *et al.* Acquired resistance and clonal evolution in melanoma during BRAF inhibitor therapy. *Cancer discovery* **4**, 80-93, doi:10.1158/2159-8290.cd-13-0642 (2014).

- 136 Aguisa-Toure, A. H. & Li, G. Genetic alterations of PTEN in human melanoma. *Cellular and molecular life sciences : CMLS* **69**, 1475-1491, doi:10.1007/s00018-011-0878-0 (2012).
- 137 Turajlic, S. *et al.* Whole-genome sequencing reveals complex mechanisms of intrinsic resistance to BRAF inhibition. *Annals of oncology : official journal of the European Society for Medical Oncology* **25**, 959-967, doi:10.1093/annonc/mdu049 (2014).
- 138 Rebecca, V. W. *et al.* Vertical inhibition of the MAPK pathway enhances therapeutic responses in NRAS-mutant melanoma. *Pigment Cell Melanoma Res* **27**, 1154-1158, doi:10.1111/pcmr.12303 (2014).
- 139 Paraiso, K. H. *et al.* PTEN loss confers BRAF inhibitor resistance to melanoma cells through the suppression of BIM expression. *Cancer research* **71**, 2750-2760 (2011).
- 140 Marampon, F., Ciccarelli, C. & Zani, B. M. Down-regulation of c-Myc following MEK/ERK inhibition halts the expression of malignant phenotype in rhabdomyosarcoma and in non muscle-derived human tumors. *Molecular cancer* **5**, 31, doi:10.1186/1476-4598-5-31 (2006).
- 141 Zawistowski, J. S. *et al.* Enhancer Remodeling During Adaptive Bypass to MEK Inhibition Is Attenuated by Pharmacological Targeting of the P-TEFb Complex. *Cancer discovery*, doi:10.1158/2159-8290.CD-16-0653 (2017).
- 142 Fattore, L. *et al.* miR-579-3p controls melanoma progression and resistance to target therapy. *Proceedings of the National Academy of Sciences of the United States of America* **113**, E5005-5013, doi:10.1073/pnas.1607753113 (2016).

- 143 Kopetz, S. *et al.* in *ASCO Annual Meeting Proceedings*. 3534.
- 144 Clarke, C. N. & Kopetz, E. S. BRAF mutant colorectal cancer as a distinct subset of colorectal cancer: clinical characteristics, clinical behavior, and response to targeted therapies. *Journal of Gastrointestinal Oncology* **6**, 660-667, doi:10.3978/j.issn.2078-6891.2015.077 (2015).
- 145 Hong, D. S. *et al.* in *ASCO Annual Meeting Proceedings*. 3516.
- 146 Chapman, P. B. *et al.* Improved Survival with Vemurafenib in Melanoma with BRAF V600E Mutation. *New England Journal of Medicine* **364**, 2507-2516, doi:doi:10.1056/NEJMoa1103782 (2011).
- 147 Shi, H. *et al.* Melanoma whole-exome sequencing identifies (V600E)B-RAF amplification-mediated acquired B-RAF inhibitor resistance. *Nature communications* **3**, 724, doi:10.1038/ncomms1727 (2012).
- 148 Prahallad, A. *et al.* Unresponsiveness of colon cancer to BRAF(V600E) inhibition through feedback activation of EGFR. *Nature* **483**, 100-103, doi:10.1038/nature10868 (2012).
- 149 Wang, R. *et al.* Regulation of Cdc25C by ERK-MAP kinases during the G 2/M transition. *Cell* **128**, 1119-1132 (2007).
- 150 Edwin, F., Anderson, K., Ying, C. & Patel, T. B. Intermolecular interactions of Sprouty proteins and their implications in development and disease. *Molecular pharmacology* **76**, 679-691, doi:10.1124/mol.109.055848 (2009).
- 151 Mao, M. *et al.* Resistance to BRAF inhibition in BRAF-mutant colon cancer can be overcome with PI3K inhibition or demethylating agents. *Clinical cancer research* **19**, 657-667 (2013).

- 152 Yaeger, R. *et al.* Pilot trial of combined BRAF and EGFR inhibition in BRAF-mutant metastatic colorectal cancer patients. *Clin Cancer Res* **21**, 1313-1320, doi:10.1158/1078-0432.ccr-14-2779 (2015).
- 153 Bendell, J. C. *et al.* in *ASCO Annual Meeting Proceedings*. 3515.
- 154 Corcoran, R. B. *et al.* Combined BRAF and MEK Inhibition With Dabrafenib and Trametinib in BRAF V600-Mutant Colorectal Cancer. *Journal of clinical oncology : official journal of the American Society of Clinical Oncology* **33**, 4023-4031, doi:10.1200/jco.2015.63.2471 (2015).
- 155 D'Autréaux, B. & Toledano, M. B. ROS as signalling molecules: mechanisms that generate specificity in ROS homeostasis. *Nature reviews Molecular cell biology* **8**, 813-824 (2007).
- 156 Brown, D. I. & Griendling, K. K. Nox proteins in signal transduction. *Free Radical Biology and Medicine* **47**, 1239-1253 (2009).
- 157 Rhee, S. G. H<sub>2</sub>O<sub>2</sub>, a necessary evil for cell signaling. *Science (New York, N.Y.)* **312**, 1882-1883 (2006).
- 158 Oberley, L. W., Oberley, T. D. & Buettner, G. R. Cell division in normal and transformed cells: the possible role of superoxide and hydrogen peroxide. *Medical hypotheses* **7**, 21-42 (1981).
- 159 Kehrer, J. P. & Smith, C. V. in *Natural Antioxidants in Human Health and Disease* 25-62 (Academic Press, 1994).
- 160 Lambeth, J. D. Nox enzymes, ROS, and chronic disease: an example of antagonistic pleiotropy. *Free Radical Biology and Medicine* **43**, 332-347 (2007).

- 161 Kamata, T. Roles of Nox1 and other Nox isoforms in cancer development. *Cancer science* **100**, 1382-1388 (2009).
- 162 Liou, G. Y. & Storz, P. Reactive oxygen species in cancer. *Free radical research* **44**, doi:10.3109/10715761003667554 (2010).
- 163 Gorrini, C., Harris, I. S. & Mak, T. W. Modulation of oxidative stress as an anticancer strategy. *Nature reviews. Drug discovery* **12**, 931-947, doi:10.1038/nrd4002 (2013).
- 164 Warburg, O., Wind, F. & Negelein, E. THE METABOLISM OF TUMORS IN THE BODY. *The Journal of general physiology* **8**, 519-530 (1927).
- 165 Yeung, S. J., Pan, J. & Lee, M. H. Roles of p53, MYC and HIF-1 in regulating glycolysis - the seventh hallmark of cancer. *Cellular and molecular life sciences : CMLS* **65**, 3981-3999, doi:10.1007/s00018-008-8224-x (2008).
- 166 DeBerardinis, R. J., Lum, J. J., Hatzivassiliou, G. & Thompson, C. B. The biology of cancer: metabolic reprogramming fuels cell growth and proliferation. *Cell metabolism* **7**, 11-20, doi:10.1016/j.cmet.2007.10.002 (2008).
- 167 Deberardinis, R. J., Sayed, N., Ditsworth, D. & Thompson, C. B. Brick by brick: metabolism and tumor cell growth. *Current opinion in genetics & development* **18**, 54-61, doi:10.1016/j.gde.2008.02.003 (2008).
- 168 Vander Heiden, M. G., Cantley, L. C. & Thompson, C. B. Understanding the Warburg effect: the metabolic requirements of cell proliferation. *Science (New York, N.Y.)* **324**, 1029-1033, doi:10.1126/science.1160809 (2009).
- 169 Dang, C. V. The interplay between MYC and HIF in the Warburg effect. *Ernst Schering Foundation symposium proceedings*, 35-53 (2007).



- 170 Warburg, O. On the origin of cancer cells. *Science (New York, N.Y.)* **123**, 309-314 (1956).
- 171 Finkel, T. Signal transduction by reactive oxygen species. *The Journal of cell biology* **194**, 7-15, doi:10.1083/jcb.201102095 (2011).
- 172 Liemburg-Apers, D. C., Willems, P., Koopman, W. J. H. & Grefte, S. Interactions between mitochondrial reactive oxygen species and cellular glucose metabolism. *Archives of Toxicology* **89**, 1209-1226, doi:10.1007/s00204-015-1520-y (2015).
- 173 Zheng, J. Energy metabolism of cancer: Glycolysis versus oxidative phosphorylation (Review). *Oncol Lett* **4**, 1151-1157, doi:10.3892/ol.2012.928 (2012).
- 174 Krause, K. H. Tissue distribution and putative physiological function of NOX family NADPH oxidases. *Japanese journal of infectious diseases* **57**, S28-29 (2004).
- 175 Bedard, K. & Krause, K.-H. The NOX family of ROS-generating NADPH oxidases: physiology and pathophysiology. *Physiological reviews* **87**, 245-313 (2007).
- 176 Cross, C. E. *et al.* Oxygen radicals and human disease. *Annals of internal medicine* **107**, 526-545 (1987).
- 177 Irani, K. *et al.* Mitogenic signaling mediated by oxidants in Ras-transformed fibroblasts. *Science (New York, N.Y.)* **275**, 1649-1652 (1997).
- 178 Lee, A. C. *et al.* Ras proteins induce senescence by altering the intracellular levels of reactive oxygen species. *J Biol Chem* **274**, 7936-7940 (1999).

- 179 Denat, L., Kadekaro, A. L., Marrot, L., Leachman, S. A. & Abdel-Malek, Z. A. Melanocytes as instigators and victims of oxidative stress. *The Journal of investigative dermatology* **134**, 1512-1518, doi:10.1038/jid.2014.65 (2014).
- 180 Meyskens, F. L., Jr., Farmer, P. & Fruehauf, J. P. Redox regulation in human melanocytes and melanoma. *Pigment cell research* **14**, 148-154 (2001).
- 181 Picardo, M. *et al.* Imbalance in the antioxidant pool in melanoma cells and normal melanocytes from patients with melanoma. *The Journal of investigative dermatology* **107**, 322-326 (1996).
- 182 Poljsak, B., Šuput, D. & Milisav, I. Achieving the balance between ROS and antioxidants: when to use the synthetic antioxidants. *Oxidative medicine and cellular longevity* **2013** (2013).
- 183 Birben, E., Sahiner, U. M., Sackesen, C., Erzurum, S. & Kalayci, O. Oxidative Stress and Antioxidant Defense. *The World Allergy Organization journal* **5**, 9-19, doi:10.1097/WOX.0b013e3182439613 (2012).
- 184 Thomas, C. *Oxygen radicals and the disease process*. (CRC Press, 1998).
- 185 Nimse, S. B. & Pal, D. Free radicals, natural antioxidants, and their reaction mechanisms. *RSC Advances* **5**, 27986-28006 (2015).
- 186 Panieri, E. & Santoro, M. M. ROS homeostasis and metabolism: a dangerous liason in cancer cells. *Cell Death Dis* **7**, e2253, doi:10.1038/cddis.2016.105 (2016).
- 187 Whitehouse, S. D. *The effects OF P22PHOX genetic polymorphisms and natural compounds on reactive oxygen species formation* Master of Science thesis, Dalhousie University, (2013).

- 188 Michaloglou, C. *et al.* BRAFE600-associated senescence-like cell cycle arrest of human naevi. *Nature* **436**, 720-724, doi:10.1038/nature03890 (2005).
- 189 Pollock, P. M. *et al.* High frequency of BRAF mutations in nevi. *Nat Genet* **33**, 19-20, doi:10.1038/ng1054 (2003).
- 190 Michaloglou, C. *et al.* BRAFE600-associated senescence-like cell cycle arrest of human naevi. *Nature* **436**, 720-724 (2005).
- 191 Bianchi-Smiraglia, A. & Nikiforov, M. A. Controversial aspects of oncogene-induced senescence. *Cell Cycle* **11**, 4147-4151, doi:10.4161/cc.22589 (2012).
- 192 Chandeck, C. & Mooi, W. J. Oncogene-induced cellular senescence. *Advances in anatomic pathology* **17**, 42-48 (2010).
- 193 Courtois-Cox, S., Jones, S. L. & Cichowski, K. Many roads lead to oncogene-induced senescence. *Oncogene* **27**, 2801-2809, doi:10.1038/sj.onc.1210950 (2008).
- 194 Block, K. & Gorin, Y. Aiding and abetting roles of NOX oxidases in cellular transformation. *Nature Reviews Cancer* **12**, 627-637 (2012).
- 195 Brar, S. S. *et al.* An NAD (P) H oxidase regulates growth and transcription in melanoma cells. *American Journal of Physiology-Cell Physiology* **282**, C1212-C1224 (2002).
- 196 Juhasz, A. *et al.* Expression of NADPH oxidase homologues and accessory genes in human cancer cell lines, tumours and adjacent normal tissues. *Free radical research* **43**, 523-532 (2009).

- 197 Yamaura, M. *et al.* NADPH oxidase 4 contributes to transformation phenotype of melanoma cells by regulating G2-M cell cycle progression. *Cancer research* **69**, 2647-2654 (2009).
- 198 Liu-Smith, F., Dellinger, R. & Meyskens, F. L., Jr. Updates of reactive oxygen species in melanoma etiology and progression. *Archives of biochemistry and biophysics* **563**, 51-55, doi:10.1016/j.abb.2014.04.007 (2014).
- 199 Fritz, G., Just, I. & Kaina, B. Rho GTPases are over - expressed in human tumors. *International journal of cancer* **81**, 682-687 (1999).
- 200 Fukuyama, M. *et al.* Overexpression of a novel superoxide-producing enzyme, NADPH oxidase 1, in adenoma and well differentiated adenocarcinoma of the human colon. *Cancer letters* **221**, 97-104 (2005).
- 201 del Pulgar, T. G., Benitah, S. A., Valerón, P. F., Espina, C. & Lacal, J. C. Rho GTPase expression in tumourigenesis: evidence for a significant link. *Bioessays* **27**, 602-613 (2005).
- 202 Piskounova, E. *et al.* Oxidative stress inhibits distant metastasis by human melanoma cells. *Nature* (2015).
- 203 Pavlova, N. N. & Thompson, C. B. The emerging hallmarks of cancer metabolism. *Cell metabolism* **23**, 27-47 (2016).
- 204 Vander Heiden, M. G. Targeting cancer metabolism: a therapeutic window opens. *Nature reviews Drug discovery* **10**, 671-684 (2011).
- 205 Zhao, Y., Butler, E. B. & Tan, M. Targeting cellular metabolism to improve cancer therapeutics. *Cell death & disease* **4**, e532 (2013).

- 206 Pelicano, H., Martin, D. S., Xu, R. H. & Huang, P. Glycolysis inhibition for anticancer treatment. *Oncogene* **25**, 4633-4646 (0000).
- 207 Allen, B. G. *et al.* Ketogenic diets as an adjuvant cancer therapy: History and potential mechanism. *Redox Biology* **2**, 963-970, doi:10.1016/j.redox.2014.08.002 (2014).
- 208 Gupta, S. C. *et al.* Upsides and Downsides of Reactive Oxygen Species for Cancer: The Roles of Reactive Oxygen Species in Tumorigenesis, Prevention, and Therapy. *Antioxidants & Redox Signaling* **16**, 1295-1322, doi:10.1089/ars.2011.4414 (2012).
- 209 Conklin, K. A. Dietary antioxidants during cancer chemotherapy: impact on chemotherapeutic effectiveness and development of side effects. *Nutrition and cancer* **37**, 1-18, doi:10.1207/s15327914nc3701\_1 (2000).
- 210 Seifried, H. E., McDonald, S. S., Anderson, D. E., Greenwald, P. & Milner, J. A. The antioxidant conundrum in cancer. *Cancer Res* **63**, 4295-4298 (2003).
- 211 Akbas, H. S., Timur, M. & Ozben, T. Concurrent use of antioxidants in cancer therapy: an update. *Expert review of clinical immunology* **2**, 931-939, doi:10.1586/1744666x.2.6.931 (2006).
- 212 Wu, L. W., Zhang, G. & Herlyn, M. Mitochondrial biogenesis meets chemoresistance in BRAF-mutant melanoma. *Molecular & cellular oncology* **3**, e1179381, doi:10.1080/23723556.2016.1179381 (2016).
- 213 Zhang, G. *et al.* Targeting mitochondrial biogenesis to overcome drug resistance to MAPK inhibitors. *The Journal of clinical investigation* **126**, 1834-1856 (2016).

- 214 Mercer, K. E. & Pritchard, C. A. Raf proteins and cancer: B-Raf is identified as a mutational target. *Biochimica et Biophysica Acta (BBA)-Reviews on Cancer* **1653**, 25-40 (2003).
- 215 Xing, M. *et al.* Detection of BRAF mutation on fine needle aspiration biopsy specimens: a new diagnostic tool for papillary thyroid cancer. *The Journal of Clinical Endocrinology & Metabolism* **89**, 2867-2872 (2004).
- 216 Tiacci, E. *et al.* BRAF mutations in hairy-cell leukemia. *New England Journal of Medicine* **364**, 2305-2315 (2011).
- 217 Tang, K. T. & Lee, C. H. BRAF mutation in papillary thyroid carcinoma: pathogenic role and clinical implications. *Journal of the Chinese Medical Association : JCMA* **73**, 113-128, doi:10.1016/s1726-4901(10)70025-3 (2010).
- 218 Houben, R. *et al.* Constitutive activation of the Ras-Raf signaling pathway in metastatic melanoma is associated with poor prognosis. *J Carcinog* **3**, 6, doi:10.1186/1477-3163-3-6 (2004).
- 219 Houben, R. *et al.* Constitutive activation of the Ras-Raf signaling pathway in metastatic melanoma is associated with poor prognosis. *Journal of carcinogenesis* **3**, 6 (2004).
- 220 Ogino, S. *et al.* Predictive and prognostic roles of BRAF mutation in stage III colon cancer: results from intergroup trial CALGB 89803. *Clinical Cancer Research* **18**, 890-900 (2012).
- 221 Xing, M. *et al.* Association between BRAF V600E mutation and mortality in patients with papillary thyroid cancer. *Jama* **309**, 1493-1501 (2013).

- 222 Di Nicolantonio, F. *et al.* Wild-type BRAF is required for response to panitumumab or cetuximab in metastatic colorectal cancer. *Journal of Clinical Oncology* **26**, 5705-5712 (2008).
- 223 Dietel, M. *et al.* A 2015 update on predictive molecular pathology and its role in targeted cancer therapy: a review focussing on clinical relevance. *Cancer gene therapy* **22**, 417-430, doi:10.1038/cgt.2015.39 (2015).
- 224 Flaherty, K. T. *et al.* Inhibition of mutated, activated BRAF in metastatic melanoma. *The New England journal of medicine* **363**, 809-819, doi:10.1056/NEJMoa1002011 (2010).
- 225 Sosman, J. A. *et al.* Survival in BRAF V600-mutant advanced melanoma treated with vemurafenib. *The New England journal of medicine* **366**, 707-714, doi:10.1056/NEJMoa1112302 (2012).
- 226 Hauschild, A. *et al.* Dabrafenib in BRAF-mutated metastatic melanoma: a multicentre, open-label, phase 3 randomised controlled trial. *Lancet (London, England)* **380**, 358-365, doi:10.1016/s0140-6736(12)60868-x (2012).
- 227 Flaherty, K. T. *et al.* Combined BRAF and MEK inhibition in melanoma with BRAF V600 mutations. *The New England journal of medicine* **367**, 1694-1703, doi:10.1056/NEJMoa1210093 (2012).
- 228 Li, Y. & Trush, M. A. Diphenyleneiodonium, an NAD(P)H oxidase inhibitor, also potently inhibits mitochondrial reactive oxygen species production. *Biochem Biophys Res Commun* **253**, 295-299, doi:10.1006/bbrc.1998.9729 (1998).
- 229 Whitehouse, S. *et al.* Resveratrol, piperine and apigenin differ in their NADPH-oxidase inhibitory and reactive oxygen species-scavenging properties.

- Phytomedicine : international journal of phytotherapy and phytopharmacology*  
**23**, 1494-1503, doi:10.1016/j.phymed.2016.08.011 (2016).
- 230 Gusman, J., Malonne, H. & Atassi, G. A reappraisal of the potential chemopreventive and chemotherapeutic properties of resveratrol. *Carcinogenesis* **22**, 1111-1117 (2001).
- 231 Jaquet, V. *et al.* NADPH oxidase (NOX) isoforms are inhibited by celastrol with a dual mode of action. *British journal of pharmacology* **164**, 507-520, doi:10.1111/j.1476-5381.2011.01439.x (2011).
- 232 Alberto, M. E., Russo, N., Grand, A. & Galano, A. A physicochemical examination of the free radical scavenging activity of Trolox: mechanism, kinetics and influence of the environment. *Physical chemistry chemical physics : PCCP* **15**, 4642-4650, doi:10.1039/c3cp43319f (2013).
- 233 Mackley, M. P. *A quantitative approach: Developing a protocol to measure mRNA level of oncogenic BRAFV600E in tumour samples by RT-qPCR* Honours Bachelor of Science thesis, Dalhousie University, (2014).
- 234 Serrander, L. *et al.* NOX4 activity is determined by mRNA levels and reveals a unique pattern of ROS generation. *Biochemical Journal* **406**, 105-114 (2007).
- 235 Bustin, S. A. *et al.* The MIQE guidelines: minimum information for publication of quantitative real-time PCR experiments. *Clin Chem* **55**, 611-622, doi:10.1373/clinchem.2008.112797 (2009).
- 236 Lefever, S. *et al.* RDML: structured language and reporting guidelines for real-time quantitative PCR data. *Nucleic acids research* **37**, 2065-2069, doi:10.1093/nar/gkp056 (2009).



- 237 Butte, A. J., Dzau, V. J. & Glueck, S. B. Further defining housekeeping, or "maintenance," genes Focus on "A compendium of gene expression in normal human tissues". *Physiological genomics* **7**, 95-96 (2001).
- 238 Hsiao, L. L. *et al.* A compendium of gene expression in normal human tissues. *Physiological genomics* **7**, 97-104, doi:10.1152/physiolgenomics.00040.2001 (2001).
- 239 VanGuilder, H. D., Vrana, K. E. & Freeman, W. M. Twenty-five years of quantitative PCR for gene expression analysis. *BioTechniques* **44**, 619-626, doi:10.2144/000112776 (2008).
- 240 Livak, K. J. & Schmittgen, T. D. Analysis of relative gene expression data using real-time quantitative PCR and the 2(-Delta Delta C(T)) Method. *Methods (San Diego, Calif.)* **25**, 402-408, doi:10.1006/meth.2001.1262 (2001).
- 241 Holland, P. M., Abramson, R. D., Watson, R. & Gelfand, D. H. Detection of specific polymerase chain reaction product by utilizing the 5'----3'exonuclease activity of *Thermus aquaticus* DNA polymerase. *Proceedings of the National Academy of Sciences* **88**, 7276-7280 (1991).
- 242 Carbonell, P. *et al.* Comparison of allelic discrimination by dHPLC, HRM, and TaqMan in the detection of BRAF mutation V600E. *The Journal of molecular diagnostics : JMD* **13**, 467-473, doi:10.1016/j.jmoldx.2011.03.009 (2011).
- 243 Barretina, J. *et al.* The Cancer Cell Line Encyclopedia enables predictive modelling of anticancer drug sensitivity. *Nature* **483**, 603-607, doi:10.1038/nature11003 (2012).

- 244 King, A. J. *et al.* Dabrafenib; preclinical characterization, increased efficacy when combined with trametinib, while BRAF/MEK tool combination reduced skin lesions. *PLoS One* **8**, e67583 (2013).
- 245 Fedchenko, N. & Reifenrath, J. Different approaches for interpretation and reporting of immunohistochemistry analysis results in the bone tissue - a review. *Diagnostic Pathology* **9**, 221, doi:10.1186/s13000-014-0221-9 (2014).
- 246 Shi, S. R. & Taylor, C. R. *Antigen Retrieval Immunohistochemistry Based Research and Diagnostics*. (Wiley, 2011).
- 247 Chung, J. Y., Braunschweig, T. & Hewitt, S. M. Optimization of recovery of RNA from formalin-fixed, paraffin-embedded tissue. *Diagnostic molecular pathology : the American journal of surgical pathology, part B* **15**, 229-236, doi:10.1097/01.pdm.0000213468.91139.2d (2006).
- 248 Penland, S. K. *et al.* RNA expression analysis of formalin-fixed paraffin-embedded tumors. *Lab Invest* **87**, 383-391, doi:10.1038/labinvest.3700529 (2007).
- 249 Lewis, F., Maughan, N. J., Smith, V., Hillan, K. & Quirke, P. Unlocking the archive--gene expression in paraffin-embedded tissue. *J Pathol* **195**, 66-71, doi:10.1002/1096-9896(200109)195:1<66::aid-path921>3.0.co;2-f (2001).
- 250 Kokkat, T. J., Patel, M. S., McGarvey, D., LiVolsi, V. A. & Baloch, Z. W. Archived formalin-fixed paraffin-embedded (FFPE) blocks: A valuable underexploited resource for extraction of DNA, RNA, and protein. *Biopreservation and biobanking* **11**, 101-106, doi:10.1089/bio.2012.0052 (2013).
- 251 Kashofer, K., Viertler, C., Pichler, M. & Zatloukal, K. Quality control of RNA preservation and extraction from paraffin-embedded tissue: implications for RT-

- PCR and microarray analysis. *PLoS One* **8**, e70714,  
doi:10.1371/journal.pone.0070714 (2013).
- 252 Evers, D. L., Fowler, C. B., Cunningham, B. R., Mason, J. T. & O'Leary, T. J. The Effect of Formaldehyde Fixation on RNA: Optimization of Formaldehyde Adduct Removal. *The Journal of molecular diagnostics : JMD* **13**, 282-288,  
doi:10.1016/j.jmoldx.2011.01.010 (2011).
- 253 Bolognesi, C. *et al.* Digital Sorting of Pure Cell Populations Enables Unambiguous Genetic Analysis of Heterogeneous Formalin-Fixed Paraffin-Embedded Tumors by Next Generation Sequencing. *Scientific Reports* **6**, 20944,  
doi:10.1038/srep20944 (2016).
- 254 von Ahlfen, S., Missel, A., Bendrat, K. & Schlumpberger, M. Determinants of RNA quality from FFPE samples. *PLoS One* **2**, e1261,  
doi:10.1371/journal.pone.0001261 (2007).
- 255 Schouten, J. P. *et al.* Relative quantification of 40 nucleic acid sequences by multiplex ligation-dependent probe amplification. *Nucleic acids research* **30**, e57 (2002).
- 256 Lake, S. L. *et al.* Multiplex ligation-dependent probe amplification of conjunctival melanoma reveals common BRAF V600E gene mutation and gene copy number changes. *Investigative ophthalmology & visual science* **52**, 5598-5604,  
doi:10.1167/iovs.10-6934 (2011).
- 257 Hayden, R. T. *et al.* Comparison of droplet digital PCR to real-time PCR for quantitative detection of cytomegalovirus. *J Clin Microbiol* **51**, 540-546,  
doi:10.1128/jcm.02620-12 (2013).

- 258 Albano, F. *et al.* Absolute quantification of the pretreatment PML-RARA transcript defines the relapse risk in acute promyelocytic leukemia. *Oncotarget* **6**, 13269-13277, doi:10.18632/oncotarget.3773 (2015).
- 259 Arena, S. *et al.* Emergence of Multiple EGFR Extracellular Mutations during Cetuximab Treatment in Colorectal Cancer. *Clin Cancer Res* **21**, 2157-2166, doi:10.1158/1078-0432.ccr-14-2821 (2015).
- 260 Bloethner, S. *et al.* Effect of common B-RAF and N-RAS mutations on global gene expression in melanoma cell lines. *Carcinogenesis* **26**, 1224-1232, doi:10.1093/carcin/bgi066 (2005).
- 261 Kingsmore, S. F., Lindquist, I. E., Mudge, J. & Beavis, W. D. Genome-Wide Association Studies: Progress in Identifying Genetic Biomarkers in Common, Complex Diseases. *Biomarker Insights* **2**, 283-292 (2007).
- 262 Boutros, P. C. The path to routine use of genomic biomarkers in the cancer clinic. *Genome research* **25**, 1508-1513, doi:10.1101/gr.191114.115 (2015).
- 263 Trape, A. P. & Gonzalez-Angulo, A. M. Breast cancer and metastasis: on the way toward individualized therapy. *Cancer genomics & proteomics* **9**, 297-310 (2012).
- 264 Perou, C. M. *et al.* Molecular portraits of human breast tumours. *Nature* **406**, 747-752, doi:10.1038/35021093 (2000).
- 265 Slamon, D. J. *et al.* Use of chemotherapy plus a monoclonal antibody against HER2 for metastatic breast cancer that overexpresses HER2. *The New England journal of medicine* **344**, 783-792, doi:10.1056/nejm200103153441101 (2001).

- 266 Piccart-Gebhart, M. J. *et al.* Trastuzumab after adjuvant chemotherapy in HER2-positive breast cancer. *The New England journal of medicine* **353**, 1659-1672, doi:10.1056/NEJMoa052306 (2005).
- 267 Santarpià, L., Lippman, S. L. & El-Naggar, A. K. Targeting the Mitogen-Activated Protein Kinase RAS-RAF Signaling Pathway in Cancer Therapy. *Expert Opin Ther Targets* **16**, 103-119, doi:10.1517/14728222.2011.645805 (2012).
- 268 Szatrowski, T. P. & Nathan, C. F. Production of large amounts of hydrogen peroxide by human tumor cells. *Cancer Res* **51**, 794-798 (1991).
- 269 Sundaresan, M., Yu, Z. X., Ferrans, V. J., Irani, K. & Finkel, T. Requirement for generation of H<sub>2</sub>O<sub>2</sub> for platelet-derived growth factor signal transduction. *Science (New York, N.Y.)* **270**, 296-299 (1995).
- 270 Bae, Y. S. *et al.* Epidermal growth factor (EGF)-induced generation of hydrogen peroxide. Role in EGF receptor-mediated tyrosine phosphorylation. *J Biol Chem* **272**, 217-221 (1997).
- 271 Huggett, J. F. *et al.* The digital MIQE guidelines: Minimum Information for Publication of Quantitative Digital PCR Experiments. *Clin Chem* **59**, 892-902, doi:10.1373/clinchem.2013.206375 (2013).
- 272 Vandesompele, J. *et al.* Accurate normalization of real-time quantitative RT-PCR data by geometric averaging of multiple internal control genes. *Genome biology* **3**, 1-12 (2002).

273 De Spiegelaere, W. *et al.* Reference Gene Validation for RT-qPCR, a Note on Different Available Software Packages. *PLoS One* **10**, doi:10.1371/journal.pone.0122515 (2015).

## APPENDIX A: SUPPLEMENTAY MATERIALS

**Table A 1 BRAF absolute quantification (copies/μl) as determined by RT-ddPCR using the QX200 ddPCR EvaGreen supermix.**

	Sample	Threshold	Concentration Copies/μl	PoissonConfMax	PoissonConfMin	Copies/20μl	MeanAmplitude of Positives	MeanAmplitude of Negatives	Positives	Negatives	Accepted Droplets
<b>Melanoma</b>	A1	21813	21.5	23.8	19.2	430	24146	16540	343	18388	18931
	A2	20174	2	2.9	1.4	40	22753	12006	31	17806	17837
	A3	20174	6.9	8.2	5.5	138	22771	12683	100	17118	17218
	B1	20112	18.3	20.6	16.1	366	23347	16091	254	16166	16420
	B2	19936	7.7	9.1	6.3	154	23332	12551	119	18141	18260
	B3	19936	1.4	2	0.9	28	24307	10303	21	18230	18251
	C1	17405	0.35	0.71	0.14	7	24144	9283.5	6	20447	20453
	C2	14915	2.4	3.3	2	48	20315	9902.3	34	16709	16743
	C3	14915	0.74	1.28	0.54	14.8	18835	10483	11	17422	17433
	D1	13992	1.08	1.69	0.84	21.6	19137	10824	17	18469	18486
	D2	13992	1.08	1.71	0.83	21.6	17700	8970.4	16	17380	17396
	D3	13992	0.36	0.79	0.22	7.2	20576	9837.8	5	16263	16268
	E1	20641	75.7	80.1	71.2	1514	23328	16910	1101	16576	17677
	E2	18703	24.5	27	22	490	22001	12256	369	17562	17931
	E3	17293	24.4	27.2	21.7	488	20955	11989	305	14545	14850
	F1	14931	14.5	16.4	12.6	290	20560	10857	227	18308	18535
	F2	15032	14	15.9	12.1	280	20915	11443	203	16979	17182
	F3	15032	9.4	10.9	7.9	188	20628	11167	148	18405	18553
<b>FTC</b>	G1	19764	68.3	72.6	64	1366	21596	15423	948	15862	16810
	G2	19663	74.4	79.3	69.6	1488	21649	16052	905	13861	14766
	G3	0	No Call				0	24216	0	17689	17689
	H1	14710	34.6	37.9	31.4	692	20028	12673	435	14574	15009
	H2	18749	252	263	247	5040	20483	15925	2139	8953	11092
	H3	18296	168	175	164	3360	20543	13970	2248	14658	16906
	I1	20024	65.3	69.6	61.1	1306	22266	15813	899	15743	16642
	I2	0	No Call				0	18558	0	16225	16225
	I3	0	No Call				0	22188	0	16869	16869
	J1	20465	70.5	74.9	68.3	1410	21773	15959	980	15866	16846
	J2	16677	10.7	12.3	9.8	214	20669	11946	158	17370	17528
	J3	18350	66.9	71.2	64.8	1338	20721	13312	958	16362	17320
	K1	16902	61.6	65.9	57.3	1232	19980	12211	788	14666	15454
	K2	0	No Call				0	19886	0	17451	17451
	K3	0	No Call				0	45081	0	5617	5617
	L1	15334	1.22	1.85	0.96	24.4	18939	9080.9	19	18357	18376
	L2	15334	2.3	3.2	2	46	19456	8702.4	36	18006	18042
	L3	15334	13	14.8	12.1	260	19958	10127	209	18812	19021
<b>CRC</b>	M1	19958	3.5	4.5	2.6	70	22130	13101	55	18665	18720
	M2	18916	1.6	2.3	1.3	32	21967	12069	25	18256	18281
	M3	19337	4.3	5.4	3.8	86	21541	11591	68	18489	18557
	N1	19764	23.1	25.5	20.7	462	21858	13573	356	17957	18313
	N2	17405	25.7	28.2	24.4	514	21346	12116	408	18486	18894
	N3	17405	20.5	22.8	19.3	410	21853	11262	308	17553	17861
	O1	19778	4.3	5.4	3.3	86	21686	12950	61	16854	16915
	O2	16786	8.5	10	7	170	21035	12120	121	16767	16888
	O3	16757	9.1	10.6	7.6	182	21269	12241	140	18047	18187
	P1	19807	1	1.6	0.6	20	21416	13183	15	17581	17596
	P2	14869	1.08	1.67	0.85	21.6	20238	10582	18	19561	19579
	P3	14869	0.6	1.5	0.3	12	18868	7569.3	3	6306	6309
	Q1	19922	0.13	0.41	0.02	2.6	46602	12271	2	18315	18317
	Q2	20024	0.21	0.56	0.05	4.2	26697	12806	3	16753	16756
	Q3	19958	0.33	0.79	0.1	6.6	22892	12461	4	14122	14126
Q3	14995	0.47	0.91	0.2	9.4	19238	11751	7	17569	17576	

**Table A 2 GUSB absolute quantification (copies/μl) as determined by RT-ddPCR using the QX200 ddPCR EvaGreen supermix.**

	Sample	Threshold	Concentration Copies/μl	PoissonConfMax	PoissonConfMin	Copies/20μl	MeanAmplitude of Positives	MeanAmplitude of Negatives	Positives	Negatives	Accepted Droplets
<b>Melanoma</b>	A1	22374	60.8	64.8	56.9	1216	24720	13996	911	17170	18081
	A2	22374	6.5	7.7	5.2	130	24319	16413	102	18487	18589
	A3	22449	13.9	15.8	11.9	278	24024	9507.1	195	16444	16639
	B1	22374	20.5	22.8	18.1	410	24734	14141	294	16744	17038
	B2	22600	6.6	8	5.4	132	24693	9545.7	99	17636	17735
	B3	22298	5.2	6.5	4.1	104	23880	14769	73	16412	16485
	C2	21036	2.4	3.2	1.7	48	22849	6944.5	40	19742	19782
	C3	20973	0.27	0.71	0.06	5.4	22310	7891.3	3	13222	13225
	D1	19672	1	1.7	0.5	20	21184	8529.2	12	13773	13785
	D2	19848	0.61	1.14	0.27	12.2	22242	6082.7	8	15512	15520
	D3	19408	4.5	5.6	3.5	90	21463	6882.3	68	17879	17947
	E1	21392	118	124	112	2360	23796	15731	1540	14636	16176
	E2	20637	39.1	42.6	35.7	782	22748	10190	493	14570	15063
	E3	20637	33.9	36.9	30.9	678	22805	10610	499	17074	17573
	F1	20407	42.2	46.1	40.2	844	22094	8529.3	450	12314	12764
F2	20344	23.3	25.7	22.1	466	22519	8677.8	369	18454	18823	
F3	20344	23.3	25.8	22.1	466	21717	10020	342	17081	17423	
<b>PTC</b>	G1	0	No Call				0	24293	0	18663	18663
	G2	20058	1460	1489	1449	29240	23962	16258	13445	5453	18898
	G3	0	No Call				0	26645	0	13481	13481
	H1	19672	20.9	23.2	18.5	418	20998	9783.2	303	16921	17224
	H2	23196	42.5	45.8	39.1	850	24699	16869	630	17144	17774
	H3	19760	93.6	98.4	88.7	1872	21303	11263	1413	17072	18485
	I1	22491	1355	1381	1330	27100	24797	18265	12270	5668	17938
	I2	23733	981	1002	961	19620	24859	20419	9195	7061	16256
	J1	22600	1157	1181	1134	23140	24341	18799	10217	6103	16320
	J2	19848	18.9	21.8	16.1	378	21166	10100	166	10228	10394
	J3	32622	0	0.4	0	0	0	17603	0	8823	8823
	K1	18598	61.3	65.8	56.9	1226	20247	11405	717	13397	14114
	K2	0	No Call				0	24142	0	17444	17444
	K3	0	No Call				0	40249	0	17047	17047
	L1	18834	0.97	1.53	0.75	19.4	19922	6822.9	16	19429	19445
L2	18834	1.7	2.4	1.4	34	19758	7155.4	26	18262	18288	
L3	19148	12.8	14.6	11.9	256	20357	9094.5	200	18270	18470	
<b>CRC</b>	M1	19903	12.9	14.7	11.1	258	21263	9866.3	199	17993	18192
	M2	21099	11.9	13.7	10.2	238	22511	10239	181	17764	17945
	M3	20721	15.9	17.9	13.9	318	22333	9109	246	18117	18363
	N1	19526	45.7	49.1	42.2	914	20645	12603	681	17205	17886
	N2	20029	37.8	41	34.6	756	21984	10714	537	16434	16971
	N3	20092	35.4	38.5	32.3	708	22032	10432	501	16413	16914
	O1	19400	11.3	13	9.6	226	20674	11125	172	17833	18005
	O2	20024	24.1	26.6	21.6	482	21628	11444	356	17196	17552
	O3	19936	19.3	21.5	17	386	21751	10701	282	17060	17342
	P1	19148	2.6	3.5	1.8	52	20213	10925	39	17821	17860
	P2	20407	3.5	4.6	2.6	70	21732	9367	52	17351	17403
	P3	21162	1.4	2	0.9	28	23229	6341.3	24	20565	20589
	Q1	19903	0.24	0.56	0.07	4.8	21715	7768.1	4	19717	19721
	Q1	20092	0.26	0.61	0.08	5.2	21226	10592	4	18215	18219
	Q2	19966	0.15	0.47	0.02	3	21465	10560	2	16189	16191
Q3	19966	2.5	3.4	1.8	50	21602	9591.5	42	19621	19663	



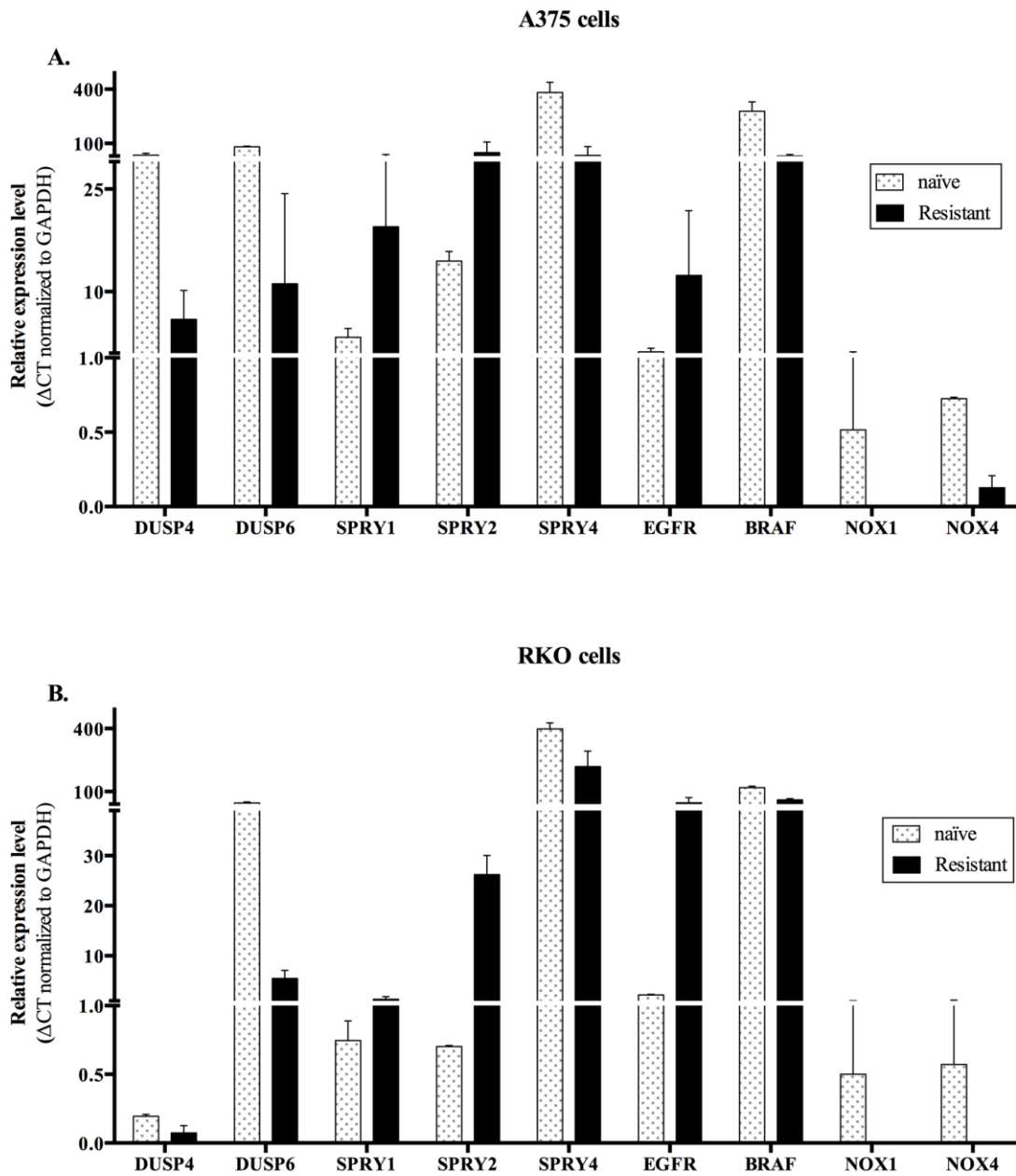


**Figure A 1 Relative expression levels.**

Bar graph showing the mean  $\pm$  SD (n=2) in  $\Delta$ Ct values of mRNA expression of our gene of interest displayed on the x-axis relative to GAPDH expression in naïve and resistance **A.** Melanoma cells A375. **B.** Colon carcinoma cells RKO.

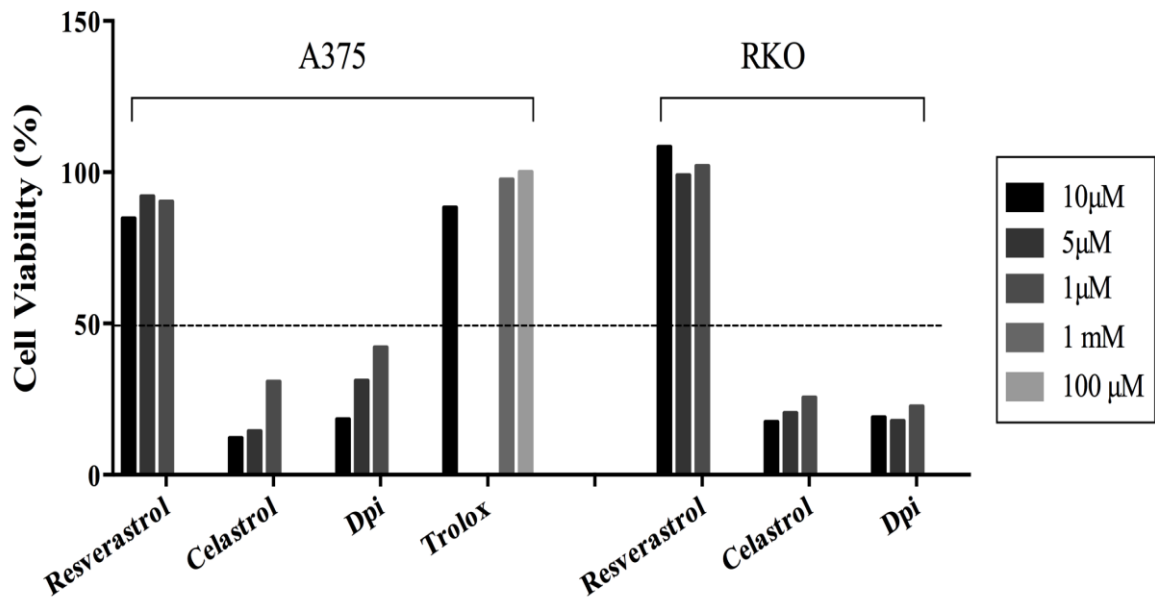


**Figure A 2 Cytotoxicity effect of four different agents with ROS scavenging activity.**

A375 and RKO cells were treated with resverastrol, DPI, and celastrol at three different concentrations 1, 5, and 10  $\mu\text{M}$  for 72 hr. In addition, A375 cells were treated with three different concentrations 1, 5, and 10  $\mu\text{M}$  for 72 hr. Cell viability was measured using Alamar Blue assay and calculated relative to the vehicle control (0.1% DMSO). Data are represented as mean (n=1).